SHIVAJI UNIVERSITY, KOLHAPUR

Volume-49 Issue-2 (July, 2023)
ISSN-Science-0250-5347

Estd. 1962
"A++" Accredited by NAAC (2021)
with CGPA 3.52

Journal of Shivaji University
SCIENCE & TECHNOLOGY

(Peer Reviewed Journal)

JOURNAL OF SHIVAJI UNIVERSITY : SCIENCE AND TECHNOLOGY

(Peer Reviewed Journal)

Volume-49, Issue-2 (July, 2023)

ISSN Science-0250-5347

EDITORIAL BOARD OF THE JOURNAL

Prof. (Dr.) D. T. Shirke
Chairman
Hon'ble Vice Chancellor, Shivaji University, Kolhapur

Prof. (Dr.) P. S. Patil
Hon'ble Pro Vice Chancellor, Shivaji University, Kolhapur

Dr. V. N. Shinde
Registrar (Ag.), Shivaji University, Kolhapur

Prof. (Dr.) Smt. S. H. Thakar
Dean, Faculty of Science & Technology, and
Head, Department of Mathematics, Shivaji University, Kolhapur

Prof. (Dr.) S. D. Delekar
Editor,
Department of Chemistry, Shivaji University, Kolhapur

MEMBERS OF THE EDITORIAL BOARD

Prof. (Dr.) K. Y. Rajpure	Head, Dept. of Physics, Shivaji University, Kolhapur
Prof. (Dr.) Smt. J. P. Jadhav	Head, Dept. of Bio-technology, Shivaji University, Kolhapur
Prof. (Dr.) K. D. Sonawane	Head, Dept. of Biochemistry, Shivaji University, Kolhapur
Dr. S. N. Sapali	Director, Dept. of Technology, Shivaji University, Kolhapur
Prof. (Dr.) R. V. Gurav	Head, Dept. of Botany, Shivaji University, Kolhapur
Prof. (Dr.) S. B. Mahadik	Head, Dept. of Statistics, Shivaji University, Kolhapur
Dr. Smt. K. S. Oza	Head, Dept. of Computer Science, Shivaji University, Kolhapur
Prof. (Dr.) A. A. Deshmukh	Head, Dept. of Zoology, Shivaji University, Kolhapur
Prof. (Dr.) K. K. Sharma	Head, Dept. of Nano Science & Technology, Shivaji University, Kolhapur
Prof. (Dr.) S. D. Shinde	Head, Dept. of Geography, Shivaji University, Kolhapur
Dr. Smt. A. S. Jadhav	Head, Dept. of Environmental Science, Shivaji University, Kolhapur
Prof. (Dr.) P. K. Gaikwad	Head, Dept. of Electronics, Shivaji University, Kolhapur

Estd. 1962
"A++" Accredited by NAAC (2021)
with CGPA 3.52

Shivaji University
Kolhapur 416 004 (INDIA)

JOURNAL OF SHIVAJI UNIVERSITY : SCIENCE AND TECHNOLOGY

(Peer Reviewed Journal)

Volume-49, Issue-2 (July, 2023)

ISSN Science-0250-5347

- Contact Details -
Prof. (Dr.) S. D. Delekar
Editor, Journal of Shivaji University : Science and Technology
and
Department of Chemistry
Shivaji University, Kolhapur 416 004 (India)
E-mail : editor.jscitech@unishivaji.ac.in
website : http://www.unishivaji.ac.in/journals/

Shivaji University, Kolhapur

JOURNAL OF SHIVAJI UNIVERSITY : SCIENCE AND TECHNOLOGY

(Peer Reviewed Journal)

Volume-49, Issue-2 (July, 2023)

ISSN Science-0250-5347

- Editor -
Prof. (Dr.) S. D. Delekar
Journal of Shivaji University :
Science and Technology

- Published by -
Dr. V. N. Shinde
Ag. Registrar,
Shivaji University, Kolhapur 416004.

- Printed by -
Shri. B. P. Patil
Superintend
Shivaji University, Kolhapur 416004.

The Editor, on behalf of the Editorial Board of the Journal of Shivaji University : Science and Technology, Vol. No. 49 (2) whises to express his thanks to the contributing authors and the experts for acting as referees for the papers included in the issue.

Published : July, 2023

Journal of Shivaji University: Science and Technology

Volume-49, Issue-2 (July, 2023)

INDEX

Department of Chemistry

Shivaji University, Kolhapur

Journal of Shivaji University : Science & Technology

Volume-49, Issue-2 (July, 2023)

Departmental Editorial Board

Silica Coated Superhydrophobic Materials for Oil-Water Separation Application-A Short Review

Rajesh B. Sawant[a,*], Mehejbin R. Mujawar[a], Amol B. Pandhare[b,f],
Sanjay S. Latthe[c], Ankush M. Sargar[d],
Raghunath K. Mane[e], Shivaji R. Kulal[a*]

[a]Department of Chemistry, Raje Ramrao Mahavidyalaya, Jath, Sangli 416 404 (MS) India.
[b]Department of Chemistry, Shivaji University, Kolhapur 416 004 (MS) India.
[c]Department of Physics, Vivekanand College, Kolhapur 416 003 (MS) India.
[d]Department of Chemistry, Bharati Vidyapeeth's Dr. Patangrao Kadam Mahavidyalaya, Sangli 416 416 (MS) India.
[e] Department of Chemistry, Smt. Kusumtai Rajarambhapu Patil Kanya Mahavidyalaya, Islampur, Sangli 416 409 (MS) India.
[f]Department of Chemistry, M.H. Shinde Mahavidyalaya, Tisangi, Gaganbavda, Kolhapur 416 206 (MS) India.
*Corresponding authors:srkulal@gmail.com and rbsawant2@gmail.com

ABSTRACT

Contamination like oil and organic pollutants in water has a severe problem for aquatic life and human being; it is a need to preserve their life. These contaminants are added due to frequent oil spill accidents, and industrial as well as domestic waste. There is a need to develop methods and materials that show excellent ability to separate the oil and organic contaminants from water. Recently, superhydrophobic coated sponges, metals mesh, membranes and porous materials plays crucial role to separate oil and water from oil-water mixture. The micro and nonporous of substrate facilitate to enter liquid into it and superhydrophobic/superoliophilic property of substrate surface resist water and allows oil to enter into porous substrate. The various surface modified organic metal oxide nanoparticles are used to develop superhydrophobic surface on porous substrate. Among them SiO_2 nanoparticles is promising material to preparation of superhydrophobic surface because of their cost-effectiveness and easy synthesis techniques. This review focused on silica modified porous sponge, metal meshes, membrane and porous substrate for scalable oil-water separation application.

KEYWORDS

Superhydrophobic, Oil-water separation, porous sponge, Metal mesh and membrane.

……

1. INTRODUCTION

Frequent oil spill accidents and industrial chemical spills occurred in the sea and the ecosystem damage; such incidents have spread to impact the offspring. Therefore, considerable surviving organisms for several years after the impact [1-2] efforts have been done to remove oil and organic solvents from water. Due to this extensive current research is focussed on the development of superhydrophobic materials for effective oil-water separation. To achieve superhydrophobic sponges, surface roughness and low surface energy materials play a crucial role. The various methods such as dip coating, immersion, spray coating; hydrothermal methods, chemical vapor deposition, surface etching, solvothermal methods, layer-by-layer assembly and electrochemical treatment describe a modification of sponges for oil and water separation [3-4]. At present, traditional technologies, including in situburning [5], bioremediation [6], chemical dispersant methods [7], skimming [8], and the use of sorbents [9] are used to clean up spilled oils or organic pollutants. However, many of these strategies involve energy intensive and slow processes, have low clean-up capacities or create secondary pollution during the clean-up process, restricting their widespread practical applications [10-11]. To realize the hierarchical structures on different material surfaces, a series of strategies, such as sol-gel coating [12], chemical vapor deposition [13], plasma etching [14], template processing [15], lithographic patterning [16], etc. have been adopted [17]. The superhydrophobic surfaces on which water achieves water contact angle higher than 150°and sliding angle less than 5°are attracting minds of researchers due to their efficient oil-water separation efficiency [18].

Recently, Wu et al. [19] have prepared a highly flexible superhydrophobic PDMS@F-SiO_2 coating for self-cleaning and drag-reduction applications via a two-step spraying of PDMS and F-SiO_2 nanoparticles. However, it is common that inorganic particles normally tend to agglomerate due to the interparticle forces stemming from the Vander Waals, capillary and electrostatic forces [20], which leads to phase separation during the fabrication process and tends to diminish the quality of the coating through cracks or weak adhesive to the substrates. Gao et al. [21] prepared PVDF/SiO_2 coated superhydrophobic porous membranes using a spraying technique. These membranes could be used to separate the oil-water mixtures but are not applicable to surfactant stabilized water-in-oil emulsions because of their large pore sizes. Li et al. [22] prepared the hydrophobic CS by incomplete combustion of hydrocarbons from the middle of a candle flame. The PU sponge was immersed in the solution of CS, SiO_2 and PU resin to achieve stable superhydrophobicity. The CS-SiO_2-PU sponge was shown excellent oil-water separation efficiency. The CS-SiO_2-PU sponge showed excellent oil-water separation efficiency from hot water, acidic solutions, alkaline solutions and salt solutions.

In this review, the sophisticated, facile and low-cost methods for fabrication of superhydrophobic porous material for oil-water separation application are discussed.

The 3D sponges, metal meshes, membrane and cotton fabrics are used as substrate for scalable oil-water separation application.

2. SUPERHYDROPHOBIC SURFACES FOR OIL-WATER SEPARATION

2.1 Superhydrophobic Sio_2 Modified Sponges for Oil-Water Separation

Zhang et al. [23] have fabricated the superhydrophobic surface by using VTMS and SiO_2 via immersion method. The schematic of preparation of superhydrophobic sponge is shown in **Figure-1.** It was shown a water contact angle of 153.2° and roll-on angle of 4.8°. The oil is quickly absorbed by superhydrophobic sponge which can be shown the superoliophilic property of a modified sponge. The IR peak at 1078 cm^{-1} shows the presence of the O-Si-O bond present in the material. It was showing the high separation efficiency of about 99.5%. It exhibited good saturated adsorption properties exceeding 70 g/g for all oils. It was shows outstanding characteristics of superhydrophobic sponge such as high porosity, small pore size and ultra-light mass. After 20 cycles, it was found that the adsorption ability of the modified melamine sponge for different oils decreased slightly. It shows outstanding stability and reusable performance. The modified sponge maintains an 89% of recovery rate even after 20 cycles. This method was used to prepare porosity and provides storage space for the adsorption of oil pollution. This superhydrophobic composite melamine sponge provided the possibility for practical application of oil-water separation.

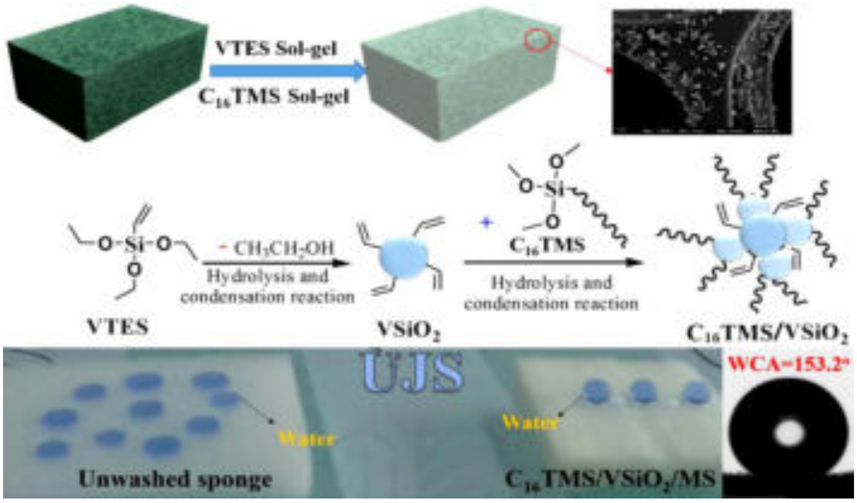

Figure-1. Schematic illustration of the preparation of superhydrophobic sponge. Images reprinted from [23], with permission from Elsevier, Journal of Chemical Engineering, Copyright 2020.

Liu et al. [24]. have fabricated a superhydrophobic sponge and polyester coated with SiO_2-DTMS through an entrapment method. The **Figure-.2** reveals the fabrication process of superhydrophobic sponge and polyester The SiO_2 particles were introduced by growth on the substrate through the polymerization process, followed by the addition of DTMS as an adhesive, leading to a homogeneous and dense superhydrophobic membrane. The modified sponge was shown the water contact angle up to 172° indicating the water repellence was superior. This superhydrophobic sample had good hydrophobic stability even in acidic condition and it can show efficient oil-water separation. The amount of the absorbed oil was about 43-65 times of sponge own weight can be shown that the evaluation of the mass based on absorbed surface tension, density, viscosity of absorbed liquids. It exhibits stable oil storage under harsh environmental conditions in oil-water separation. The performance remained constant after 100 recycling sequences, even in a harsh water environment.

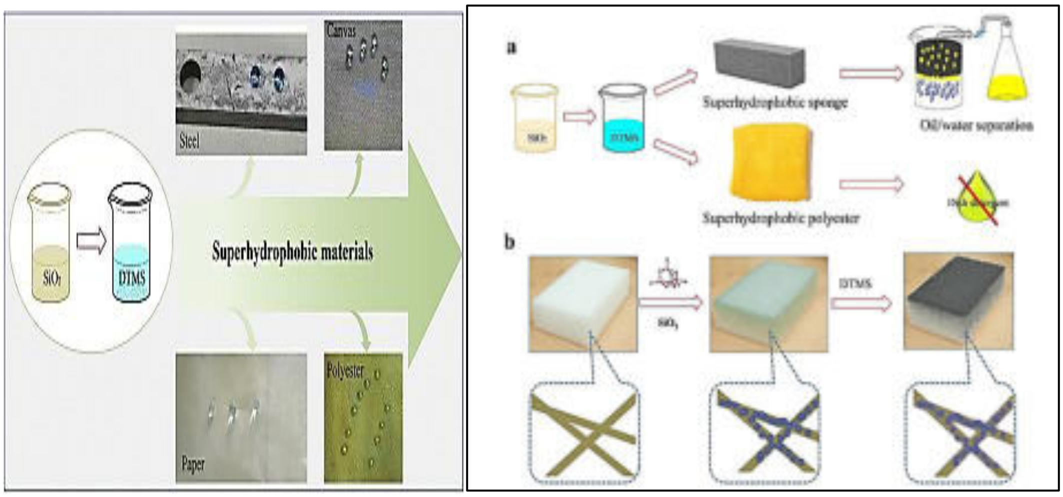

Figure-2. Schematic illustration of the fabrication of a modified sponge and polyester. Images reprinted from [24], with permission from Elsevier, Copyright 2019.

2.2 Superhydrophobic Sio$_2$ Modified Metal Meshes for Oil-Water Separation

Zhao et al. [25] have prepared superhydrophobic SiO_2 nanoparticles by improved Stober method and then coated on a chemically etched stainless steel mesh by one step dipping method to fabricate superhydrophobic SiO_2 coated stainless steel mesh. The preparation process was simple, efficient and environmentally friendly. The experimental procedure is shown in **Figure-3.** It shows excellent oil-water separation properties, which can be widely used in oil-water separation. It was showing 153.3° water contact angle and 0° oil contact angle. The oil-water separation efficiency was nearly 96% by using this modified stainless-steel mesh.

The separation efficiencies were obtained repeatedly even after 40 cycles without noticeable deterioration. The superhydrophobic modified stainless steel mesh shows stability, durability and reusability. The SiO_2 modified stainless steel mesh indicates good material for treating real oil-polluted water in different practical applications. This method shows high performance, oil-water separation in a short time and repeatedly in comparison with earlier works.

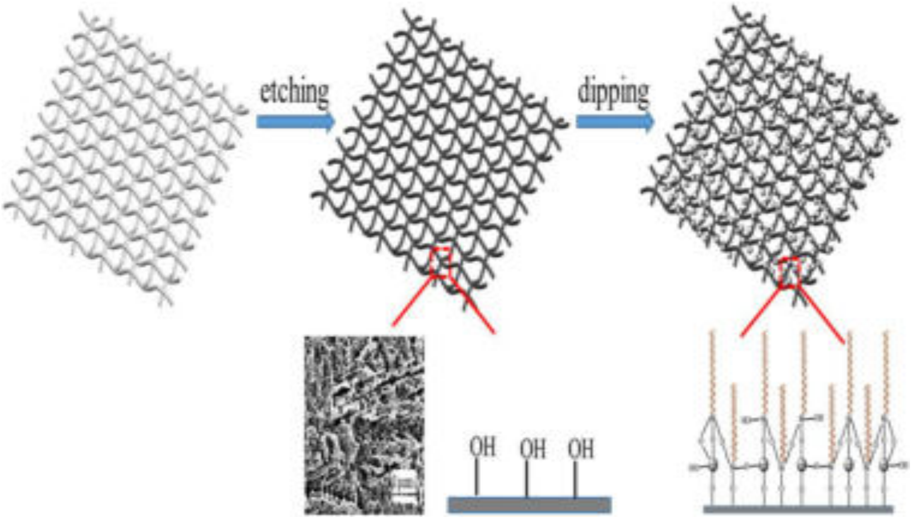

Figure-3. Schematic illustration of the preparation of FSSM. Images reprinted from [25], with permission from Elsevier, Copyright 2019.

Xiong et al. [26] have prepared SiO_2 nanoparticles by an improved modified method by using TEOS and then coated on a stainless-steel mesh by spraying method to fabricate SiO_2 coated stainless steel mesh. The **Figure-4** illustrates schematic of preparation of the superhydrophobic stainless-steel mesh. The preparation process was efficient, simple and environmentally friendly. It shows good mechanical properties and oil/water separation performance. It was showing 156.4° oil contact angle and less than 10^0water contact angles. The oil-water separation efficiency was nearly 98.69% by using this modified stainless-steel mesh. The separation efficiencies obtained repeatedly even after 20 cycles without noticeable deterioration. The superhydrophobic modified stainless stell mesh shows stability, durability and reusability. The SiO_2 modified stainless steel mesh indicates excellent material for treating oil-polluted water in different practical applications. This method shows an easily scaled-up preparation process, stable mechanical and thermal properties, offering new prospects for efficient oil/water separationin comparison with earlier works.

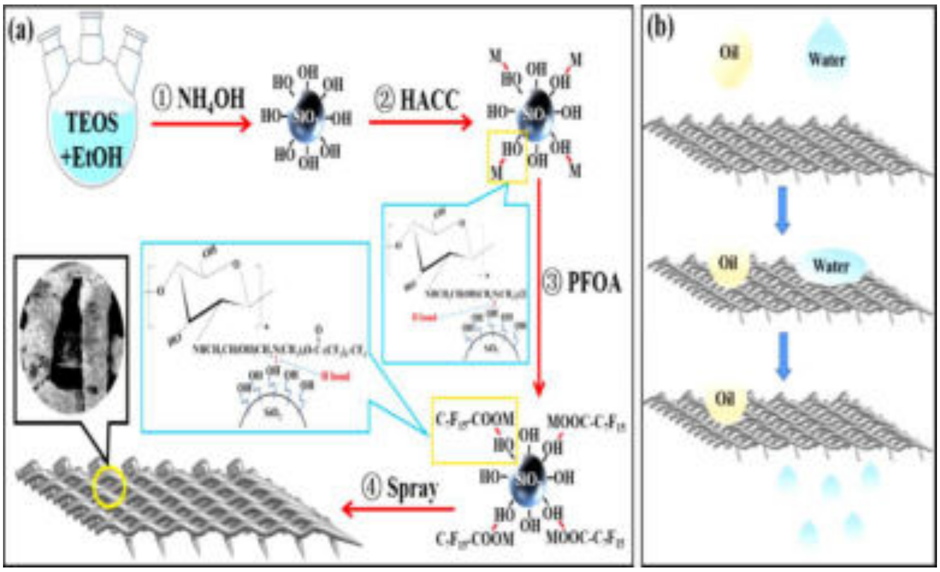

Figure-4 (a) Schematic diagram illustrating the fabrication of air superhydrophilic-superoleophobic membrane. (b) Scheme of the oil/water separation. Images reprinted from [26], with permission from Elsevier, Journal of Colloid and Interface Science, Copyright 2021.

2.3 Superhydrophobic Sio2 Modified Porous Substrates for Oil-Water Separation

Gu et al. [27] have prepared a membrane (SiO_2/Polyurethane membrane) with porous structure rough surface and hydrophobic epidermis by surface modification to construct a rough surface and low-energy epidermis on electrospun polyurethane membrane. The schematic of experimental procedure is shown in **Figure-5.** The superhydrophobic SiO_2/PU porous membrane prepared by chemical modification on the membrane shows a water contact angle 152.1° and low sliding angle 6°. This membrane was used for different aqueous solutions like water, saline solution, alkaline solution acidic solution. The porous membrane shows low air permeability and high-water vapor transmission rate. It shown good oil absorption capacity. It was shows high oil-water separation efficiency above 98.5%. The absorption capacity of the modified membrane does not show severe degradation even after 30 separation cycles which indicating a highly stable absorption performance of modified membrane. It provided the potential for eater repellent, breathable applications and oil-water separation in long term use.

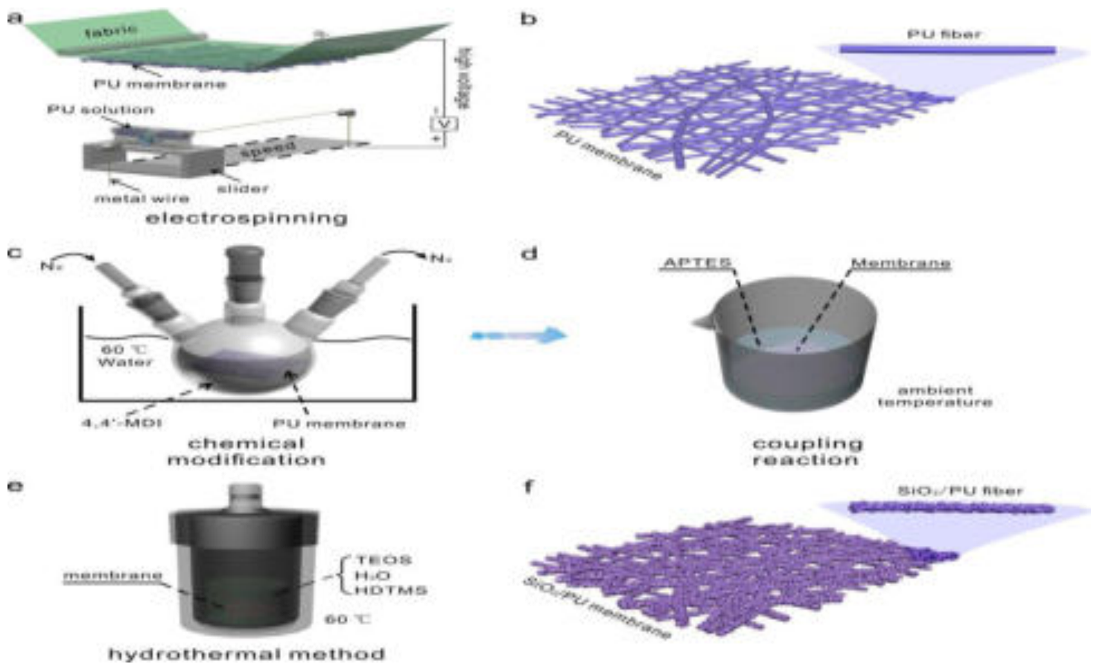

Figure-5. The preparation scheme of superhydrophobic SiO_2/PU membrane. Images reprinted from [27], with permission from Elsevier, App. Sur. Sci. Copyright 2019.

Wei and their co-researchers [28] have obtained the SiO_2 nanoparticles from ethanol and ammonium hydroxide with TEOS. TheSiO_2 nanoparticles were isolated by repeated centrifugation in ethanol followed by drying in a vacuum oven. A facile strategy was presented to prepare silica particles grafting. The sprayable solution be easily applied to different porous substrates to achieve durable superhydrophobic coating (schematically shown in **Figure-6**). The surface shows a separation efficiency of 98.8% dealing with oil-water mixture. The oil absorption capacity of immersion coated polyurethane sponge was demonstrated higher than pristine polyurethane sponge an 39 g/g which would benefit from the presence of lipophilic PSAN and higher porosity contributed by abundant nanoparticles. After 10 cycles of abrasion test the remained separation efficiency of above 96% and water contact angle of 151° confirmed the mechanical durability. This sponge shows facile, environmentally friendly, mechanical and chemical stability.

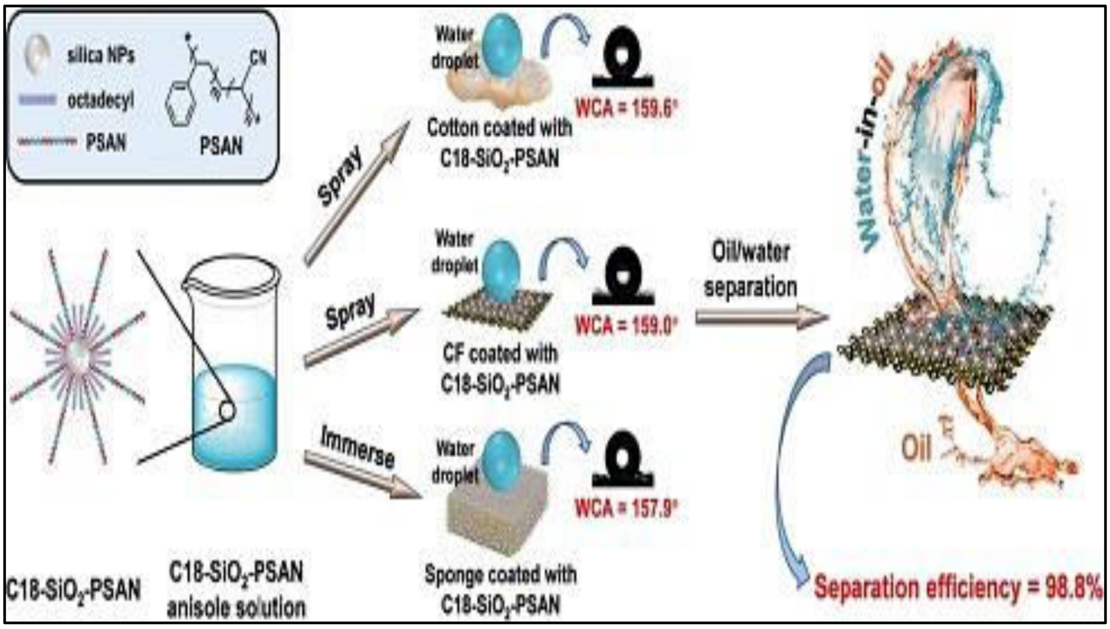

Figure-6. Schematic illustration of preparation of modified superhydrophobic surface for oil-water separation. Images reprinted from [28], with permission from Elsevier, Copyright 2021.

2.4 Superhydrophobic Sio_2- Polymer Composite Based Membrane for Oil-Water Separation

Li and their co-workers [29] have fabricated the superhydrophobic surface by using PVDF and SiO2 via sugar template method. The schematic of preparation method is shown **Figure-7.** It was shown in a water contact angle of 155.68° and roll-on angle of nearly 6°. The prepared superhydrophobic PVDF oil/water separation membrane had low water adhesion performance and ultrahigh separation efficiency of nearly 99.98% in terms of the oil purity in the filtrate. The recycling performance over 20 cycles. This membrane has excellent potential for use in various large-scale practical applications, water purification treatment and the separation of commercially relevant emulsions. The possibility of large-scale production and low manufacturing costs of this sponge is very promising advantages for oil-water separation application.

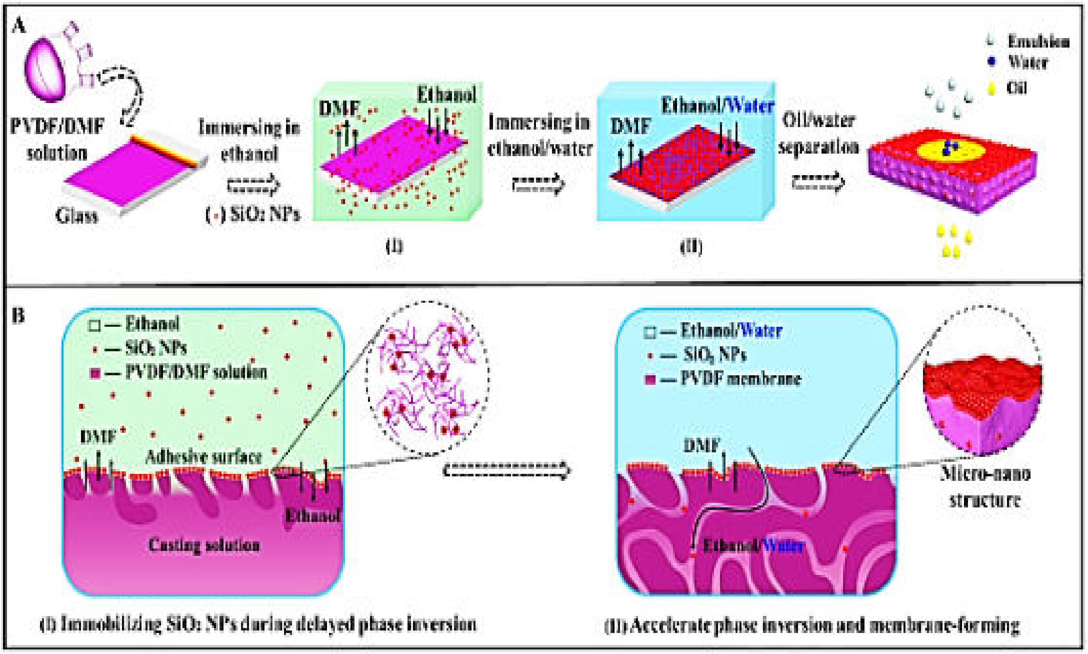

Figure-7. Schematic illustration (A) and structural evolution (B) for the formation of adhesive-free superhydrophobic SiO_2 nanoparticles decorated PVDF oil-water separation membranes [29]. Images reprinted from [29], with permission from Elsevier, Copyright 2018.

Bai et al. [30] have coated cotton fabric by sol-gel processed SiO_2 The as-prepared fabric was immersed in the solution of $FeCl_3$, thiophene and CH_2Cl_2 solution. Then, the modified fabric was washed with ethanol and dry it. **Figure-8** reveals the experimental procedure of preparation of superhydrophobic fabric. The modified fabric shows water contact angles above 160°. The strongest peak at 1050 cm^{-1} belongs to the Si-O bond indicating that SiO_2 particles have been coated on the cotton fabric. The modified cotton fabric shows outstanding resistance to ultraviolet irradiation, high temperature, low temperature, organic solvent, immersion and excellent durability even after 8 months. The as-prepared fabric was showing the capability in various chemical exposures. It was showing good anti-dirt and anti-frost properties. The modified superhydrophobic cotton fabric was used as filter membrane for the gravity driven oil-water separation with high separation efficiency and excellent reusability. By using, this modified cotton fabric, both immiscible and emulsified oil-water mixtures could be separated. The efficient oil-water separation was also achieved under harsh conditions. The superhydrophobic fabric shows potential for the fast, coat-effective treatment of oil spill accidents and industrial oily sewage.

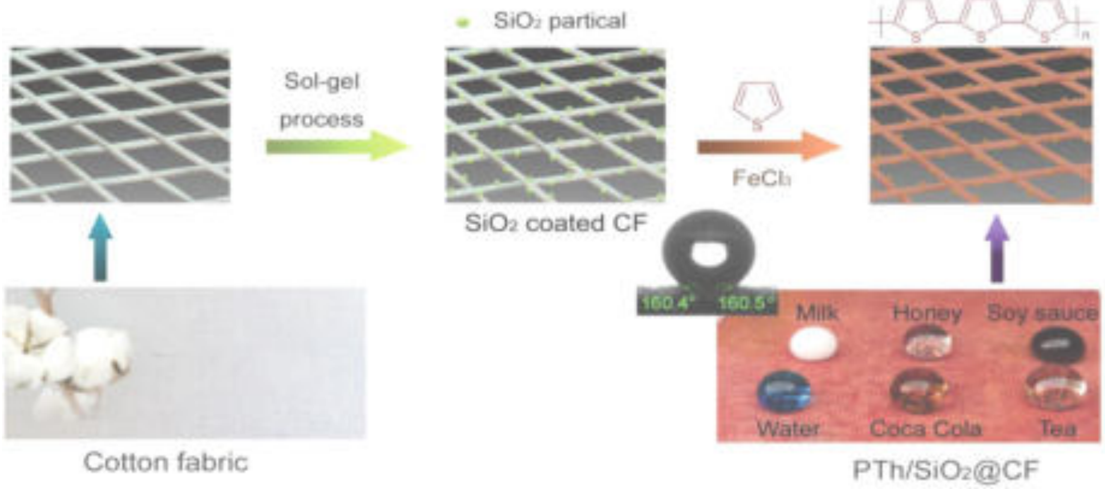

Figure-8. Schematic Illustration of the fabrication process of the PTh/SiO_2@CF [30]. Images reprinted from [30], with permission from Elsevier, Adv. Mater. Interfaces, Copyright 2021.

3. CONCLUSION

This review highlights, SiO_2 nanoparticles are unique, their fabrication requires little control of external parameters such as surface modification. It is very beneficial economically, facile and straightforward to synthesize. The SiO_2nanoparticles coated sponge/mesh has been developed by using SiO_2nanoparticles and different polymers. The absorption/separation investigation demonstrates that, the SiO_2surface is highly efficient and stable in absorbing a wide range of oil and organic solvents. It can be believed that, the SiO_2coated superhydrophobic materials are very useful for oil-water separation. It shows various tremendous results with SiO_2-polymer composite in various mechanical conditions. Hence this review is helpful to upcoming researchers to develop highly scalable superhydrophobic surfaces for efficient oil-water separation applications.

ACKNOWLEDGEMENT

This work was supported by Department of Chemistry and Department of Physics, Raje Ramrao Mahavidyalaya, Jath. We also acknowledge Prof. (Dr.) Suresh S. Patil, Principal, Raje Ramrao Mahavidyalaya, Jath.

REFERENCES

1. Alsbaiee A., Smith B. J., Xiao L., Ling Y., Helbling D. E. & Dichtel W. R. (2016) Nature, 529, 190-194.
2. Li Y., Zhang Z., Ge B., Men X., and Xue Q. (2016) Green Chemistry, 18, 5266-5272.
3. Ma Q., Cheng H., Fane A. G., Wang R., and Zhang H. (2016) Small, 12, 2186-2202.
4. Li L., Li B., Dong J., and Zhang J. (2016) Journal of Materials Chemistry A, 4, 13677–13725.
5. Yuan J., Liu X., Akbulut O., Hu J., Sui S. L., Kong J., Stellacci F. (2008) Nature, 3, 332-337.
6. Broje V., Keller A. A. (2006) Environmental Science & Technology, 40, 7914-7918.
7. Wu Z. Y., Li C., Liang H. W., Zhang Y. N., Wang X., Chen J. F. & Yu S. H. (2014) Science Reports, 4, 4079-4091.
8. Keshavarz A., Zilouei H., Abdol maleki A. (2015) Journal of Environmental Management, 157, 279-286.
9. Wang Z., Xu Y., Liu Y., Shao L. (2015) Journal of Materials Chemistry A, 3, 266-273.
10. Li J., Zhao Z., Kang R., Zhang Y., Lv W., Li M., Jia R., Luo L. (2017) Journal of Sol-Gel Science and Technology, 3, 817–826.
11. Keshavarz A., Zilouei H., Abdolmaleki A., Asadinezhad A. (2015) Journal of Environmental Management, 157, 279-286.
12. Sam E. K., Sam D. K., Lv X., Liu B., Xiao X., Gong S., Yu W., Chen J., Liu J. (2019) Chemical Engineering Journal, 19, 1103-1109.
13. Jin M., Feng X., Xi J., Zhai J., Cho K., Feng L., Jiang L. (2005) Macromolecular Rapid Communications, 26, 1805-1818.
14. Yao T., Zhang Y., Xiao Y., Zhao P., Guo L., Yang H., Li F. (2016) Journal of Molecular Liquids, 218, 611–614.
15. Gao Y., Zhou Y. S., Xiong W., Wang M., Fan L., Golgir H. R., Jiang L., Hou W., Huang X., Jiang L., Silvain J. F., Lu Y. F. (2014) ACS Applied Materials & Interfaces, 6, 5924–5929.
16. Erbil H. Y., Demirel A. L., Avcı Y., Mert O. (2003) Science, 299, 1377-1391.

17. Fard A. K., Mckay G., Manawi Y., Malaibari Z., Hussien M. A. (2016) Chemsphere, 164, 142-155.

18. Ren G., Song Y., Li X., Zhou Y., Zhang Z., Zhu X. (2018) Applied Surface Science, 428, 520-525.

19. Gu J., Xiao P., Chen J., Liu F., Huang Y., Li G., Zhang J., Chen T. (2014) Journal of Materials Chemistry A, 2, 15268–15272.

20. Li J., Kang R., Tang X., She H., Yang Y., Zha F. (2016) Nanoscale, 8, 7638–7645.

21. Gao Y., Zhou Y. S., Xiong W., Wang M., Fan L., Golgir H. R., Jiang L., Hou W., Huang X., Jiang L., Silvain J. F., Lu Y. F. (2014) ACS Applied Materials & Interfaces, 6, 5924–5929.

22. Li J., Zhao Z., Kang R., Zhang Y., Li M. (2017) Journal of Sol-Gel Science and Technology, 83, 817-826.

23. Zhang R., Zhou Z., Ge W., Lu Y., Liu T., Yang W., Dai J. (2020) Chinese Journal of Chemical Engineering, 5, 30292-30310.

24. Liu D., Yu Y., Chen X., Zheng Y. (2017) RSC Advances, 7, 12908–12915.

25. Zhao L., Du Z., Tai X., Ma Y. (2021) Colloids and Surfaces A: Physicochemical and Engineering Aspects, 623, 126404-126415.

26. Xiong W., Li L., Qiao F., Chen J., Chen Z., Zhou X., Hu K., Zhao X., Xie Y. (2021) Journal of Colloid and Interface Science, 6, 118–126.

27. Gu J., Xiao P., Chen J., Liu F., Huang Y., Li G., Zhang J., Chen T. (2014) Journal of Materials Chemistry A, 2, 15268–15272.

28. Wei C., Deu F., Lin L., An Z., He Y., Chen X., Chen L., Zhao Y. (2018) Journal of Membrane Science, 555, 220-228.

29. Li X., Wang X., Yuan Y., Wu M., Wu Q., Liu J., Yang J., Zhang J. (2021) European Polymer Journal, 159, 110729-110742.

30. Bai W., Lin H., Chen K., Zeng R., Lin Y., Xu Y. (2021) Advanced Materials Interfaces, 254, 725-740.

Green Synthesis of NiO Nanoparticles from *Parthenium hysterophorus* Plant

Sneha V. Koparde[a], Akanksha G. Kolekar[a], Shital S. Shendage[a], Aniket H. Sawat[a], Snehal D. Patil[a], Snehal S. Patil[a], Reshma B. Darekar[a], Amol B. Pandhare[a,c], Vijay S. Ghodake[a,d], Samadhan P. Pawar[b], Govind B. Kolekar[a,]*.

[a] Department of Chemistry, Shivaji University, Kolhapur 416 004 (MS) India.

[b]Department of Chemistry, Rajarshi Chhatrapati Shahu College, Kolhapur 416 005 (MS) India.

[c]Department of Chemistry, M.H. Shinde Mahavidyalaya, Tisangi, Gaganbavda, Kolhapur 416 206 (MS) India.
[d]Department of Chemistry, Yashwantrao Chavan Mahavidyalaya, Halkarni, Kolhapur 416 552 (MS) India.
*Corresponding author: gbk_chem@unishivaji.ac.in

ABSTRACT

Plant-mediated synthesis of nanomaterials has been increasingly gaining popularity due to its eco-friendly nature and cost-effectiveness. In the present study, we have synthesized NiO nanoparticles by a simple and cost-effective green synthesis method using "parthenium hysterophorus" leaf extract. The leaf extract of Parthenium hysterophorus acts as a reducing as well as a capping agent for the synthesis of nickel oxide (NiO) nanoparticles. This method allows the synthesis of nanoparticles, which was confirmed by UV-vis spectroscopy and X-ray diffraction (XRD) Characterization. The absorbance of NiO nanoparticle is seen at 313 nm while it has 11.5 nm crystallite size.

***KEYWORD*S**

Parthenium hysterophorus, Green synthesis, NiO nanoparticles.

……………………………………………………………………………………………

1. INTRODUCTION

Nanoparticles represent a particle with a nanometer size of 1-100 nanoscale materials has unique and superior physical and chemical properties compared to their bulk structure, due to an increase in the ratio of the surface area per volume of the material /particles. Nanostructure Science and technology is a broad and interdisciplinary area of research and development activity that has been growing explosively worldwide in the past few years. It has the potential for revolutionizing the ways in which materials and products are created and the range and nature of functionalities that can be accessed [1]. The most widely studied nanomaterials are metal nanoparticles because they are easier to synthesize [2]. For these reasons, many research groups have an increasing interest in the development and study of these materials.

Nickel oxide (NiO) is widely used in catalysis [3], optical fibers [4], magnetic materials [5], as a cathode material in the battery [6], gas sensors [7], fuel cells [8], and electrochromic films [9], etc. because of their high chemical stability, electrocatalysis, electron transfer capability, and super-capacitance properties. Many researchers are greatly motivated due to their quantum size effect, surface effect, macroscopic tunnel effect, and volume effect, and also have a low material cost.

NiO is used as a catalyst in organic transformation but in various organic solvents at elevated temperatures. To accomplish the manipulation of nanostructure nickel oxide a variety of strategies such as evaporation [10], thermal decomposition, sputtering, electro decomposition [11], and sole-gel [12] techniques have been employed. But the drawback of conventional methods is high cytotoxicity with low productivity and is not environment friendly. Therefore, we have selected a cost-effective, productive, eco-friendly biogenic method for nanoparticle synthesis.

Nickel oxide nanoparticles has been synthesized by using *Nephelium lappaceus L peel* extract [14], *Moringa laoleifera* extract [15], aqueous extract of *Tamarix serotine* [16], *Agathosma Betulina* natural extract [17], *hydrongea paniculata* [18] flower extract, *calotropis procera* leaf extract [19], using Arabic Gum, *aegle marmelos* leaf extract [20].

Parthenium hysterophorus is species of flowering plant in the aster family in the native American tropics. It is common invasive species in India, Australia, and part of Africa. The leaf extract gives Allelopathic chemicals, *P. hysterophorus* act as a reducing as well as a stabilizing agent in the synthesis of nanoparticles and commercial enzyme production and additive in biogas production.

2. MATERIALS AND METHOD

Nickel chloride ($NiCl_2$), and 90% Ethanol were purchased from Loba Chemicals Pvt. Ltd, Mumbai, (MAH), *Parthenium hysterophorus* leaves were collected from the university campus.

2.1 Instrumentation

The absorption spectrum was acquired at room temperature by using Specord 210 plus, Analytikjena UV-Vis spectrophotometer with the use of 1 cm quartz cuvette. High speed centrifugation model REMI R-24 was applied for centrifugation operation. The phase and purity of the synthesized NiO NPs was confirmed by using XRD analysis (Bruker D8 Advance) using CuKα radiations.

2.2 Preparation of Leaf Extract

Leaves of *Partheninum hysterophoruos* were collected, washed 2 times with distilled water, and dried naturally. The dried leaves were ground gently in mortar pestle to form a fine powder of leaves. This powder reflux with 90% ethanol in a 250 mL round bottom flask with the help of an electric heating mantle for 20 min. then the leaf extract was filtered through Whatman filter paper No. 41. The filtrated leaf extract was then centrifuged in order to remove unwanted biomaterials from the leaf extract. This leaf extract is used for further experiments **(Figure- 1.).**

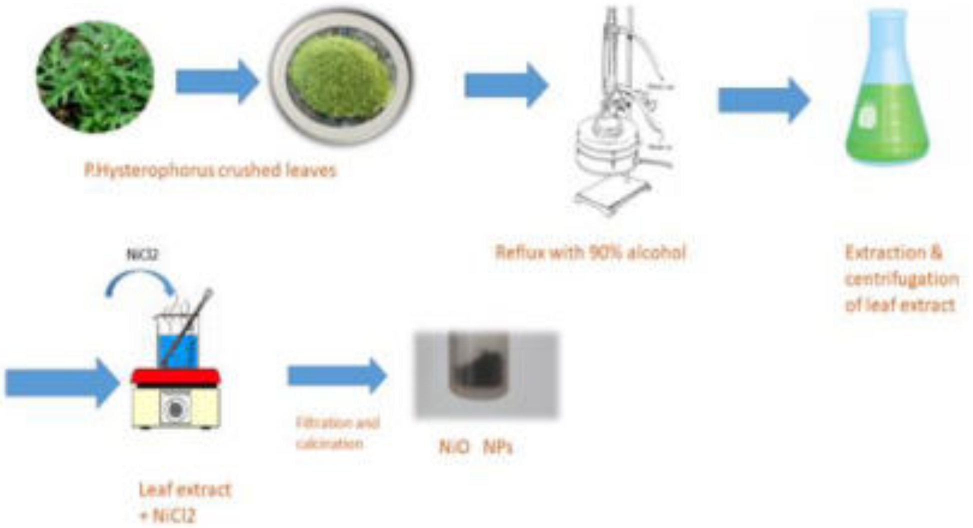

Figure- 1. Schematic of Green Synthesis of NiO Nanoparticles from *P. Hysterophorus* Leaves.

2.3 Preparation of Nickel Oxide Nanoparticles

The NiO nanoparticles were synthesized by using analytical reagent grades such as $NiCl_2$ (99%). About 100 mL of leaf extract was heated in a 250 mL beaker by using an oil bath up to 80 °C consequently $NiCl_2$ (4.0 g) was added to the heated leaf extract and stirred constantly with help of a magnetic stirrer the solution was further heated up to its complete dryness. The dried powder is washed with 500 mL distilled water and calcined to 400 °C for 6 hr. to lead to the formation of NiO nanoparticles **(Figure- 1.).**

3. RESULT AND DISCUSSION

As synthesized NiO NPs were characterized and confirmed through different analytical techniques**.**

3.1 Uv Visible Spectroscopy Technique

The optical absorption of NiO was studied by UV-visible spectrometer. The optical absorption of NiO NPs was described within the wavelength range of 300-400 nm. The absorption edge was seen at 313 nm for NiO NPs. [21] **(Figure- 2.).**

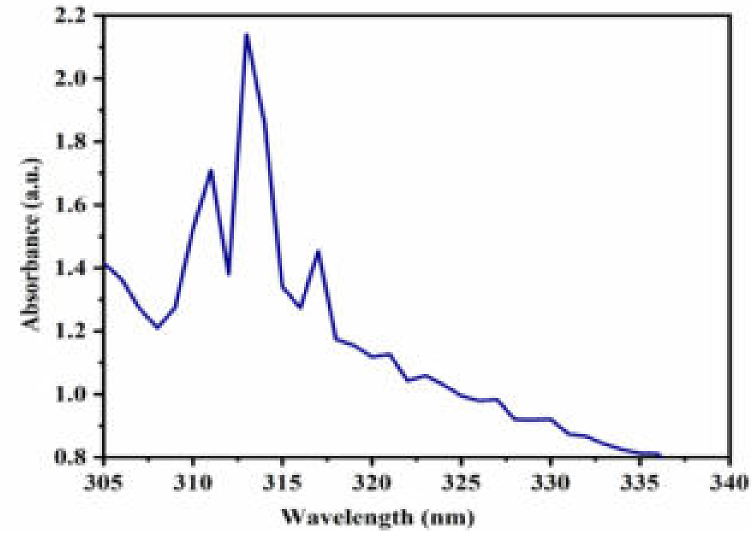

Figure- 2. UV-vis spectra of NiO NPs.

3.2 X-Ray Diffraction Technique

The crystal structure of NiO NPs was studied via X-ray diffraction (XRD) technique having Cu Kα radiation (λ- 1.54 Å) in the range (2Ɵ- 10 to 80^o). The X-ray diffraction data **(Table- 1.)** have been recorded for the powder sample of NiO NPs shown in **Figure- 3.** The data shows distinct peaks at 2Ɵ of 37.08, 43.15, 62.70, 75.24, and 79.13. These peaks were identified as peaks of cubic NiO crystallites with various diffraction planes (111), (200), (220), (311), and (222).

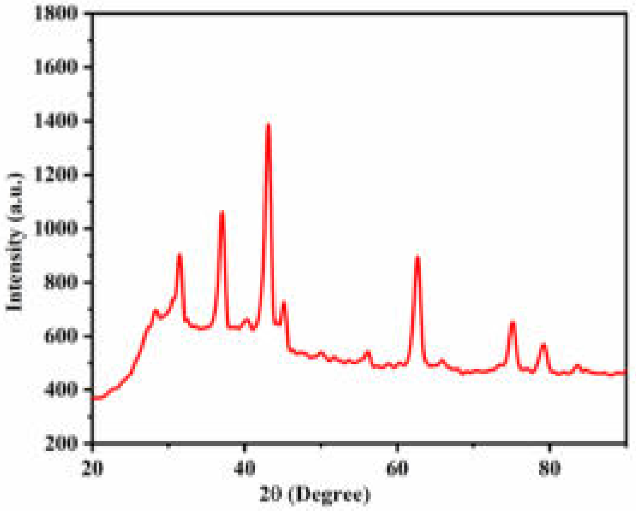

Figure- 3. XRD spectra of NiO NPs.

The XRD pattern revealed the formation of the cubic phase of NiO with lattice constant *a* = 4.1771 Å. The other peak observed at (2ϴ) of 31.500 which have identified as Ni_2O_3 corresponds to the [002] crystal plane.

Table -1. 2ϴ Values, hkl Planes, Observed 'd' Values, The Standard 'd' Values of NiO Nano Particles.

Sr. No.	**2ϴ (Degree) Observed**	**2ϴ (degree) Standard**	**hkl planes**	**Observed 'd' values**	**Standard 'd' values**
1	37.08	37.06	111	2.4221	2.4110
2	43.15	43.095	200	2.1335	2.0880
3	62.70	62.62	220	1.4801	1.4764
4	75.24	75.09	311	1.2614	1.2591
5	79.13	79.185	222	1.2089	1.2055

A peak observed at 2ϴ of 45.23 has been identified for Ni [111] phase. 'd' value calculated by the formula (**Equation -1**).

$$n \lambda = 2d \sin \Theta \qquad -(1)$$

where 'λ' is the wavelength, 'n' is integral, 'ϴ' is the angle of diffraction.

Further, the average crystallite size was calculated using a well-known Debye-Scherrer's formula (**Equation- 2**).

$$D = \frac{0.9\lambda}{\beta \cos \theta} \qquad -(2)$$

where, λ is the wavelength of X-rays (1.5406 Å), β the full width at half maximum (in radian) of the peak, D is the diameter of the crystallite, and ϴ is Bragg's angle of the XRD peak. Further, the average crystallite size estimated using Scherrer's formula is approximately 11.5 nm [13].

4. CONCLUSION

The cost-effective, sustainable green synthesis of NiO nanoparticles has been investigated using *parthenium hysterophorus* leaf extract, which act as a capping and reducing agent. Here, green leaf extract helps with the reduction of nickel material at the nanoscale. The XRD features have revealed the formation of the cubic phase of

NiO nanoparticles with a crystallite size of 11.5 nm. The NiO nanoparticles show maximum absorbance at 313 nm wavelength.

ACKNOWLEDGEMENT

The author Ms. Sneha V. Koparde is thankful to the Mahatma Jyotiba Phule Research Fellowship (MJPRF-22) (MAHAJYOTI/2022/Ph.D. Fellow/1002 (909) for financial support.

REFERENCE

1. He X., Deng H., Hwang H. (2019) Journal of Food and Drug Analysis, 27, 1–21.
2. Rane A. V., Kanny K., Abitha V. K., Thomas S.,Thomas S. (2018) Elsevier Ltd,. 12, 362–378.
3. Liu J. (2020) Green Chemistry, 22, 7387–7397.
4. Wang P., Zhang X., Wei Y., Yang P. (2019) Internatonal Journal of Hydrogen Energy, 44, 19792–19804.
5. Chatterjee S., Maiti R., Chakravorty D. (2020) RSC Advance, 10, 13708–13716.
6. Pu J. (2022) Electrochimica Acta, 435, 141396.
7. Li P. (2021) Sensors Actuators B:Chemical, 339, 129886.
8. Fuku X., Modibedi M., Matinise N., Mokoena P., Xaba N., Mathe M. (2019) Journal of Colloid and Interface Science, 545, 138–152.
9. Jung H . K. (2019) Electrochimica Acta, 330, 135203.
10. Al-Sehemi A. G., Al-Shihri A. S., Kalam A., Dud G., Ahmad T. (2014) Journal of Molecular Structure, 1058, 56–61.
11. Sahila S., Prabhu N., Simiyon G . G., Jayakumar L. S. (2022) Chemical Data Collections, 38, 100837.
12. Ghazal S. (2020) Jornal of Molecular Structure, 1217, 128378.
13. Wardani M., Yulizar Y., Abdullah I., Bagus Apriandanu D. O. (2019) IOP Conference Series: Materrials Science and Engineering, 509.
14. Adinaveen T., Karnan T., Samuel Selvakuma S. A. (2019) Heliyon, 5, 01751.
15. EzhilarasA . A., Vijaya J. J., Kaviyarasu K., Maaza M., Ayeshamariam A ., Kennedy L. J. (2016) Journal of Photochemistry and Photobiology B: Biology,164, 352–360.

16. Nasseri M. A., Ahrari F., Zakerinasab B. (2016) Appllide Organometalic Chemistry, 30, 978–984.
17. Karthik K., Shashank M., Revathi V.,Tatarchuk T. (2018) Molecular Crystal and Liquide Crystal, 673, 70–80.
18. Kundu M., Karunakaran G., Kuznetsov D. (2017) Powder Technology, 311,. 132–136.
19. Shinde B., Kamble S. B., Jadhav H. S., Karale B. K., Kanade K. G.,Burungale A. S. (2018) ChemistrySelect, 3, 13140–13153.
20. Ezhilarasi A. A., Vijaya J. J., Kaviyarasu K., Kennedy L. J., Ramalingam R. J., Al-Lohedan H. A. (2017) Journal of Photochemistry and Photobiology B: Biology, 180, 39–50.
21. Sabouri Z., Akbari A., Darroudi M. (2020) Polyhedron, 178, 114351.

Microwave-Assisted Synthesis of Pyrazole and Its Hybrid Scaffolds as Potent Biological And Pharmacological Agents: A Short Review

Pravin. R. Kharade[a, b], Uttam. B. Chougale[a, b], Satish. S. Kadam[c], Kiran. N. Patil[d], Prakash S. Pawar[e,f,] Savita. S. Desai[b]
[a]Department of Chemistry, Karmaveer Hire Arts, Science, Commerce, and Education College, Gargoti 416 209 (MS) India.
[b]Research Laboratory in Heterocyclic Synthesis, Devchand College, Arjunnagar 591 237 (MS) India.
[c]Department of Chemistry, Vivekanand College, Kolhapur 416 106 (MS) India.
[d]Department of Chemistry, Dr. Ghali College, Gadhinglaj 416 502 (MS) India.
[e]Nanoscience Research Laboratory, Department of Chemistry, Shivaji University, Kolhapur,416 004 (MS), India.

[f]Department of Chemistry, Shri Yashwantaro Patil Science College, Solankur
Tal-Radhanagari Dist-Kolhapur, 416 212 (MS), India.

*Corresponding author: pravinkharade03@gmail.com

ABSTRACT
Pyrazole and its derivatives, due to their diverse biological activities, have gained tremendous attention from researchers in synthetic as well as application perspectives. Due to such promising activities, the study of pyrazole-containing compounds has the utmost importance in the heterocyclic field. Many methods and procedures have been developed and used for the synthesis of pyrazole derivatives during the last two decades. The traditional methodologies used for the synthesis of pyrazole compounds were found to possess certain disadvantages like prolonged reaction time, use of organic/toxic solvents, high-temperature reaction, lesser yield of products, purity of compounds, etc. To overcome these difficulties, researchers have been using an eco-safe way i.e., use of microwaves for the synthesis of pyrazole compounds. The synthesis of pyrazole has been made very easy and simple by using the microwave-assisted protocol. The present review provides information about microwave-assisted synthetic procedures of bioactive pyrazole compounds. Researchers may utilize this information for their future endeavours.

KEYWORDS
Pyrazole, Microwave, Antimicrobial, Eco-friendly synthesis, etc.

……

1. INTRODUCTION

Among the five-membered heterocycles, pyrazoles are the most studied class of moieties from azole family. Pyrazole based compounds possess promising and diversified applications in the medical, agriculture and technology fields [1-2] as well as they are used as brightening agents [3]. The presence of this nucleus in pharmaceutical agents like potent anti-inflammatory drug, celecoxib, antipsychotic drug, CDPPB, an analgesic, betazole, anti-depressant, fezolamine have described the wide pharmacological potential of the pyrazole compounds [4]. Further, these compounds were found to exhibit anticancer [5-15], antidepressant [16-17], anticonvulsant [18-19], anti-inflammatory [20], anti-tubercular [21], antiviral [22], antipyretic [23], antimicrobial [24-26], antioxidant [27], antifungal [28-30], as well as pyrazole derivatives, serve as sodium channel blockers [31], potent neuraminidase inhibitors [32], etc. In spite of these, they show other wide biological properties [33-36].

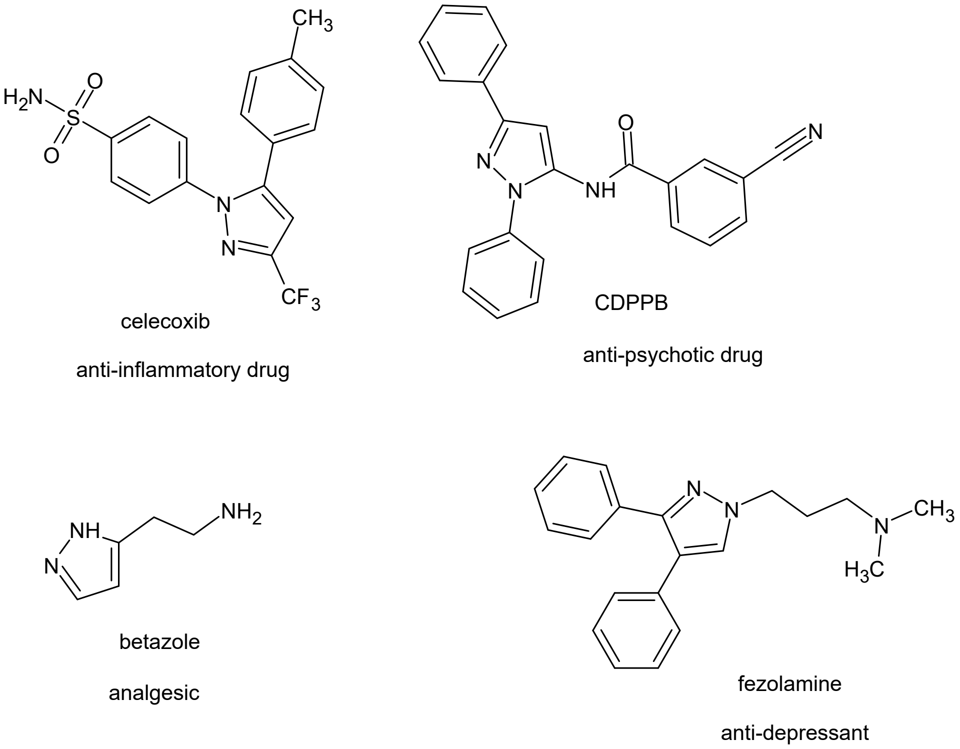

Figure-1. Some representative pyrazole compounds as drugs.

Researchers are focusing on design and development of greener and eco-friendly methodologies to carry of heterocyclic synthesis in an efficient and easy manner. The best tool that can be utilized for this purpose is the use of microwaves in synthetic method. It is now considered an emerging technology in the field of organic synthesis. Microwave synthesis represents a major breakthrough in synthetic chemistry methodology, a dramatic change in the way chemical synthesis is performed and in the way it is perceived in the scientific community. Microwave provides a powerful way to do synthetic chemistry in green approach. Nowadays, drug discovery and development in the pharmaceutical and academic areas carried out through new enabling technology like microwave irradiation. Microwave provides a powerful way to do synthetic chemistry in green approach [37]. The advantages to carry microwave assisted organic transformations are the higher yield of product with excellent purity, minimization of time and prominent acceleration of reaction rate [38-39]. Due to microwave synthesis technique, expansion of scientific creativity in organic chemistry takes place. By using this technique organic reaction carried out in minutes or in seconds, instead of spending hours or even days by convention way [40]. Microwave synthesis effectively carried out to any reaction scheme which occurs rapidly with improving yields and producing cleaner chemistries [41-44]. So, the use of microwaves could be very useful technique for the synthesis of biologically active pyrazole derivatives.

2. Synthesis of pyrazole and its hybrid compounds-

Sumit Sood et. al. [45] **(2020)** have synthesized pyrazole-4-carbonitriles and 1-(thiazol-2-yl)-1H-pyrazole-4-carbonitriles. In first step, they prepared the OPC-VH reagent **(Scheme 1)** by the reaction of DMF with o-phthaloyl dichloride in 2-chlorotoluene as solvent. Then, the condensation of pyrazole-4-carbaldehydes with hydroxylamine hydrochloride generated corresponding oxime derivative in situ which was on subsequent treatment with OPC-VH reagent in DMF afforded the pyrazole-4-carbonitrile derivatives **(Scheme 2)**. Further, this procedure has been successfully employed in the synthesis of 1-(thiazol-2-yl)-1H-pyrazole-4-carbonitriles **(Scheme 3)**. The prepared derivatives were screened against Gram-positive Bacteria *Bacillus cereus* and *Staphylococcus aureus*; Gram negative bacteria *Escherichia coli* and *Yersinia enterocolitica* and antifungal activity checked using *Candida albicans*. These derivatives showed moderate to good antibacterial and antifungal activities.

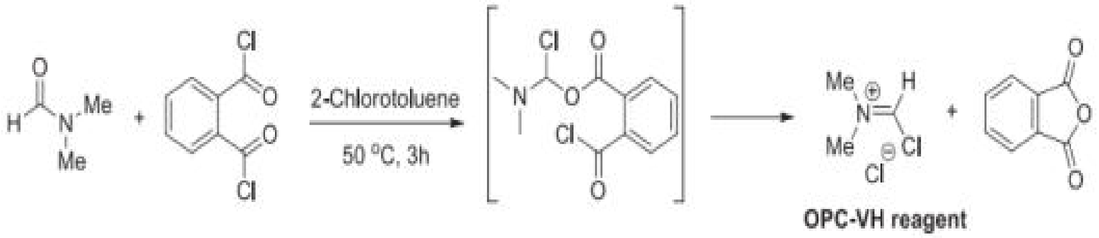

Scheme 1

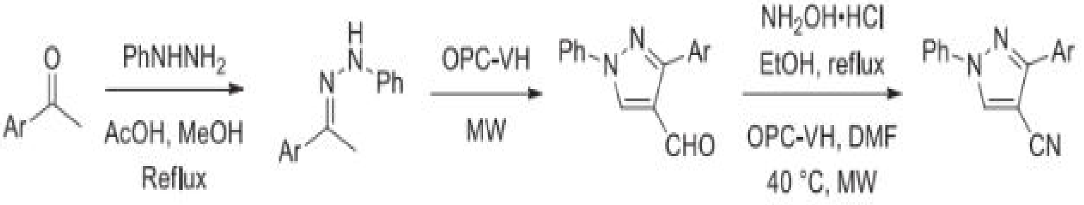

Scheme 2

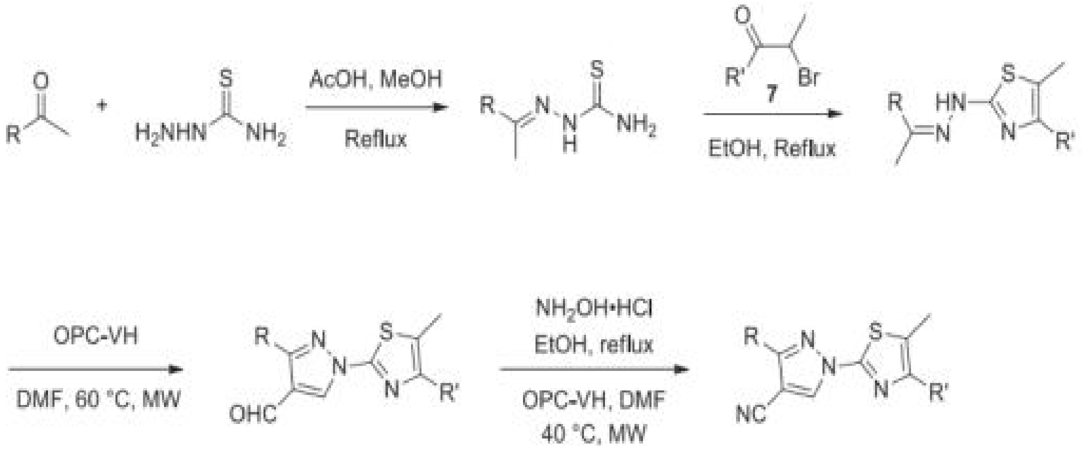

Scheme 3

Sarkate et. al. [46] **(2020)** reported the synthesis of new Substituted-3-Methyl-1-Substituted Phenyl-1H-Pyrazole. In this method, substituted 1-phenylbutane-1,3-dione (1 mmol), phenylhydrazine (1 mmol), ZnO (10 mmol) with solvent was added and this mixture subjected to MW irradiation (800 W), for 2–4 min to give the products **(Scheme 4**). The yield of products found in the range of 96-98%. The mild reaction conditions, stirring at reflux temperature, good to excellent yields, easy workup, and easily available substrates are some advantages of this method over conventional protocol.

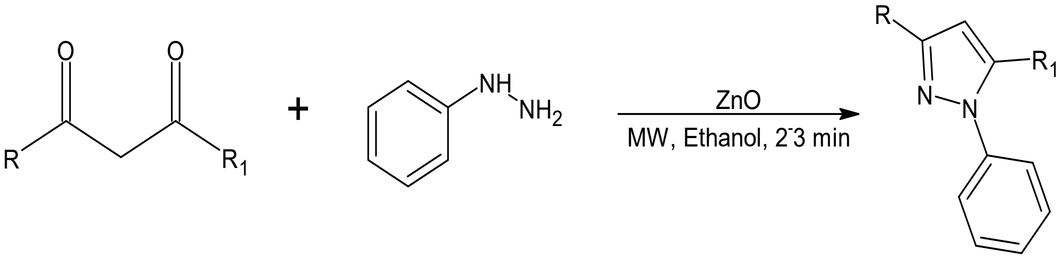

Scheme 4

Jasril et. al. [47] **(2019)** reported the synthesis of four pyrazoline derivatives viz. 3-(4-methoxyphenyl)-5-naphthalene-1-yl-1-phenyl-4,5-dihydro-pyrazole, 3-(4-methoxyphenyl) -5-naphthalene-1-yl-4,5-dihydro-1H-pyrazole, 3-(2-methoxyphenyl)-5-naphthalene-1-yl-1-phenyl-4,5-dihydro pyrazole and 3-(2-methoxyphenyl)-5-naphthalene-1-yl-4,5-dihydro-1H-pyrazole were obtained via intermolecular cyclization of substituted chalcones and hydrazine derivatives. The mixture was irradiated under MW radiations for 2-4 minutes at 180 W power to give target pyrazolines **(Scheme 5)**. The synthesized compounds were screened for toxicity and antioxidant activity. The two chalcone compounds was found to be more toxic with LC_{50} 0.97 and 11.47 µg/mL, respectively. Further, the compound 3-(2-methoxyphenyl)-5-naphthalene-1-yl-4,5-dihydro-1H-pyrazole possessed high antioxidant activity with IC_{50} of 4.47 µg/mL.

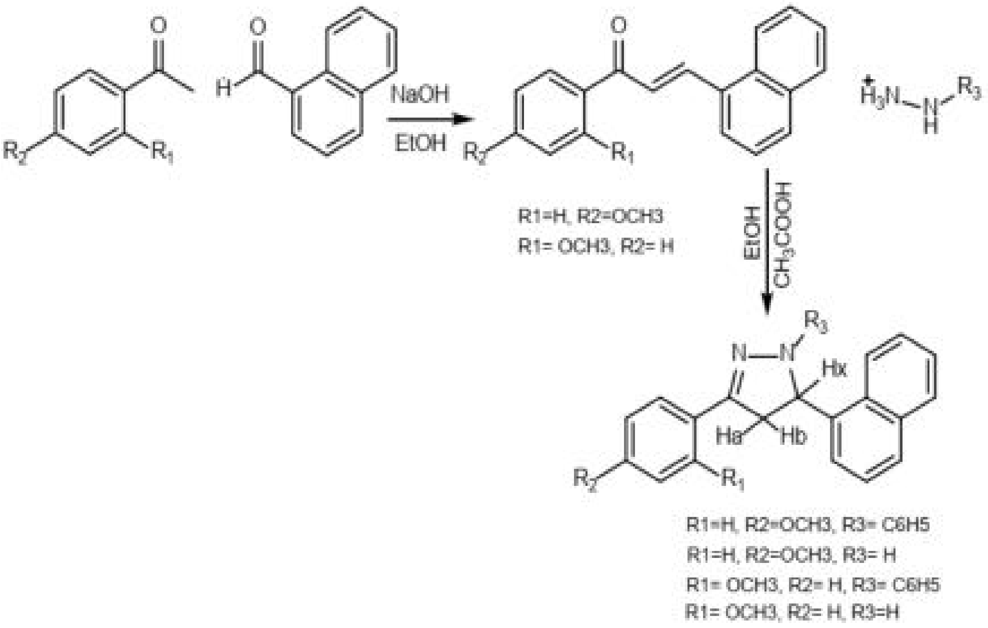

Scheme 5

Ch. Subramanyam et. al. [48] **(2018)** treated a mixture of chalcone (0.01 mole) with phenyl hydrazine hydrochloride (0.01 mole) under the influence of microwave irradiation in microwave oven at the power of 490 W for 2-3 minutes to give 4-[(1,5-diphenyl-4,5-dihydro-1H-pyrazol-3-yl)amino]phenol derivatives **(Scheme 6)**. The prepared pyrazole compounds were subjected to in vitro anti-inflammatory screening by using Albumin denaturation method and Membrane test method. Among the all compounds, 4-{[5-phenyl-1-(pyridin-4-yl)-4,5-dihydro-1H-pyrazol-3-yl]amino}phenol, 4-{[1-(4-fluorophenyl)-5-phenyl-4,5-dihydro-1H-pyrazol-3-

yl]amino}phenol and 4-{[1-(4-nitrophenyl)-5-phenyl-4,5-dihydro-1H-pyrazol-3-yl]amino}phenol have shown potent anti-inflammatory activity.

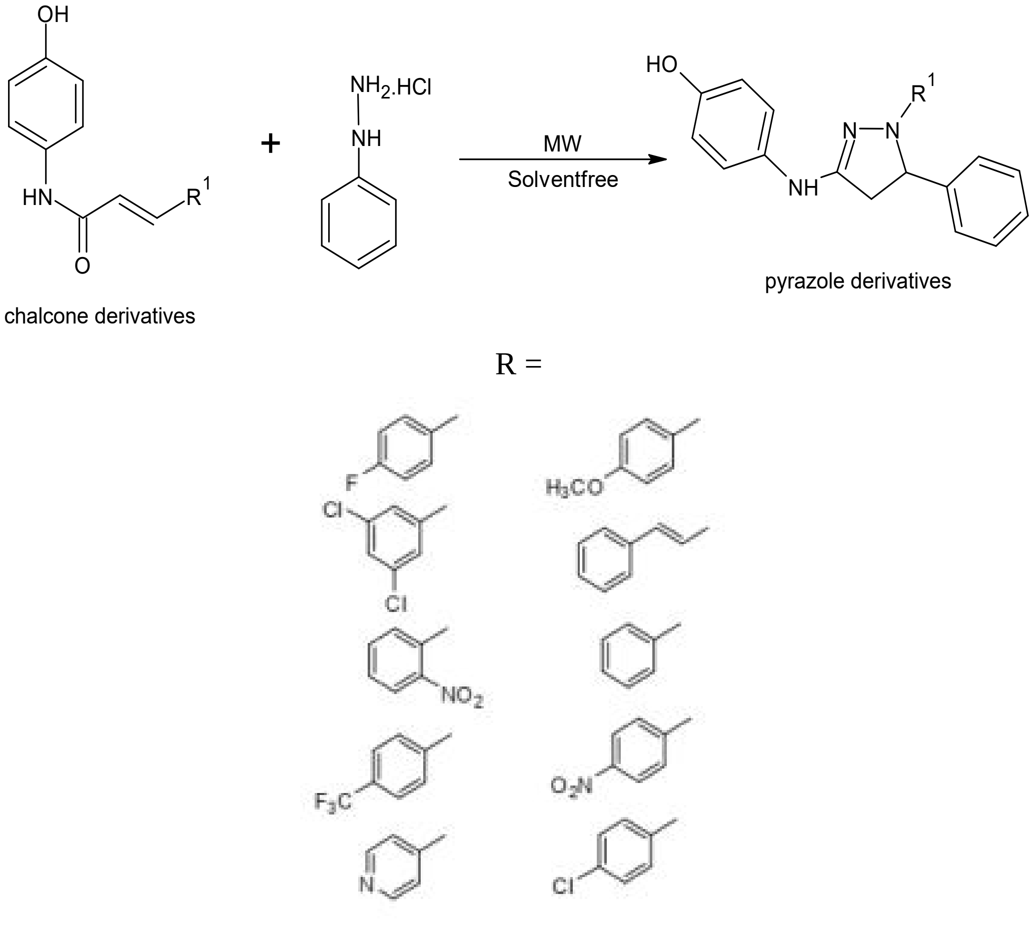

Scheme 6

Shailendra Jain [49] **(2018)** have reported the microwave-assisted synthesis of benzimidazolyl pyrazole derivatives. Different benzimidazolyl chalcone dibromides treated with hydrazine hydrate under microwave irradiation at 300-Watt power for 3-5 minutes **(Scheme 7).** The synthesized compounds were tested for antifungal activity against *C. albicans and A. niger* and for antibacterial activity against *E. coli, P. aerginusa, B. subtilis* and *K. pneumonia* in vitro at a concentration of 300mg/ml. Amongst the all derivatives, the compound 2-(4-bromo-5-phenyl-4,5-dihydro-1H-pyrazol-3-yl)-1H-indole has shown highest antifungal activity against *C. albicans and A. niger*. Then, compounds 2-[4-bromo-5-(4-chlorophenyl)-4,5-dihydro-1H-pyrazol-3-yl]-1H-indole and 2-{4-bromo-5-[4-(furan-2-yl)phenyl]-4,5-dihydro-1H-pyrazol-3-yl}-1H-indole have shown highest antibacterial activity against *E. coli, K.*

pneumonia and *P. aeruginosa*. Diflucan and coffrioxane were used as standard drugs for the comparison of antifungal and antibacterial activities respectively.

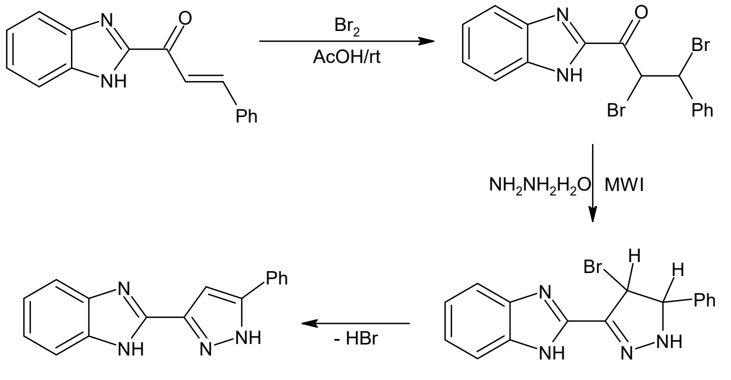

Ph = Phenyl,4-methoxyphenyl, 3,4-dimethoxyphenyl, 3,4,5-trimethoxyphenyl, 4-chlorophenyl, 4-furanyl

Scheme 7

S. M. Gomha et. al. [50] **(2017)** reported thiophene incorporated pyrazole derivatives under microwave irradiation. The reaction of (2E)-1-(thiophen-2-yl)-3-(thiophen-3-yl)prop-2-en-1-one with hydrazine derivatives in presence of catalytic amount of acetic acid in microwave oven was carried out at the power of 500 W (120 ^{0}C) for 5-10 minutes to generate corresponding pyrazoline derivatives **(Scheme 8)**. Antimicrobial activity of prepared compounds was done using agar disc diffusion method. Some of the derivatives have shown promising results for their antimicrobial activity.

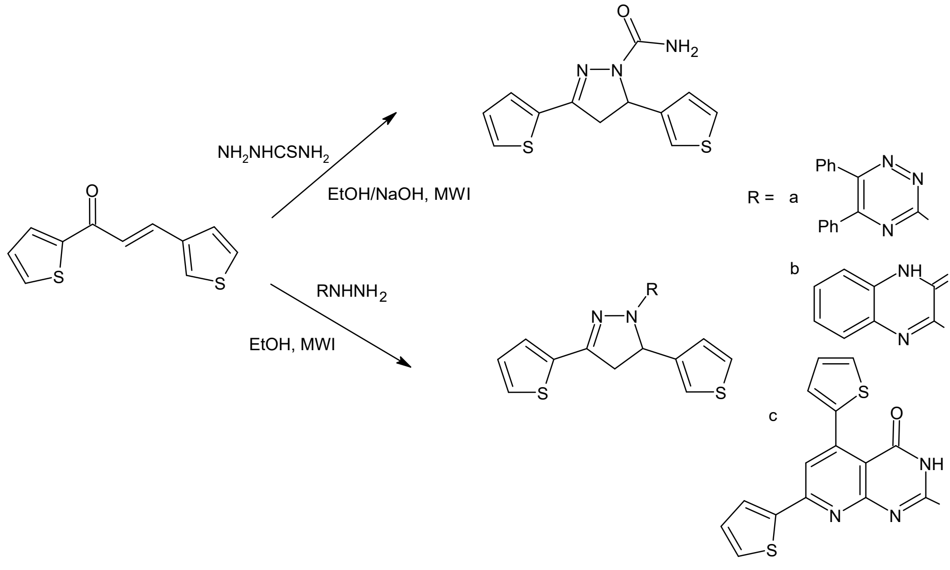

Scheme 8

Dhivare et. al. [51] **(2016)** synthesized bis-pyrazole derivatives using microwave irradiation having antibacterial and antifungal activity. In this method, different bis-chalcones with N-phenyl glutamide moiety were prepared which on further treatment with hydrazine hydrate under microwave irradiation of the power of 640 W generated bis-pyrazole compounds within 3-6 minutes **(Scheme 9)**. The compound (3Z,4Z)-3,4-bis-(4-hydroxy-3-methoxybenzylidene)-7-(4-chlorophenyl)-3,3a,3b,4,5,7-hexahydro-2H- piperidine-[2,3-c,5,4-c] dipyrazole, (3Z,4Z)-3,4-bis-(4-hydroxy-3-methoxybenzylidene)-7-(3-chloro-4-fluorophenyl)-3,3a,3b,4,5,7-hexahydro-2H- piperidine-[2,3-c,5,4-c] dipyrazole and (3Z,4Z)-3,4-bis-(4-hydroxy-3-methoxybenzylidene)-7-(2,4,5-trichlorophenyl)-3,3a,3b,4,5,7-hexahydro-2H-piperidine-[2,3-c,5,4-c] dipyrazole were found to be active as antifungal agents.

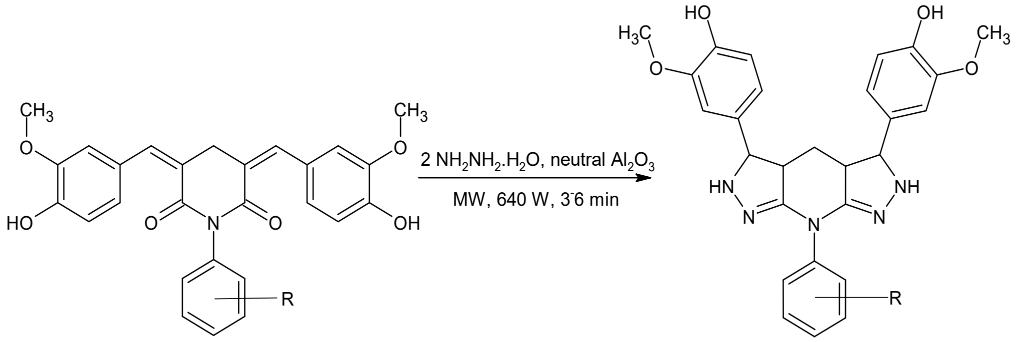

R = H, -4Br, -4Cl, $-4CH_3$, $-4OCH_3$, -4F, $-4NO_2$, -phenyl, -3Cl4F, -2,4,5Cl

Scheme 9

Novel pyrazole-4-carbaldehyde derivatives were synthesised using microwave irradiation method by Selvam et. al. [52] **(2014)** The synthesized compounds were confirmed by spectral methods and subjected to screen analgesic and anti-inflammatory activities. 1-(4-fluorophenyl)-3-phenyl-1H-pyrazole-4-carbaldehyde, 1-(4-chlorophenyl)-3-phenyl-1H-pyrazole-4-carbaldehyde and 1-(4-chlorophenyl)-3-phenyl-1H-pyrazole-4-carbaldehyde showed good analgesic and anti-inflammatory activities **(Scheme 10)**.

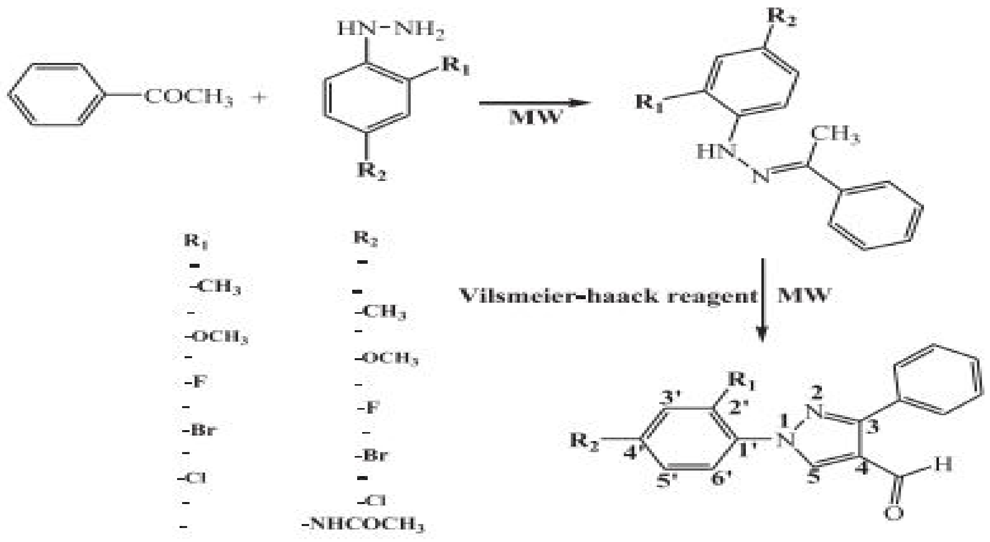

Scheme 10

Kalirajan, et al. [53] **(2013)** synthesized novel pyrazole substituted 9-anilino acridine derivatives by reacting a solution of 0.0025 mol of the corresponding chalcones in 20 ml of absolute ethanol and 0.2503 g (0.005 mol) of hydrazine hydrate (99%) under microwave irradiation. The reaction was carried out at the power of 140 W (20% power) for about 15 to 20 minutes **(Scheme 11).** The synthesized derivatives when tested for anti-microbial activity, 5-phenyl and 5-(4-OH)-phenyl derivatives showed highest activity.

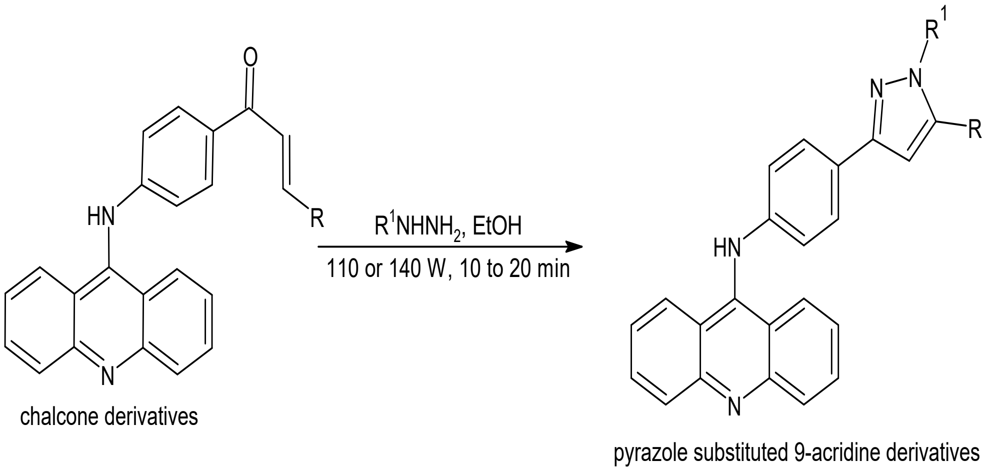

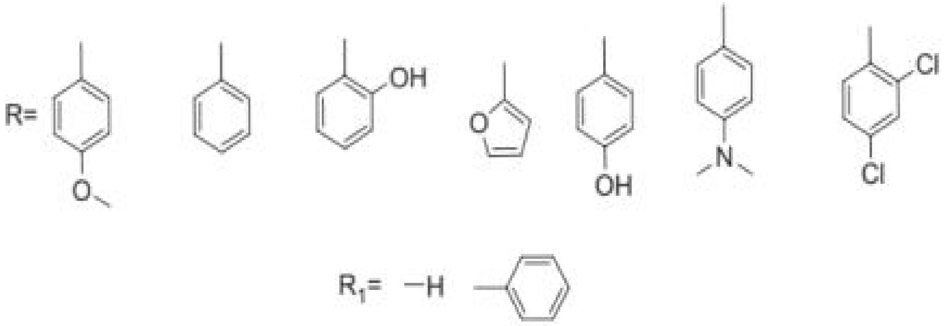

Scheme 11

Harendra K. Sharma and Manoj Sharma [54] **(2012)** subjected a mixture of 6-chloropriazine-2-carboxylic acid hydrazide (0.001 mole), benzoyl nitriles (0.001 mole), catalytic amount of glacial acetic acid (≈5-6 drops) and dry methanol (2 mL) to microwave irradiation for 10-15 minutes to give (5-amino-3-arylpyrazol-1-yl)(6-chloropyrazin-2-yl)-methanones **(Scheme 12)**. The condensation of 6-chloropriazine-2-carboxylic acid hydrazide with benzoyl nitriles generate hydrazone intermediate which undergo intramolecular attack of nitrogen atom on cyano group to produce target compounds. All the compounds were confirmed with the help of spectral analysis. The yield of synthesized derivatives found to be good.

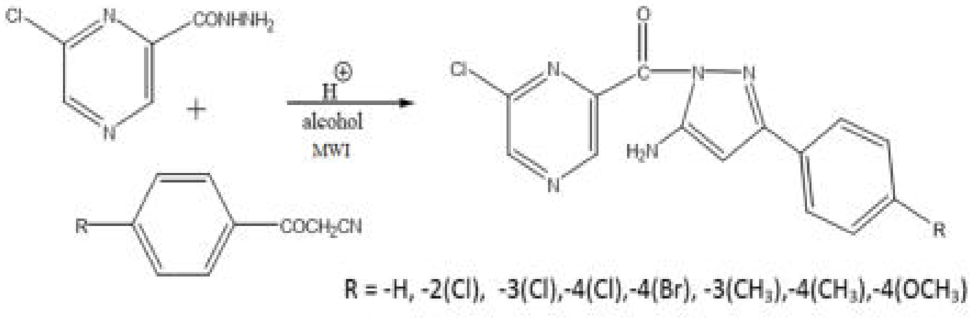

Scheme 12

Sahu Sudeep et. al. [55] **(2011)** have reported the synthesis of fluro-pyrazoles containing 5-[(Z)-benzylideneamino]-2-fluoro-N-phenylaniline moiety. The different chalcones (0.01 mol) were reacted with phenyl hydrazine (0.01 mol) in a beaker containing ethanol and few drops of glacial acetic acid under microwave irradiation to give pyrazole derivatives **(Scheme 14)**. The synthesized compounds were screened for anti-inflammatory activity using formali induce rat paw edema model. The derivatives have shown moderate to good anti-inflammatory activity after comparison with standard drug diclofenac sodium.

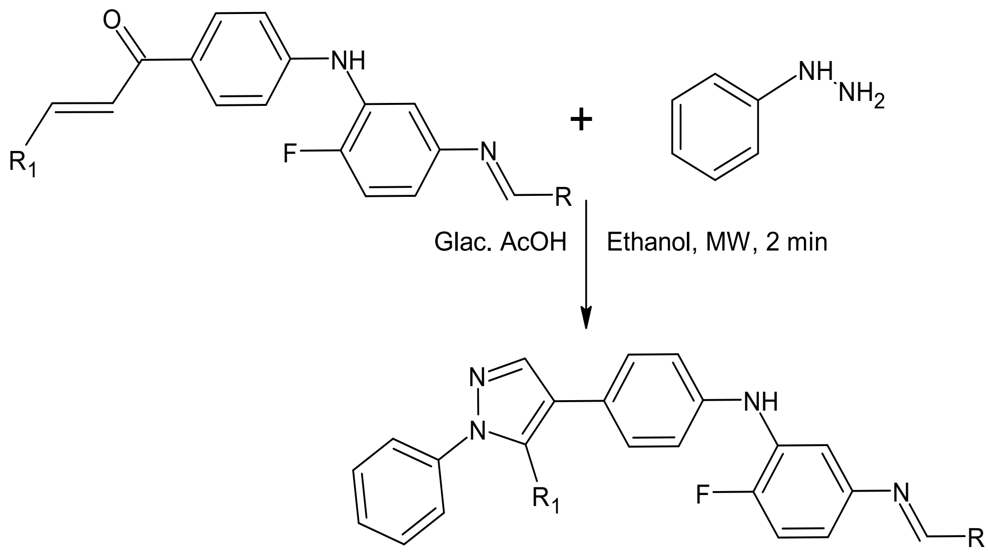

Scheme 14

Biradar and Mugali [56] **(2008)** have synthesized different thiadaizinyl-pyrazole compounds containing indole moiety from microwaves induced reaction of ethyl 2-hydrazinyl-5-oxo-5,6-dihydro-4H-1,3,4-thiadiazine-6-carboxylate with chalcones of substituted acetophenone and substituted indole-3-carboxaldehydes in presence of AcOH in ethanol as solvent **(Scheme 15)**.

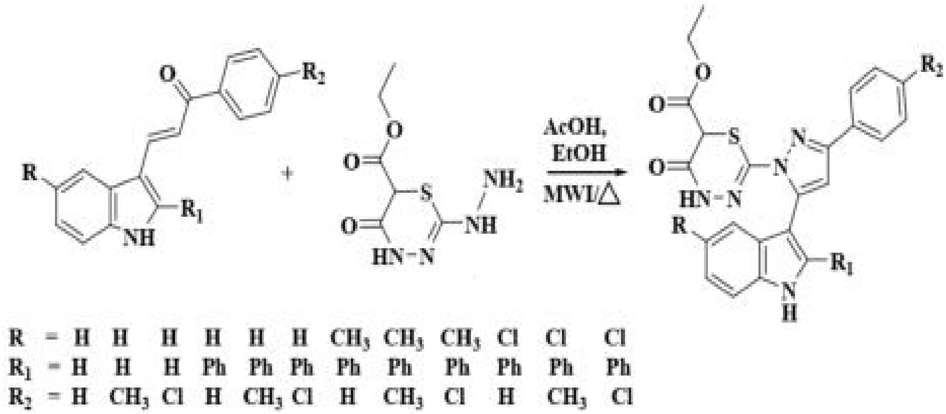

R =	H	H	H	H	H	H	CH_3	CH_3	CH_3	Cl	Cl	Cl
R_1 =	H	H	H	Ph	Ph	Ph	Ph	Ph	Ph	Ph	Ph	Ph
R_2 =	H	CH_3	Cl	H	CH_3	Cl	H	CH_3	Cl	H	CH_3	Cl

Scheme 15

Sauzem et. al. [57] **(2008)** reported the microwave-assisted synthesis of novel 3- or 4-substituted 5-trifluoromethyl-5-hydroxy-4,5-dihydro-1H-1-carboxyamidepyrazoles by rapid one-pot cyclocondensation of 4-alkoxy-1,1,1-trifluoromethyl-3-alken-2-ones with semicarbazide hydrochloride **(Scheme 16)**. The synthesized compounds were confirmed by spectral analyses and X-ray crystal structure studies. The synthetic pathway designed in the exploration of the bioisosteric replacement of benzene present in salicylamide with a 5-trifluoromethyl-4,5-dihydro-1H-pyrazole scaffold. The prepared derivatives could be used as promising moieties for future development of novel analgesic and anti-inflammatory drugs. Higher yields, shorter reaction time and operationally simple method are some key advantages of the reported work.

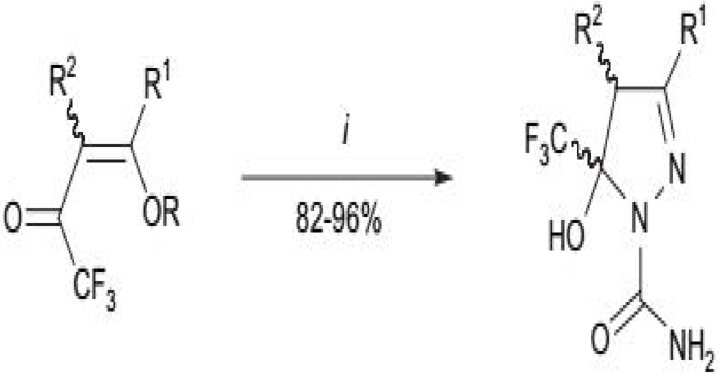

R	R1	R2	Yield (%)
Et	H	H	90
Me	Me	H	96
Me	Et	H	91
Me	Pr	H	87
Me	*i*-Pr	H	90

R	R1	R2	Yield (%)
Me	Bu	H	89
Me	*t*-Bu	H	82
Me	Ph	H	85
Me	4-Br-Ph	H	91
Et	H	Me	94

Reagents and conditions:

(i) $NH_2NHCONH_2.HCl$, $MeOH/H_2O$, Py, MW, 100 W, 70 ^{0}C, 2.2 bar, 4 min

Scheme 16

Table: Summary of activities of pyrazole derivatives

Pyrazole derivative	**Biological/Pharmacological activity**
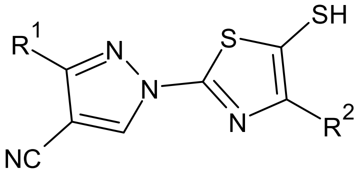	Anti-bacterial Anti-fungal
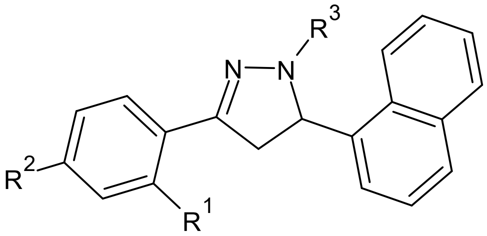	High anti-oxidant activity with IC_{50} =4.47 µg/mL
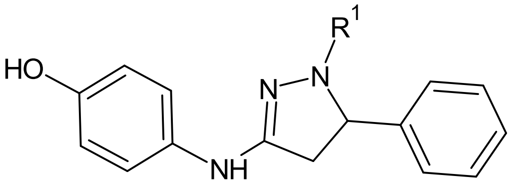	Anti-inflammatory
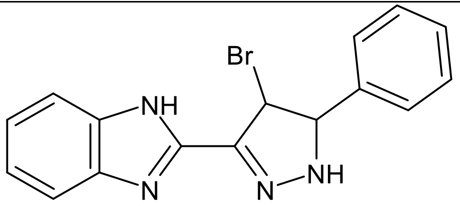	Anti-fungal Anti-bacterial
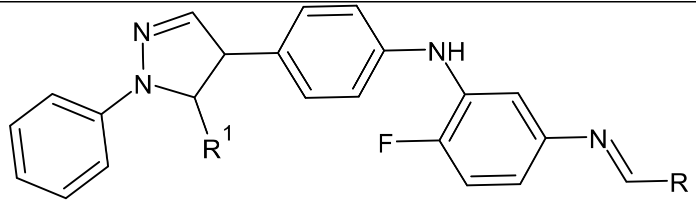	Anti-inflammatory

3. CONCLUSION

Pyrazole based compounds have been used as therapeutic agents. Pyrazole nucleus represents major pharmacophore with diverse biological activities. The study of bioactive character of pyrazole has become interesting field of drug discovery. The modification on the position 1, 3, 4 and 5 in pyrazole moiety affect or enhance the biological properties drastically. The structure-activity relationship studies of reported pyrazole derivatives give more focus on improvement of the inherent biological and pharmacological properties. The synthesis of pyrazole derivatives can be accomplished by using microwave irradiation in easiest way. Here, we have described an overview of some microwave assisted and operationally simple synthetic procedures to find out library of functionalized pyrazole compounds and a wide range of biological and pharmacological activities shown by these pyrazole derivatives.

REFERENCES

1. Fustero, S., Sanchez-Rosello, M., Barrio, P., Simon-Fuentes, A. (2011) Chemical Reviews, 111, 6984-7034.
2. Ansari, A., Ali A., Asif, M., Shamsuzzaman. (2017) New Journal of Chemistry,41, 16-11.
3. Wang, M., Zhang, J., Liu, J., Xu, C., Ju, H. (2002) Journal of Luminescence, 99, 79-83.
4. Chavan, R. R., Hosamani, K. M. (2018) Royal Society Open Science, 5, 172435.
5. Nitulescu, G. M., Matei, L., Aldea, I. M., Draghici, C, Olaru, O. T., Bleotu, C. (2015) Arabian Journal of Chemistry, 12, 816-824.
6. Xia, Y., Dong, Z. W., Zhao, B. X., Ge, X., Meng, N., Shin, D. S., Miao, J. Y. (2007) Bioorganic and Medicinal Chemistry, 15, 6893-6899.
7. Daidone, G., Maggio, B., Raffa, D., Plescia, S., Schillaci, D., Raimondi, M. V. (2004) Il Farmaco, 59, 413-417.
8. Farghaly, A. R. (2010) Arkivoc, 11, 177-187.
9. Soliman, A. S., El-Zahar, M. I., El-Masry, A. H., Kamel, M., Gohar, R. S. (2010) Der Pharma Chemica, 2, 507-521.
10. El-Zahar, M.I., El-Karim, S. S. A., Haiba, M. E., Khedr, M. A. (2011) Acta Poloniae Pharmaceutica-Drug Research., 68, 357-373.
11. Tanitame, A., Oyamada, Y., Ofuji, K., Terauchi, H., Kawasaki, M., Wachi, M., Yamagishi, J. (2005) Biorganic Medicinal Chemistry Letters, 15, 4299-4303.
12. Dawood, K. M., Eldebss, T. M. A., El-Zahabi, H. S. A., Yousef, M. H., Metz P. (2013) European Journal of Medicinal Chemistry, 70, 740–749.
13. Magedov, I. V, Manpadi M., Slambrouck, S. V., Steelant, W. F. A., Rozhkova E., Przhevalskii, N. M., Rogelj, S., Kornienko, A. (2007) Journal of Medicinal Chemistry, 50, 5183–5192.

14. Dhongade, S. R., Chougale, U. B., Chavan, H. V., Deshmukh, S. M., Kharade, P. R., Kenawade, S. A., Shetake, P. K. (2019) Research Journal of Life Sciences, Bioinformatics, Pharmaceutical and Chemical Sciences, 5 (2), 1164-1175.
15. Swanepoel, B., Mitulescu, G. M., Olaru, O. T., Venables, L., van de Venter M. International Journal of Molecular Sciences. 20, 5559.
16. Prasad, Y. R., Rao, A. L., Prasoona, L., Murali, K., Kumar, P. R. (2005) Bioorganic and Medicinal Chemistry Letters. 15, 5030–5034.
17. Aziz, M. A., Rahma, G. E., Hassan, A. A. (2009) European Journal of Medicinal Chemistry. 44, 3480–3487.
18. Priyadarsini, P., Ujwala, B., Rao C. V., Rao V. M. (2012) Der Pharmacia Lettre, 4, 1123-1128.
19. Ozdemir Z., Kandilici H. B., Gumusel B., Calis U., Bilgin A. A. (2007) European Journal of Medicinal Chemistry, 42, 373–379.
20. Tewari, A. K., Srivastava, P., Singh, V. P., Singh, A., Goel R. K., Mohan, C. G. (2010) Chemical and Pharmaceutical Bulletin. 58, 634–638.
21. Pattan, S. R., Rabara, P. A., Pattan, J. S., Bukitagar, A. A., Wakale, V. S., Musmade, D. S. (2009) Indian Journal of Chemistry B, 1453–1456.
22. Gokhan-Kelekci, N., Yabanoglu, S., Kupeli, E., Salgin, U., Ozgen, O., Ucar, G., Yesilada, E., Kendi, E., Yesilada, A., Bilgi, A. (2007) Bioorganic and Medicinal Chemistry, 15, 5775.
23. Sener, A., Kasımogullari, R., Sener, M. K., Bildirici, I., Akcamur, J. Y. (2002) Journal of Heterocyclic Chemistry, 39, 869.
24. Prakash, O., Pundeer, R., Ranjan, P., Pannu, K., Dhingra, Y., Aneja, K. R. (2009) Indian Journal of Chemistry B, 563–568.
25. Takate, S. J., Shinde, A. D., Karale, B. K., Akolkar, H., Nawale, L., Sarkar, D., Mhaske, P. C. (2019) Bioorganic and Medicinal Chemistry Letters, 29, 1199-1202.
26. Prabhudeva, M. G., Vivek, H. K., Kumar, K. A. (2019) Chemical Data Collections, 20, 100193.
27. Padmaja, A., Rajasekhar, C., Padmavati, V. (2011) European Journal of Medicinal Chemistry, 46, 5034- 5038.
28. Verma, A. K., Nagarju, B., Shanmuga, P. S., Maurya, R., Kumari, R. (2014) International Journal of Pharmaceutical Sciences and Research, 4, 792-801.
29. Chen, H. S., Li, Z. M., Han, Y. F. (2000) Journal of Agriculture and Food Chemistry, 48, 5312-5315.
30. Vicentini, C. B., Romagnoli, C., Andreotti, E., Mares, D. (2007) Journal of Agriculture and Food Chemistry, 55, 10331-10338.

31. Tyagarajan, S. (2010) Bioorganic and Medicinal Chemistry Letters, 20, 7479–7482.
32. Meng, F. J., Sun, T., Dong, W. Z., Li, M. H., Tuo, Z. Z. (2016) Archiv Der Pharmazie, 349 (3), 168–174.
33. Rangaswamy, J., Kumar, H. V., Harini, S. T., Naik, N. (2012) Bioorganic and Medicinal Chemistry Letters, 22, 4773–4777.
34. Horrocks, P., Pickard, M. R., Parekh, H. H., Patel, S. B., Pathak, R. B. (2013) Organic and Biomolecular Chemistry, 11, 4891–4898.
35. Vijesh, A. M., Isloor, A. M., Prashant, S., Sundershan, S., Fun, H. K. (2013) European Journal of Chemistry, 62, 410–415.
36. Mamaghani, M., Nia, R. H., Shirini, F., Tabatabaeian, K., Rassa, M. (2015) Medicinal Chemistry Research, 24, 1916–1926.
37. Singh, K. N., Singh, S. K. (2009) Arkivoc, 13, 153–160.
38. Kappe, C. O., Dallinger, D. (2009) Molecular Diversity, 13, 71–193.
39. Jiang, B., Shi, F., Tu, S. T. (2010) Current Organic Chemistry, 14, 357–378.
40. Karimi, F., Peppley, B. A. (2017) International Journal of Hydrogen Energy, 42, 5083-5094.
41. Hayes, B. L. (2002) CEM Publishing, Matthews, NC.
42. Polshettiwar, V., Varma, R. S. (2010) Aqueous Microwave Assisted Chemistry, Royal Society of Chemistry, Cambridge, U. K.
43. Ahluwalia, V. K., Varma, R. S. (2008) Alternate Energy Processes in Chemical Synthesis, Narosa Publishing House, New Delhi.
44. Sood, S., Kumari, P., Yadav, A. N., Kumar, A., Singh, K. (2020) Journal of Heterocyclic Chemistry, 1-9.
45. Sarkate, A. P., Pansare, D. N., Tiwari, S. V., Nikalje, A. P. G., Seija, J. A. (2020) Chemical Proceedings, 1, 1- 10.
46. Jasril, J., Teruna, H. Y., Aisyah, A., Nurlaili, N., Hendra, R. (2019) Journal of Chemistry, (3), 583-591.
47. Subramanyam, C., Sujatha, B., Kumar, D. R., Raju, C. N. (2018) International Journal of Research in Engineering and Management. 307-312.
48. Jain, S. (2018) Research and Reviews: Journal of Chemistry 7(3), 32-36.
49. Gomha, S. M., Farglay, T. A., Mabkhot, Y. N., Zayed, M. E. M., Mohamed A. M. G. (2017) Molecules, 22, 346-356.
50. Dhivare, R. S., Rajput, S. S. (2016) International Letters of Chemistry, Physics and Astronomy, 65, 53-63.
51. Selvam, T. P., Kumar, P. V., Saravanan, G., Prakash C. R. (2014) Journal of Soudi Chemical Society, 18, 1015–1021.

52. Kaliranjan, R., Muralidharan, V., Jubie, S., Sankar, S. (2013) International Journal of Health Allied Sciences, 2 (2), 81-87.
53. Sharma, H. K., Sharma, M. (2012) Asian Journal of Biomedical and Pharmaceutical Sciences, 2(9), 20-24.
54. Sudeep, S., Tathagata, D., Somila, K., Jyothi, Y. (2011) Research Journal of Pharmaceuticals and Technology, 4 (3), 413-419.
55. Biradar, J. S., Mugali, P. S. (2008) Organic Chemistry - An Indian Journal, 4, 9-11.
56. Sauzem, P. D. (2008) European Journal of Medicinal Chemistry, 43, 1237-1247.

Biosynthesis and Catalytic Transformation of Ruthenium Nanoparticles in Biomimetic Applications

Komal M. Dhumal[a], Anita R. Mali[b*]
[a]Department of Chemistry, Balwant cCollege, Vita 415 311 (MS) India.
[b]Department of Chemistry, Yashvantarao Chavan Institute of Science, Satara 415 002 (MS) India.
[*]Corresponding author: anita.mali009@gmail.com

ABSTRACT

Nanoparticles have generated interest among researchers because of their numerous applications. Among the noble metals Ru NPs and Ru containing nanoparticles such as bimetallic nanoparticles eg. Ru/Pd, Ruthenium oxide nanoparticles RuO_2, *supported nanoparticles. Ruthenium supported on CNTs etc. is in focus due to its wide applications in biocatalyst, antimicrobial, anticancer, antifungal, photocatalysis and supercapacitor. Now a days researchers are focused on to the development of a green, biocompatible, and eco-friendly method for the synthesis of NPs. Biosynthesis is one such method that involves the use of natural resources for reducing and stabilizing agents for Nanoparticle synthesis. In the present review, we are summarizing the biosynthesis of ruthenium-containing nanoparticles their characterization, and their applications and to highlight its potential.*

KEYWORDS

Biosynthesis, Green synthesis, Ru NPs.

……

1. INTRODUCTION

Nanotechnology involves the design, synthesis, and application of particles ranging from 1-100 nm range. Nanotechnology is an emerging field yet challenging field for modern research. Nanoparticles show different physical, chemical, and optical properties from that of the bulk material [1]. Metal nanoparticles attain the attentions of researchers. Because due to their higher surface area to volume ratio, they show wide applications range. NPs can be synthesized by different methods which are chemical, Physical, and biological methods. These methods include two main approaches for the synthesis of NPs which are top-down and bottom-up methods. In the top-down approach, we go from bulk material to nanoscale and in the bottom up from atoms clusters towards the nanoparticles [2-3]. Bottom-up method involves physical vapor deposition [4]. sol-gel method [5], chemical reduction method[6], biological method[7]. Top-down methods include ball milling[8], laser ablation [9], and sputtering[10], (**as shown in Fig.1)** Among these methods biological methods gain lots of attention because it overcomessome disadvantages of conventional physical and chemicalmethods. It is an environment-friendly method which less toxic, cost-effective,simple method, and less chemical waste. Nanocatalysts synthesized from this show selectivity, high yield, recyclability, and less chemical deposition [11-12], (**as shown in Fig.2)**. Ru NPs Synthesized by this method can efficiently shows these characteristics. Biosynthesis of Ru involves Plants, and microorganisms. Ru NPs synthesized by using bio-reductionwork as agood catalyst and significant anticancer and antibacterial agent [13-14] **(as shown in Fig. 3)**. Present review containsbiosynthesis of ruthenium containing nanoparticles, their characterization by various techniques and their application.

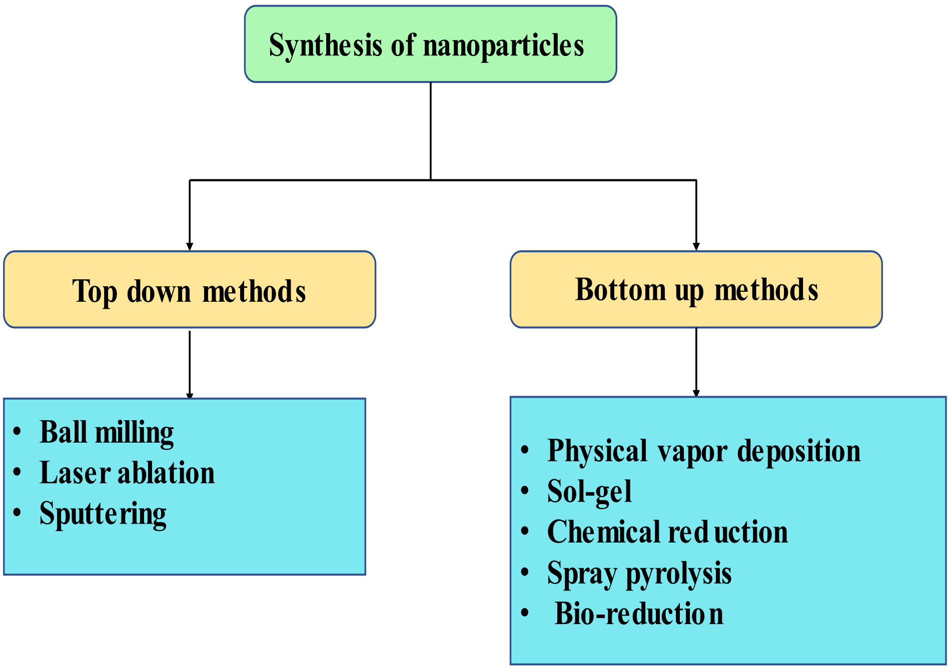

Fig.1: Methods of synthesis of nanoparticles.

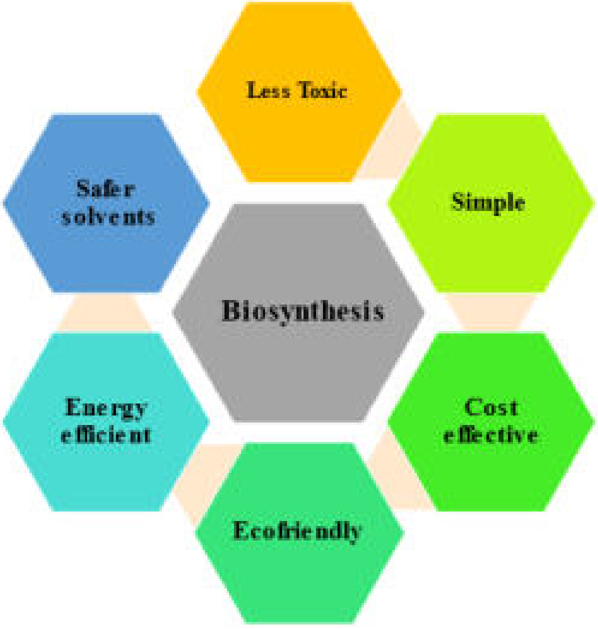

Fig. 2: Key merits of Biosynthesis.

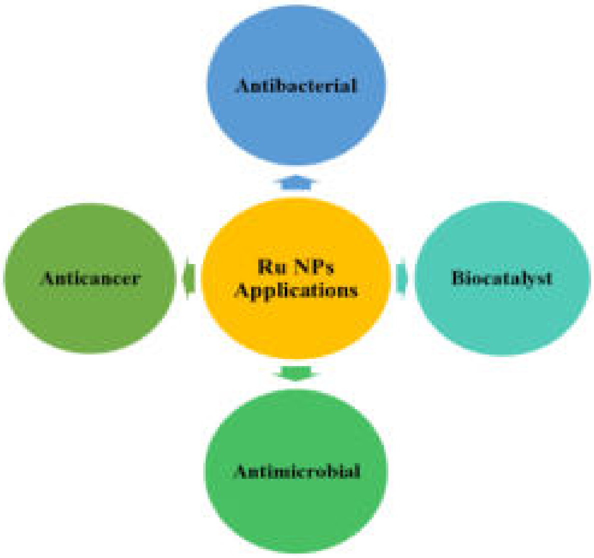

Fig. 3:Applications of Ru NPs.

2. BIOSYNTHESIS

In the early days, noble metal nanoparticles like platinum, silver,palladium,and ruthenium are widely used in different areas. Conventional methods used for the synthesis of NPs require high-temperature, pressure also there may occur binding or deposition of toxic chemicals or material on the surface of nanomaterial which reduces their use in biomedicine [15-16]. So, there is a need to develop a green, biocompatible method for the synthesis of these nanoparticles. Biosynthesis is a green method in which nanoparticles are synthesized by using natural resources such as bacteria, yeast,fungi, and plant parts like leaves, stem, seeds, flowers, fruit, roots, and bark [17-19]. From the study biomolecules present in natural resources like proteins, flavonoids, and phenols work as reducing as well as capping agents [20-21].

2.1Biosynthesis of Ru NPs

Among noble metal nanoparticles, Ru NPs are cheap and productive [22]. Ruthenium nanoparticles and ruthenium oxide nanoparticles show various applications like a catalyst in hydrogenation[23], nanocatalyst in redox reactions[24], an electrocatalyst for hydrogen evolution[25].

2.1.1 Biosynthesis of Ru/CNTs NPs from *Gloriosa superba* leaf extract:

Kasi Gopinath *et al.* reported the synthesis of Ru NPs from Gloriosa superba leaf extract, Ru NPs were synthesized by stirringaqueous leaf extract with a solution of $RuCl_3$ at 100^0 c for 20 min. Synthesized nanoparticles were characterized by UV Vis, fluorescence spectra,FTIR, XRD, SEM, and EDX. FTIR shows that cholidonic, superbine, Colchicine, glorisol, phytosterils, and stigmasterol biomolecules present in leaf extract are responsible for the reduction and capping of synthesized nanoparticles. A fluorescence emission peak observes at 464 nm which shows the Ru=N Pi bond. XRD confirms hexagonal crystalline structure with peaks at 38.42^0(100), 42.2^0(002), 43.98^0(101), 58.32^0(102), and 69.42^0(110). SEM analysis Shows spherical morphology with a size range of 25-90 nm.Ru NPs show good antibacterial activity against gram-positive and gram-negative bacteria[26].

2.1.2 Synthesis of Ru NPs supported on carbon nanotube

In another work, Yao Ma *et al.* synthesizeRu NPs supported on carbon nanotubes from *Cacumen platycladi* leaf extract by adsorption- reduction method. Supported nanoparticles were synthesized by stirring CNTs with an aqueous solution of $RuCl_3$ on an oil bath for 1 hr. at 60^0c after that leaf extract was added to it. These NPs were Examined by various analytical techniques. TEM analysis showswell-dispersedspherical NPs on CNTs with an average sizeof 3.6nm. Various polyols like flavones and reducing sugars help in bioreduction this was revealed by FTIR **(as shown in Fig.5).**EDX shows the synthesis of Ru NPs. nanoparticle shows catalytical activity in hydrogenation of benzene to cyclohexane **(Scheme:1)** at temperature 80^0c, 4 MPA pressure, with time length 0.5 hr.gives 99.9% yield with turnover Frequency (TOF) value 6983.09 h^{-1}. It shows recyclability up to six cycles (Ma Y. *et al.*2014).

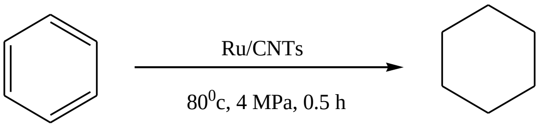

Scheme 1: Ru/CNTs catalyzed hydrogenation of benzene to cyclohexane.

2.1.3 Green synthesis of RuO_2NPs by *Acalypha indica*

Leaf extract of *Acalypha indica*potentially used for synthesis RuO_2 NPs by S.K.Kannan.Leaf of *Acalypha indica*extract was stirred with $RuCl_3.xH_2O$ solution at 90^0c for 2 hr. and obtained powdered sample was calcinated at 600^0c. Synthesized ruthenium oxide nanoparticles were elliptical spherical with size ranging from 6-25 nm. XRD shows an orthorhombic structure with Bragg's diffraction plan at 28.27^0(110), 40.65^0(020), 43.00^0 (210), 58.25^0 (220), 69.08^0(301), and 73.61^0(311). Non-defined morphology with agglomerate particles observed by SEM. Thepresence of elemental Ru was confirmed by EDX. Elliptical spherical nature of NPs observed by TEM analysis. The size distribution of synthesized NPswas examined from DLS which shows the average size distribution was 386.4 (d.nm). These RuO_2NPs show good antibacterial activity against S. marcescens, P. aeruginosa, E. coli, and S. aureus microorganisms [27].

2.1.4 RuO_2 NPs synthesis by *Aspalathus Linearis*:

E. Ismail *et al.* show that RuO_2 nanoparticles were synthesized by using leaf extract of *Aspalathus linearis* which was originally found in Southern Africa. Leaf extract contains various phenolic groups mainly aspalathin, a dihydrochalcone C-glucoside, flavones, and flavonols. Extract of *Aspalathus linearis* works as both a chelating and capping agent for nanoparticles. To synthesize RuO_2 NPaqueous leaf extract was reacted with $RuCl_3.H_2O$ solution of PH 3.8 at room temperature for 2 hr. and precipitate was further subject to annealing at 400^0 c for 2hr for effective crystallization. Synthesized Np was 1.4- 4.3 nm in size and quasi-monodisperse spherical in shape.NPs were Characterized by using TEM, EDX, XRD, XPS Raman,SAED,and UV-VIS-NIR techniques. XRD shows Rutile Np with Braggs reflection plane at 28.0^0(110), 35.05^0(101), 40.5^0(111), and 54.24^0(211).BET surface area of such NPs was observed to be 136.1 m^2/g Synthesized NPs show Water photo-splitting response[28].

2.1.5 Synthesis of Ru/Pt Bimetallic nanoparticles by *Diospyros kaki*

Zhiguo Zhang *et al.* demonstrate the biosynthesis of Ru- Pt nanocatalyst from leaf extract of *Diospyros kaki*. nanoparticles were prepared by mixing a solution of $RuCl_3$

and $H_2PtCl_6 \cdot 6H2O$ with leaf extract ina controlled thermostatic water bath for 1 hr. after that carbon support was added to it and the solution was again stirred for 1 hr. synthesized bimetallic Ru-Pt Np were characterized by using XPS,TEM,XRD, N_2 adsorption-desorption, TEM, HRTEM, TG analysis, and EDX.XPS analysis shows binding energy of 71.2 eV was for metallic Pt and 462.2 eV for metallic Ru and this result shows reduction of metal salt. TEM and HRTEM image shows quasi-sphere-like particles. From XRD there is a decrease in crystalline form.Bimetallic Pt/Ru NPs show good catalytical activity in the hydrogenation of chloronitrobenzene**(Scheme:2)**in different condition but suitable conditions for hydrogenation was reaction temperature 50^0C, 1 MPa H_2 pressure, about 300^0calcinated temperature, Ru/Pt molar ratio 1:1, 300 mg catalyst amount. Bimetallic NPs can be used up to five cycles [29].

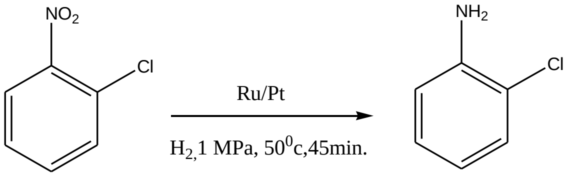

Scheme.2.: Ru/Pt nanoparticles catalyzed hydrogenation of o-chloronitrobenzene to o-Chloroaniline.

2.1.6 Biosynthesis of bimetallic Pd/Ru nanoparticles from *Escherichia coli*

Jaime Gomez-Bolivar *et al.* investigated the synthesis of Ruthenium and bi-metallic Pd/Ru nanoparticles from *Escherichia coli*by using Na_2PdCl_4 and $RuCl_3.2H_2O$ salts. Synthesized bimetallic nanoparticles were characterized by using EDX,HAADF,XPS,XAS,and STEM. XPS shows the presence of Pd (II), Pd(0),Ru (III), and Ru (IV) which was confirmed by X-ray absorption near edge structure (XANES) and extended X-ray absorption fine structure (EXAFS).This shows Pd/Ru core-shell structure.Synthesized Pd/Ru and Ru Np show upgrading of 5-hydroxymethyl furfural (5-HMF) to 2,5 dimethylfuran (DMF) [30].

2.1.7 Green synthesis of Pd/Ru Bimetallic nanoparticles from *Bacillus benzeovorans*

Jacob B. Omajali *et al.*synthesize Pd/Ru bimetallic nanoparticles from *Bacillus benzeovorans*.Synthesized Pd/Ru NPs were characterized by using HAADF, XPS, XAS, XRD, STEM, and EDX analysis.1-2 nm (Pd/Ru mixture) and 4-8 nm Pd@Ru Core shells these two NPs populations observed from HAADF analysis.The presence of Pd(0), Pd(II), Ru (III), and Ru(VI) were analyzed from XPS, but Ru (0) was not found to indicate RuO_2 NPs were apparent.Bimetallic nanoparticles show catalytical activity in the conversion of 5-hydroxymethyl furfural to the fuel precursor 2,5-dimethyl furan**(Scheme:3)**[31].

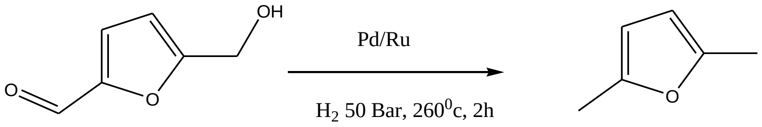

Scheme:3 Ru/Pd Nanocatalyst catalyzed conversion of -hydroxymethyl furfural to the fuel precursor 2,5-dimethyl furan

2.1.8 Biosynthesis of RuO_2 NPs from Akarkara *Anacyclus pyrethrum*

Nisha B. *et al.* reported the synthesis of RuO_2 nanoparticles. For this synthesis root extract of Akarkara *Anacyclus pyrethrum*was used.Akarkara *Anacyclus pyrethrum*is a medicinal Indian herb.RuO_2 nanoparticles were synthesized by treating root extract with $RuCl_3.3H_2O$ solution,then obtained precipitate was calcinated at 600^0c for 3hr. The crystalline nature of NPs was observed by XRD analysis and the average crystalline sizecalculated by the Scherrer formula was 9.52 nm.SEM analysis shows uniform morphology. Spherical shape was observed by TEM with an average size of 13 nm. Cyclic Voltammetry analysis indicates a high degree of charge-discharge reversibility and long-term electrochemical stability. Synthesize nanoparticles were characterized by using XRD, SEM, TEM with SAED and FTIR spectroscopy, and Cyclic voltammetry. RuO_2 NPs show supercapacitor application [32].

2.1.9 Synthesis of Ru NPs from *Pseudomonas aeruginosa* SM1

Sarvesh Kumar Srivastava *et al.*biosynthesize Ru NPs from *Pseudomonas aeruginosa* SM1 without the use of an external stabilizing agent, PH adjustment, or High temperature.Ru NPs were synthesized by adding Ammonium hexachlororuthenate(IV) $[(NH_4)_2RuCl_6]$ solution to the cell pellet at room temperature for 24 hr. TEM analysis shows that synthesized nanoparticles were spherical and some disk shape with size 8.3 ± 5.4 nm. Primary and secondary amines in organic compounds involved in reaction responsible for stabilization of NPs observed from FTIR. NPs were characterized by using FTIR, TEM, and XRD [33].

2.1.10 Biosynthesis of Ru NPs from *Dictyota dichotoma*

Mohamed Yacoob Syed Ali *et al.* stem and leaf extract of *Dictyota dichotoma* marine algae used for the synthesis of Ru nanoparticles. Ru NPs were synthesized by incubating a mixture of a leaf-stem extract with Ruthenium aqueous solution for a 10 min change in color to dark brown indicating the formation of Nanoparticles. Synthesized nanoparticles were examined by UV-visible spectroscopy SEM, EDAX,PXRD, and FTIR analysis. The presence of various functional groups of alcohols, esters, ethers, and alcohols binds with NPs and also provides stabilization which is confirmed by FTIR. XRD analysis shows two peaks at 38^0(111), and 44^0(200) which indicate Face centered cubic structure. From SEM examination synthesized nanoparticles were average of 30 nm in size.These Ru nanoparticles show anticancer activity against human cancer cell lines. Ru (II) NPs shows

efficiency to develop anticancer agent because they show low general toxicity, can mimic iron binding to molecule, and affinity to cancer tissues[34].

2.1.11Bio-synthesis of Ru NPs supported on nitric acid modified activated carbon from *Cacumen platyclade.*

Yangqiang Huang *et al.* used *Cacumen platycladi* leaf extract for the synthesis of Ruthenium nanoparticles supported on Nitric acid-modified active carbon.Supported nanoparticles were prepared by impegrating modified activated carbon with $RuCl_3$ solution in a water bath at 60^0c for 1 hr. then leaf extract was added to it and stirred for 5 hr. synthesized nanoparticles were characterized by using BET, XRD, TEM, and FTIR.XRD analysis shows peaks at 26.5^0,and 44.5^0corresponding to hexagonal carbon, and ruthenium diffraction peaks were not observed which show Ru was highly dispersed on carbon.From FTIR modified Carbon support by HNO_3 increases the oxide group on the surface which work as an anchor site and interacts with the catalytic site.these nanoparticles act as catalyst inliquid phase hydrogenation of 2,2,4,4-tetramethylcyclobutane-1,3-dione to2,2,4,4-tetramethylcyclobutane-1,3-diol**(Scheme:4)**(Hung Y. *et al.*2015).

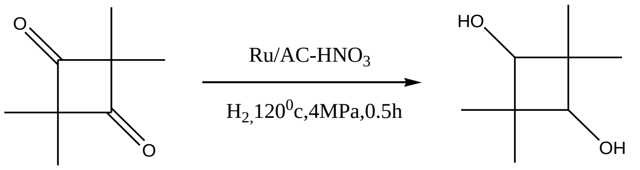

Scheme:4 Ru Ru/AC-HNO$_3$ NP catalyzed conversion of of 2,2,4,4-tetramethylcyclobutane-1,3-dione to 2,2,4,4-tetramethylcyclobutane-1,3-diol

2.1.12 Green synthesis of RuO_2 Nanoparticles from *Catharanthus roseus* and *Moringa oleifera* leaf extract

Table No. 1 Biosynthesis of Ru NPs fromPlant Parts.

S. M. Anjum and co-worker synthesized RuO_2 NPs from leaf extract of Catharanthus roseus and Moringa oleifera leaf extract. For this 10 g dried leaf powder of

Plant	**Plant part used**	**Size(nm)**	**Characterization**	**Applications**	**Reference**
Gloriosa superba	Leaves	25- 90	UV-Vis, Fluorescencespectra,FTIR, XRD, SEM, EDX	Antibacterial activity	[26]
Cacumen platycladi	Leaves	3.06	BET, TEM, HAADF-STEM-EDX, XRD, XPS, FTIR,TG, DTG	Catalyst for hydrogenation of Benzene to cyclohexane	[17]
Acalypha indica	Leaves	6-25	FTIR, XRD, SEM, EDX,TEM, DLS,TGA/DSC	Antibacterial activity	[14]
Aspalathus linearis	Leaves	1.4-4.3	TEM, EDX, XRD,XPS,Raman,SAED,UV-VIS-NIR	Water Splitting response	[28]
Diospyros kaki	Leaves	-	XPS, TEM,XRD,N_2 adsorption-desorption, TEM, HRTEM, TGA	Catalyst in the hydrogenation of ortho-chloronitrobenzene	[29]
Akarkara (*Anacyclus pyrethrum*)	Root	13	XRD, SEM, TEM with SAED and FTIR spectroscopy,Cyclic voltammetry.	Supercapacitor	[33]
Dictyota dichotoma	Stem and leaves	30	UV-Vis,FTIR,SEM,EDAX,PXRD.	Anticancer activity	[34]
Cacumen platcladi	Leaves	1.19 - 0.08	BET, XRD, TEM, FTIR, EDS	Used as catalyst in the liquid phase hydrogenation of 2,2,4,4-tetramethylcyclobutane-1,3-dione to 2,2,4,4-tetramethylcyclobutane-1,3-diol	[35]
Catharanthus roseus and *Moringa oleifera*	Leaves	5.6 and 4.6	UV-Vis. XRD, FTIR, EDX, HRTEM, DLS	antibacterial activity and shows good catalytical activity against Methylene Blue dye.	[12]

Catharanthus roseus and Moringa oleifera was taken and boiled at 80^0c in water bath for about 30 min. This leaf extract was filtered through Whatman No. 1 Paper. 20 ml of each leaf extract was added dropwise to 0.1 M $RuCl_3.xH_2O$ solution at 80^0c for 2 h. Color change from yellowish green to dark brown indicated formation of Nanoparticles. RuO_2 NPs were characterized by various techniques such as UV-Vis., XRD, FTIR, HRTEM, EDX, DLS. UV-Vis shows an intense sharp peak for Catharanthus roseus at 320 nm and for Moringa oleifera at 330nm. XRD pattern shows orthorhombic crystal structure forCatharanthus roseusextract with crystal plane (110), (020), (210), (220),(301) andMoringa oleifera extract with crystal plane (110), (020), (210), (220), (301) and (311). HR-TEM shows a spherical structure with a particle size 5.6 nm for Catharanthus roseus and a spherical structure with 4.6 nm size. These synthesized NPs shows antibacterial activity and shows good catalytical activity against Methylene Blue dye.

Table No. 2 Biosynthesis of Ru NPs from Microorganisms.

Microorganism	**Size (nm)**	**Characterization**	**Applications**	**Reference**
Escherichia coli	-	EDX, HAADF, XPS, XAS, STEM.	Catalyst in upgrading 5-Hydxoxy methyl into liquid fuel precursors	[30]
Bacillus benzeovoran	-	HAADF, XPS, XAS, XRD, STEM, EDX.	Catalyst in 5-hydroxymethyl furfural (5-HMF) to the fuel precursor 2,5-dimethyl furan	[31]
Pseudomonas aeruginosa SM1	8.3-5.4	TEM, FTIR, XRD	-	[32]

3. CONCLUSION

Among noble metal nanoparticles, ruthenium metal attracted the attention of researchers because of its numerous applications in biology, catalysis, photocatalysis, and many more.biosynthesis method follows green chemistry principle using water as a green solvent and non-toxic biomass extract alga, bacteria, fungi, plant extract like leaves, stem, flower, bark, seeds for synthesis. The Ru NPs were characterized by using UV-Vis, SEM, TEM, XRD, EDAX, FTIR, DLS, SAED,and TG techniques. Ru NPs show application in antibacterial activity,Anti-cancer activity, bio-catalysis,etc. Our study will help the researcher to develop biocompatible, ecofriendly biocatalyst, anticancer, and antimicrobial agents containing Ru NPs. In future Ru NPs will be in demand as biocatalyst and biomedical applications.

ACKNOWLEDGMENT

The Authors arethankful to Balwant College, Vita, Yashvantarao Chavan Institute of Science, Satara, and Shivaji University, Kolhapur for providing support.

REFERENCES

1. Henglein, A. (1989) Chemical Reviews.**,**89,1861–1873.
2. Pacioni, N.L., Borsarelli, C.D., Rey V., Veglia, A. V. (2015) Engineering Materials, 13–46.
3. Rajput, N. (2015) International Journal of Advances in Engineering and Technology. 7 (6), 806-1811.
4. Pandey, P.A., Bell, G.R., Rourke, J.P., Sanchez, A.M., Elkin, M.D., Hickey, B.J., Wilson, N.R. (2011). Small, 7(22), 3202-3210.
5. Cushing, B.L., Kolesni, V.L., Connor, C.J. (2004) Chemical Reviews, 104 (9),3893–3946.
6. Pantidos, N., Horsfall, L.E. (2014) Nanomedicine & Nanotechnology., 5 (5),1218-1220.
8. Ullah, M., Ali, M., Hamid, S.B. (2014) Reviews on Advanced Materials Science, 37, 1356-1359.
9. Simakin, A.V., Voronov, V.V., Kirichenko, N.A., Shafeev, G.A. (2004) Applied Physics A Materials Science & Processing, 79 (4), 1127–1132.
10. Swihart, M.T. (2003) Current Opinion in Colloid & Interface Science, 8 (1) 127–133.
11. Ahmad, A., Mukherjee, P., Senapati, S., Mandal, D., Khan, M. I., Kumar R., and Sastry, M. (2003) Colloids and Surfaces B: Biointerfaces, 28, 313– 318.
12. Shankar, S.S., Rai, A., Ankamwar, B., Singh,A., Ahmad A.,and Sastry, M. (2004) Nature Materials,3, 482–488.
13. Gopinath, K., Karthika, V., Gowri, S., Senthilkumar, V., Kumaresan S., and Arumugam, A. (2014*)* Journal of Nanostructure in Chemistry volume, 4, (1), 4–9.
14. Kannan, S. K., Sundrarajan, M.(2015) Advanced Powder Technology, 26 (6), 1505–1511.

15. Ahmed, S., Ahmad, M., Swami B. L., and Ikram, S. (2016) Journal of Advanced Research,7, 17-28.
16. Marambio, J. C.and Hoek, E. M. (2010) Journal of Nanoparticle Research, 2, 1531-1551.
17. Mallick, K. M., Whitcomb, J., Scurrella, M.S. (2005) Materials Chemistry and Physics, 90, 221–224.
18. Liu, Y.C., Lin, L.H. (2006) Clinical Microbiology and Biomedical Sciences. 6, 1163–1168.
19. Smetuna, A.B., Klabunde, K.J., Sorensea, C.M. (2005) Journal of Colloid and Interface Science, 284, 521–526.
20. Collera Z. O., Jimenez, F.G. and Gordillo, R.M. (2005) Food Chemistry, 90, 1-2,109–114.
21. Jagadeesh, B.H., Prabha, T.N., and Srinivasan, K. (2004) Indian Journal of Plant Physiology,9, (2), 164–168.
23. Mishra, D. K., Dabbawala, A. A., Hwang, J. S. (2013) Journal of Molecular Catalysis A: Chemical Volumes, 376, 63–70.
24. Veerakumar, P., Ramdass, A., Rajagopal, S. (2013) Journal of Nanoscience and Nanotechnology., 13 (7), 4761–4786.
25. Sadhanala, H. K., Harika, V. K., Penki, T. R., Aurbach, D., Gedanken, A. (2019) Chem.Cat.Chem,11 (5), 1495–1502.
26. Nisha, B., Vidyalaxmi, Y., Abdul, R. S. (2020) Advanced Powder Technology, 31 (3), 1001–1006.
27. Ma, Y., Huang, Y., Cheng, Y., Wang, L., Li, X. (2014) Applied Catalysis A: Generals, 484, 154–160.
28. Ismail, E., Diallo, A., Khenfouch, M., Dhlamini, S. M., Maaza, M. (2016) Journal of Alloys and Compounds, 662, 283–289.
29. Zhang, Z., Suo, Y., He, J., Li, G., Hu, G., Zheng, Y. (2016) Industrial & Engeering Chemistry Research, *55* (26), 7061–7068.
30. Gomez-B. J., Mikheenko, I. P., Orozco, R. L., Sharma, S., Banerjee, D., Walker, M., Hand, R. A., Merroun, M. L., Macaskie, L. E. (2019) Frontiers in Microbiology,10,1–17.
31. Omajali, J. B., Gomez-Bolivar, J., Mikheenko, I. P.,Sharma, S., Kayode, B., Al-Duri, B., Banerjee, D., Walker, M., Merroun, M. L., Macaskie, L. E. (2019) Scientific Reports, 9 (1), 1–12.
32. Anjum S. M., Riazunnisa K. (2022) Journal of Cluster Science, 33, 1103-1117.
33. Srivastava, S. K., Constanti, M.(2012) Journal of Nanoparticle Research,14 (4), 831.
34. Yacoob, M., Ali, S., Anuradha, V., Abishek, R., Yogananth, N., Sheeba, H., Mohamed-Y. A. (2017) Nano World Journal, 66–71.

Third Generation Solar Cells: Importance and Measurements Techniques for knowing Photovoltaic Device Performance

Prakash S. Pawar[a,b], Pramod A. Koyale[a], Amol B. Pandhare[a,d],
Vijay S. Ghodake[a,c], Swapnijit V. Mulik[a], Ankita K. Dhukate[a],
Waleed Dabdoub[a], Sagar D. Delekar[a,*]

[a]Department of Chemistry, Shivaji University, Kolhapur 416 004 (MS) India.

[b]Department of Chemistry, Shri Yashwantaro Patil Science College,
Solankur, Kolhapur 416 212 (MS) India.

[c]Department of Chemistry, Yashwantrao Chavan Mahavidyalaya, Halkarni, Kolhapur 416 552 (MS) India.

[d]Department of Chemistry, M.H. Shinde Mahavidyalaya, Tisangi, Gaganbavda, Kolhapur 416 206 (MS) India.

*Corresponding author: sdd_chem@unishivaji.ac.in

ABSTRACT

Solar cells are one of the emerging tools for utilization of solar energy effectively and further solar energy conversion for sustainable development. As moving from first generation solar cells to third generation solar cells, the cost of fabrication, performance and feasibility of devices observed to be altered which primes to focus on third generation solar cells. Hence forth, the DSSCs, perovskite solar cells, QDSSCs, organic solar cells, etc. have been highly appreciated throughout research community in terms of wide variety of materials and strategies deployed to design such devices. Subsequently, the photovoltaic device performance can be analyzed using various techniques such as current-voltage measurement, solar efficiency calculation, electrochemical impedance spectroscopy, Mott Schottky analysis, etc. This review focusing on the brief overview to emerging solar cells as well as various measurement techniques for knowing solar photo voltaic devices.

KEYWORDS

Solar cells, third generation solar cells, IV, IPCE, Mott-Schottky, EIS

……………………………………………………………………………………………

1. INTRODUCTION

In the 21st century, renewable sources such as wind, water, solar, and geothermal, etc., have the potential to replace the existing non-renewable sources to meet the energy needs of human beings. This is due to their various features such as giant availability, environmental benign, cheaper or cost effective, available everywhere [1], etc. According to the Perez et al, the availability of renewable and non-renewable energy reserves available on the plant is shown in **Figure-1**. [© R. Perezet al.]

`

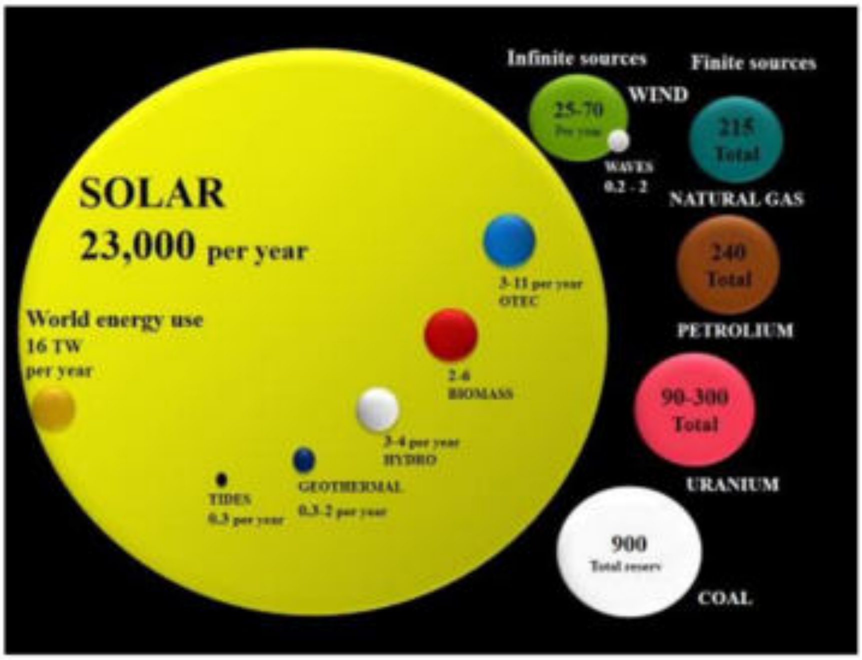

Figure-1. Comparing finite and renewable planetary energy reserves (Terawatt-years). Total recoverable reserves are shown for the finite resources. Yearly potential is shown for the renewables.

From the **Figure-1**, it is revealed that the sun is emitting an energy of 23000 TW per year; while wind, biomass, hydro, geothermal, tides resources providing the energy of 70-120, 2-6, 3-4, 0.3-2, 0.3 TW per year, respectively. Comparatively, the non-renewable resources are called as finite energy resources; which having total available energy are of around 1655 TW only. Therefore, among both the resources, solar energy is most abundant, freely available for maximum days per year, eco-friendly, etc. Therefore, solar energy has been considered as an important source for energy harvesting. Solar energy is converted into electrical energy using a device through photovoltaic effect called as solar device. With invention of first solar cell by American Scientist Charles Fritts in 1883 onwards, investigators continuously progressing in terms of designing the different materials, device architectures and assembly so as to reach the next-generation performance, as well as low-cost devices [2]. Since last few decades, the solar cell technology has grown as extraordinary source of renewable energy to meet the global energy needs. This can be illustrated with the help of **Figure-2**, which displays the dominance of solar cells over other strategies to generate electricity. For last three years i.e., 2018, 2019 and 2020, out of total electricity generation among renewable sources, solar cells comprised the most effectual conversion about 33%, 22% and 16% respectively. So, it is conceivable to say that this technology has been playing a vital role in concern with scientific, economic as well as social point of the view.

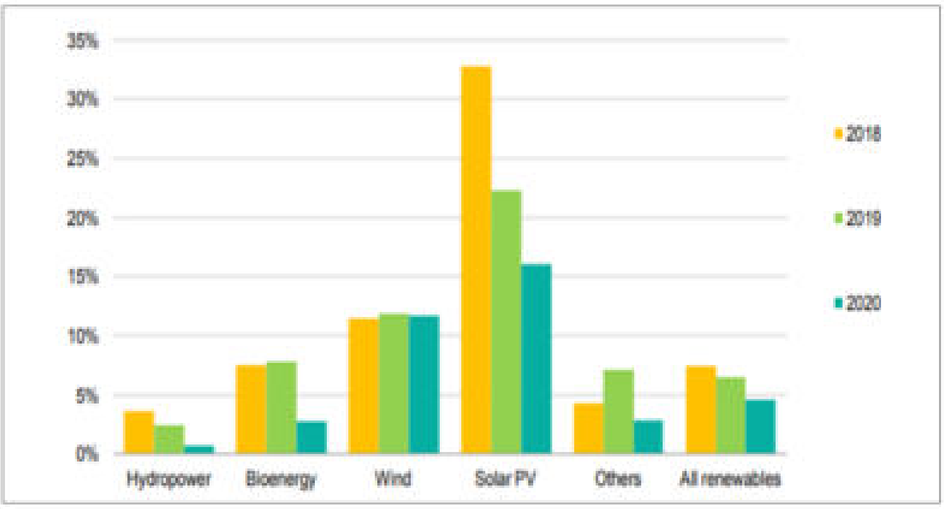

Figure-2.The annual growth for renewable electricity generation by sources, 2018-20.(IEA(2020),Global Energy Review 2020, IEA, Paris.)

Generally, the solar cells are categorized into three different generations, depending on type of materials deployed for their fabrication. Among these generations, first generation is highly matured solar cell technology and hence it is dominated in the market. In the first generation, the photovoltaic devices are fabricated either by crystalline silicon (c-Si) or Gallium Arsenide (GaAs) wafers. In connection to the materials properties, GaAs has thedirectopticalbandgapof1.43eVat300K, while c-Si have an indirect optical band gap of 1.12 eV at 300K and hence GaAs exhibits remarkable optical properties compared to silicon [3],[4]. Therefore, GaAs based solar devices offer the highest conversion efficiency (29.1%) to that of c-Si based photovoltaic devices (26.7%) [5],[6], but still have not yet been chosen for commercialization. Because, the starting materials (such as gallium and arsenic) are much expensive, rare, and toxic. But silicon is most abundant, less toxic compared to GaAs, and hence the c-Si-based photovoltaic devices are commercialized well than that of GaAs [7]. However, the fabrication process for making silicon wafers is tedious, highly expensive and hence having higher overall cost of such devices; which limits the excessive use of silicon-based solar devices. In order to overcome the laggings of first-generation solar devices, scientists have been focusing on the development of the materials under second generation solar devices [8]. Second-generation solar devices are also known as thin-film devices, fabricated by depositing one or more thin layers of the materials on the substrates viz. glass, plastic, and metals, etc. [9]. Copper indium gallium diselenide (CIGS), cadmium telluride (CdTe), and amorphous thin-film silicon (a-Si), etc. are the different materials utilized in this generation. The advantages of this second-generation device are ease thin film deposition, cheap starting materials, lower amount of the materials, thickness dependent properties controls, etc.;

however, the efficiency is somewhat lower than the first-generation solar devices. The reported laboratory efficiency of CIGS and CdTe-based devices is around 20% [10]. Though the devices under second generation are cheaper, but less efficient than conventional c-Si as well as having less film life time (below20years), are the major constraints and hence their commercialization share is less than 20% worldwide in the last three decades [11]. In addition, according to Schokley-Quiseer limit, the another major constraint for these first-generation and second generation solar cells (single-junction) is in terms of their theoretical efficiency; which would be reached up to 33.7 % under the standard conditions (unconcentrated, AM 1.5 solar spectrum, 1.34 eV optical band, 1000 W/m2)[12]. In order to overcome these constraints of first- and second-generation solar cells, researchers have been focused towards the new generation, which is commonly known as third generation solar cells or emerging photovoltaic or hybrid solar cells [13]. This is due to the different ways such as intermediate band positions [14], photon up-conversion [15], hot electron capture [16], multiple exciton generation [17], thermal photon up-conversion [18], etc. In addition, the fabrication processes as well as material architectures of third generation solar devices are easier than the first and second generations. Above **Figure-3** indicates the number of publications related to the third-generation solar cells from last five years, which reflects the dominance over the development of third generation solar cells which include dye sensitized solar cells (DSSCs), quantum dot sensitized solar cells (QDSSCs), Perovskite as well as organic solar cells [19],[20]. In addition, emerging hybrid solar devices such as quantum dot sensitized, dyad-sensitized, etc. have been focused highly so as overcome the constraints of the mono-type sensitized solar devices [21]. Further, in connection to analyze the performance of solar devices in terms of current density, charge transfer resistance as well as carrier density, the various measurement techniques have been utilized to date. It is beneficial to study such techniques for knowing the solar cell performance.

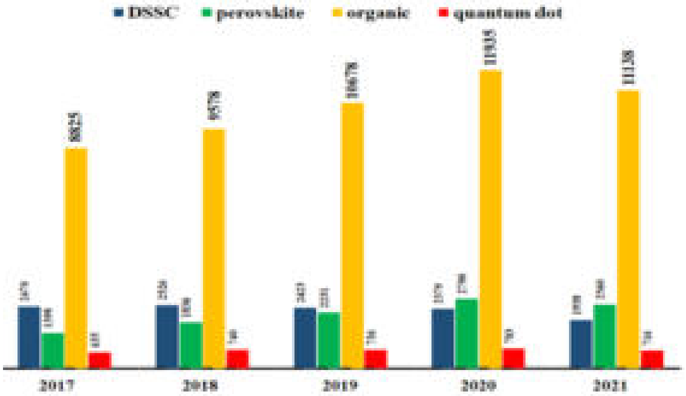

Figure-3. Year wise number of publications related to third generation photovoltaic from2017 onwards based on the number of articles published on Elsevier platform dated up to13th July 2021.

In this connection, the present review focuses on the various measurement techniques like current-voltage (IV), incident photon to current conversion (IPCE), electrochemical impedance spectroscopy (EIS) and Mott Schottky analysis to recognize the performance of photovoltaic devices. Along with this, different factor which are affecting the solar efficiency, are also being described in this review.

2. MEASUREMENTS FOR KNOWING PHOTOVOLTAIC DEVICES PERFORMANCE

2.1.Current-Voltage(I-V) Measurements

The power conversion efficiency of a solar device is studied through the measurement of photocurrent formed with respect to the bias potential and hence it is measured through the current-voltage plot. Therefore, I-V measurement is essential for the evaluation of the various parameters of the solar cells include short-circuit current, open-circuit voltage, fill factor, efficiency, etc. [22]. Basically, I-V plot is measured by using three different methods such as, photovoltaic output with constant illumination (variable resistor), photovoltaic output with variable illumination and diode forward in dark current. Among these methods, the photovoltaic output with constant illumination is commonly used method. With constant illumination of known intensity, a resistive load is varied between short-circuit and open-circuit (zero to infinity) conditions by measuring the voltage and the current output at the respective terminals. **Figure-4** shows the circuit diagram used during the measurement of I-V of the solar cells. This method is only applicable to low-power devices since resistors for higher power are hardly available. Load resistors are not recommended for photovoltaic module characterization because short-circuit is not exactly measured. In addition, the reverse bias characteristics cannot be determined using this method. However, the use of load resistors to evaluate the performance of a solar device or module can provide an inexpensive way of approximating its performance. In **Figure-4**, the load resistor is increased manually in the different steps. In each step, the voltage and the current (actually the voltage across a shunt resistor) are sensed using a pair of handed digital multi-meter. It is reported that change in the load resistor makes the process very slow, so solar radiation and thermal conditions could be changed during the measurement. The system presented employs a set of resistors as load. An array of relays, controlled by a computer card, is used to select the combination of resistors to achieve a specific resistive load. The resistors are chosen to obtain a good spread of points around the “knee” of the curve. Two A/D channels of the computer card are used in order to measure each I-V pair. With this approach, manual operation over the resistor is avoided and the acquisition time is improved [23].

`

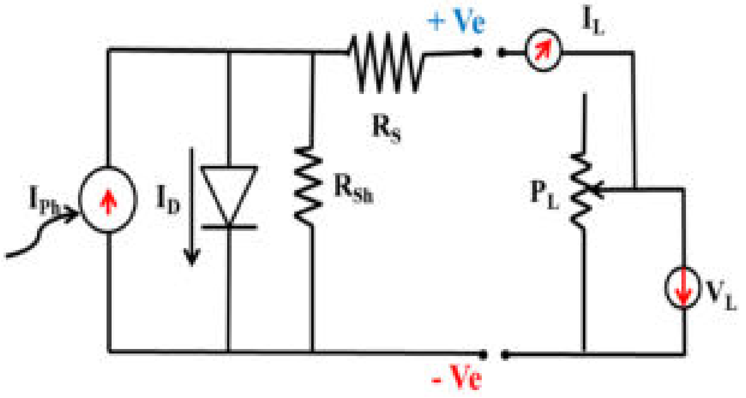

Figure-4. Schematic representation of equivalent circuit of a solar cell with series and shunt resistance.

For an ideal solar cell, the shunt resistance is very high and hence its contribution in I-V measurement is neglected. The photovoltaic output can be measured as (equation-1),

$$I = I_L - I_O\left\{\exp\left[\frac{e}{nKT}(V_L - I_L R_S)\right] - 1\right\} - I_{Ph} \ldots\ldots\ldots\ldots..(1)$$

Where, I_L is the light or photo-generated current, I_o is the reverse saturation current, e is charge on charge carrier, n is ideality factor, K is Boltzmann constant, T is temperature, V_L is the applied voltage across the terminals of the diode, R_s is series resistance, I_{ph} is light generated current. Since solar cell acts as a generator, I-V measurement can also be obtained in fourth quadrant through four quadrant power supply. The circuit diagram with nature of I-V plot of fourth quadrant system is indicated in **Figure-5(a-b)**.

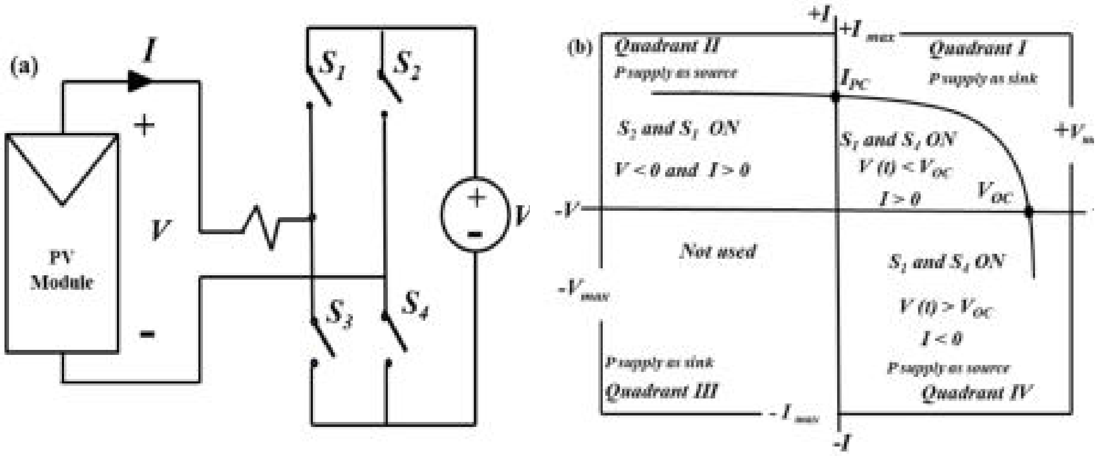

Figure-5. Schematic representation of a) Four-Quadrant power supply scheme, b) I-V characteristics in 1^{st}, 2^{nd} and 4th quadrant. Reprinted with the permission of reference [21].

`

In 2nd method, the light generated current (I_{Ph}) of solar device can also be measured with respect to change in illumination intensity. In this method, at every light intensity setting, the short-circuit current (I_{SC}) and open circuit voltage (V_{OC}) of the solar devices can be measured as indicated in equation-2:

$$I_{Ph} = I_{SC} - I_O\left[\exp\left(\frac{e}{nKT}\ V_{oc}\right) - 1\right] \ldots\ldots\ldots\ldots..(2)$$

In 3rd method, solar device is tested like a diode in dark by applying the external dc power supply in the forward bias. The I-V characteristics can be observed into the first quadrant of the I-V plane. It is described by equation-3 as follow:

$$I = I_O\left\{\exp\left[\frac{e}{nKT}(V_L - I_L R_S)\right] - 1\right\} \ldots\ldots\ldots\ldots..(3)$$

In concern with all three methods, the ideal current-voltage plot of a solar cell is shown in **Figure-6**.

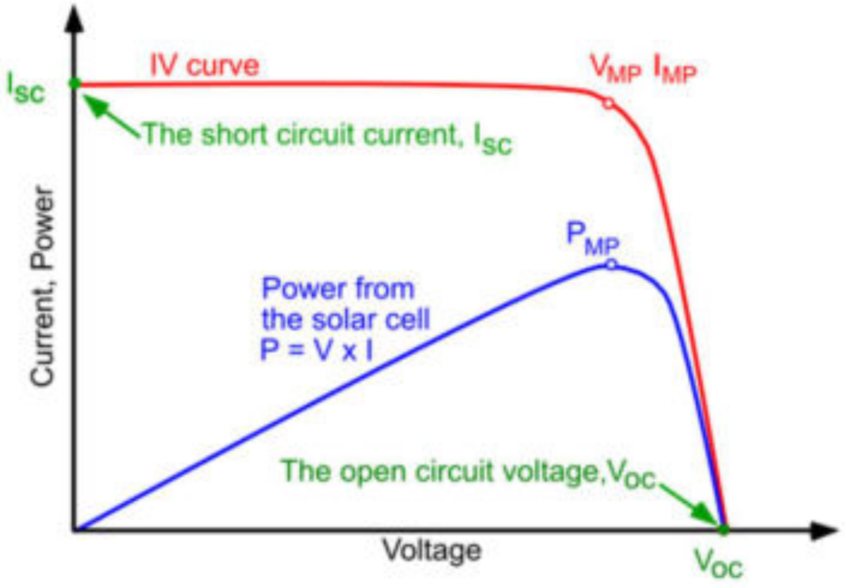

Figure-6. Current voltage (I-V) curve of solar cell

On the basis of I-V characteristics curve, the following solar cell parameters are measured for knowing the overall performance.

2.1.1. Short-circuit current (I_{SC})

Current flows through a cell at zero bias voltage called as the short-circuit current (I_{SC}); which is shown in the **Figure-7**. The generation and collection of I_{SC} is due to the light generated carriers. For ideal photovoltaic devices with moderate resistive loss, I_{SC} and the light generated current are identical. The I_{SC} depends on the different factors such as, the area of the solar cell, number of photons, the spectrum of incident

`

light, optical properties and collection probability. In addition, the variation in illumination intensity significantly affects the I_{SC}. Changes in the illumination intensity between 10^2 to10^{-2} mW·cm^{-2} causes a proportional change in the I_{SC} for all solar cells. In representative investigations, I_{SC} is directly proportional to the number of the photons absorbed by the semiconducting material. The I_{SC} is also evaluated by taking the product between short-circuit current density (J_{SC}) and cell area and it is, represented as in equation-4.

$$I_{SC}=J_{SC}.A \ldots\ldots\ldots\ldots\ldots\ldots\ldots (4)$$

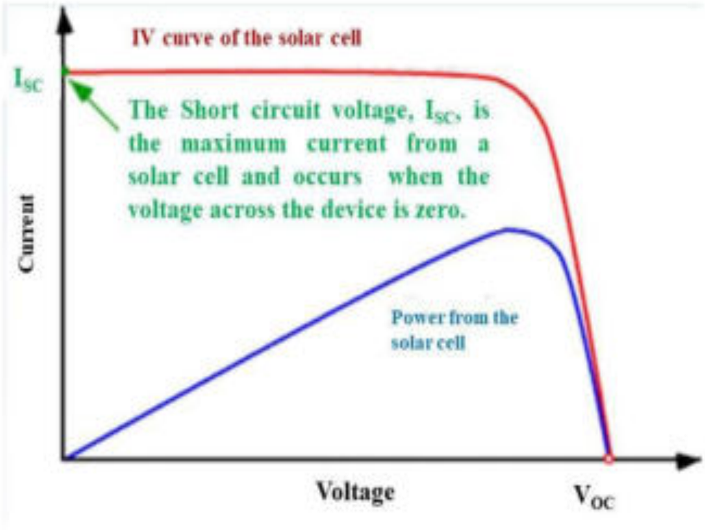

Figure-7. Current flows through a cell at zero bias voltage called as the short-circuit current (I_{SC}).

2.1.2. Open-circuit current (V_{OC})

The open circuit voltage (Voc), is the maximum voltage available from a solar cell at zero current density in that device. The open – circuit voltage corresponds to the amount of forward bias on the solar cell. Due to the bias of the solar cell junction with the light generated current. In solar device, the Voc depends on the work function of the Fermi energy of the photo anode and electrolyte as well. The equation of open circuit current is found by setting the net current equal to zero in the solar cell and it gives equation,

$$V_{OC} = \frac{nKT}{q} ln\left[\left(\frac{I_L}{nKT}\right) - 1\right] - I_L \ldots\ldots\ldots\ldots\ldots (5)$$

2.2.3. Fill Factor

Fill factor is one of the parameters used to know performance of photovoltaic devices; which measures the maximum power (deliverable power) of a solar cell at conjunction of Voc and Isc.

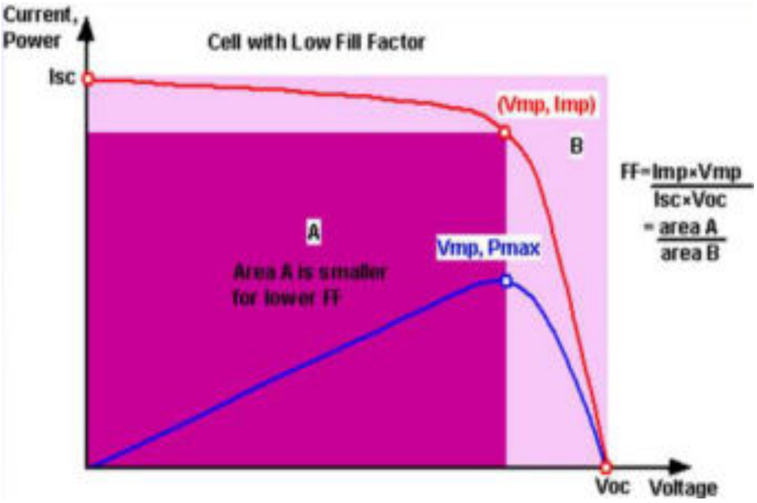

Figure-8. Indication I-V curve for measurement of fill factor.

So, the fill factor is a measure of the squareness of the solar cell and is also the area of the largest which fit in the I-V curve. In above figure the red line (output current), blue line (incident voltage), as a function of voltage. Also, short circuit current (I_{SC}) and open-circuit voltage (V_{OC}) as well as maximum power point (Vmp, Imp) are shown in above figure. The fill factor is calculated by using the following equation-6,

$$\text{FF}\ \% = \frac{Pmax}{Jsc\,.Voc} = \frac{Jmax.\ Vmax}{Jsc\ .\ Voc}\text{............ (6)}$$

The diode characteristics of solar cells can be measured with this factor. For an ideal diode, the parameter must be unity. As the higher fill factor, the diode will be more ideal. In solar device, due to the losses occurring by recombination and transport, the fill factor is usually found between 0.6 and 0.85. In solar cells, it is observed that shunt and series resistance act as limiting factors. Large shunt resistance and low series resistance in solar cells lead to high fill factor FF.

2.1.3. *Solar cell efficiency (η)*

The photovoltaic device is a device, which converts the solar energy into electricity, such conversion is measured in terms of power conversion efficiency (PCE) of the device, and it is indicated as 'η'. The efficiency of solar cell is defined as the ratio of output electrical power at maximum power point on the curve is divided by incident light power. It can be illustrated in equation-7,

$$PCE\ (\eta) = \frac{FF\ \times\ \mathrm{J_{sc}}\ \times\ \mathrm{V_{oc}}}{P_{in}}\text{..................... ..... (7)}$$

Where, η is called efficiency of solar cell, J_{sc} is short circuit current density, V_{oc} is open circuit current voltage, FF is fill factor and P_{in} is incident input power. To allow for effective comparison of device performance, an international standard for input power is used. This standard is an incident spectrum of AM 1.5 G, with an intensity of 1000 W/m^2 (100 mW/cm^2), whereas the cell is at a temperature of 25^{0}C. These solar output parameters reveal the overall performance of solar devices.

2.1.4. Shunt resistance (R_{sh})

The shunt resistance, simply estimates the slope of any I-V curve at the short circuit point (V = 0) and this is equal to -1/R_{Sh}. The shunt resistance is defined as the resistor having very low value of resistance in a circuit (see **Figure-9**).

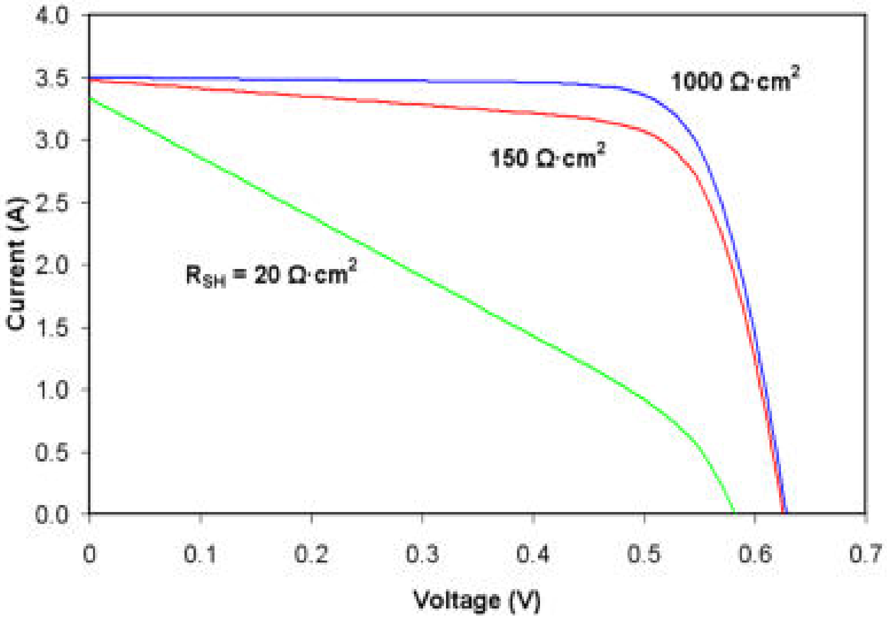

Figure-9. Representation for shunt resistance.

2.1.5. Series Resistance (Rs)

The series resistance is a bulk resistance of the of the diode and contact resistance. The main effect of series resistance is to reduce the fill factor, and also change the Isc, but it does not change the V_{OC} [24],[25]. These changes affected on the efficiency and the performance of photovoltaic devices. Various methods are used to measure the series resistance such as, illumination curve method (Wolf and Rauchenbach 1963), p-n junction dark forward characteristics method (Imamura and Portscheller 1970), the method due to Rajkanan and Shewchun (1979) and high level of excitation method due to Agarwal et al (1981). Among these method, the series resistance can be calculated by using the illumination curve method and it can be represented in equation-8.

$$R_S = R_{SO} - \left(\frac{nV_{th}}{I_O}\right)\exp\left(-\frac{V_{OC}}{nV_{th}}\right) \ldots\ldots\ldots\ldots..(8)$$

Where, V_{OC} is the open circuit voltage (V), R_S is the series resistance, R_{Sh} is the shunt resistance (Ω). R_S is the reciprocal of slope of *I-V* curve at open circuit

`

point (Ω) (see **Figure-10**).

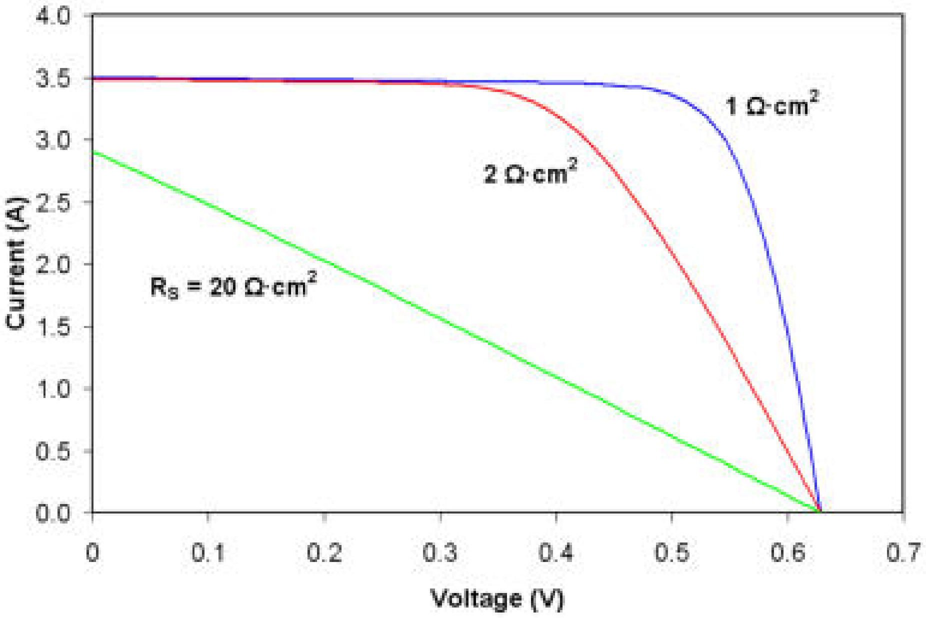

Figure-10. Representation for series resistance

2.1.6. Reverse saturation current

Reverse saturation current is defined as a measure of the "leakage" of carriers across the p-n junction in reverse bias[26]. This lekage is the result of carrier recombination in the neutral regions on the either side of the junction.

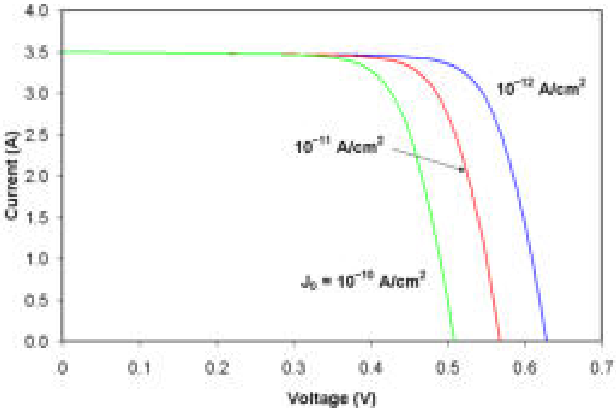

Figure-11. The effect of reverse satuartion current of solar cell.

The **Figure-11** indicates the effect of reverse satuartion current of solar cell. The reverse saturation current can be calculated by using following equation-9,

$$I_O = \left(I_{SC} - \frac{V_{OC}}{R_{Sh}}\right)\exp\left(-\frac{V_{OC}}{nV_{th}}\right) \ldots\ldots\ldots\ldots..(9)$$

2.1.7. Light or Photo-generated current

The photo generated current involves two key processes, the first is the absorption of incident photons to create electron-hole pairs. The generation of electron-hole pairs occurred by the energy of incident photon is greater than the band gap. However, the electrons carrier from p-type materials and holes carriers from n-type materials are always in meta-stable form. While in in second process, it collects these electron-hole carriers by the p-n junction. And also, separate these electron and holes by the action electric filed in the p-n junction without the recombination. After that, these electron-hole pairs can be calculated by using the following formula-10 [27].

$$I_L = I_{SC}\left(1 + \frac{R_S}{R_{Sh}}\right) + I_O\left\{\exp\left(\frac{I_{SC}R_S}{nV_{th}} - 1\right)\right\} \ldots\ldots\ldots\ldots..(10)$$

Where, I_L is the light or photo generated current, I_0 is the reverse saturation current, R_S is the series resistance, R_{Sh} is the shunt resistance, V_{th} is thermal voltage at 300 K (V), n is the ideality, I_{SC} is the short-circuit current.

2.2. Effect other Parameters on Photovoltaic Devices

2.2.1. Ideality Factor

This factor is also said to be emissivity factor, which gives the information about how closely diodes track the ideal diode equation, which is very convenient formula for current as the function of voltage [28]. So, with help of this parameter one can comment on second order effects present in material since the diode not follow the ideal equation. The ideality factor can be measured by using equation-11.

$$n = \frac{[V_m + R_{SO}\,I_m - V_{OC}}{[V_{th}\,\{\ln(I_{SC} - V_m/R_{Sho} - I_m) - \ln(I_{SC} - V_{OC}/R_{Sh}) + I_m/(I_{SC} - \{V_{OC}/R_{Sho}\})\}]} \ldots\ldots(11)$$

Where, R_{ShO} is the reciprocal of slope of *I-V* curve at short circuit point (Ω). Vm is the voltage at MPP (V), I_m is the current at MPP (V).

It is useful to describe the possible recombination arisen via band to band. When there is no recombination within space charge region, the ideality factor relates the standard efficiency of device with value of n=1. As recombination occurs, the value of ideality factor undergoes variation. This behavior of ideality factor can be illustrated with the help of following **Figure-12** and **Table-1**.

`

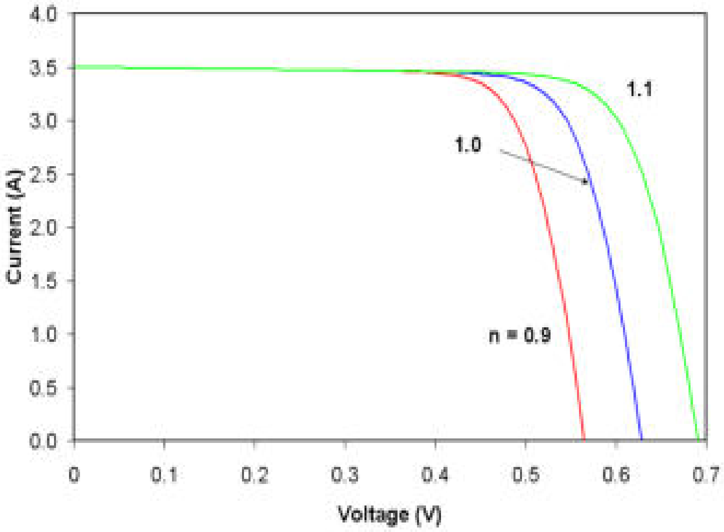

Figure-12. Typical current voltage performance of solar cell with respect to ideality factor.

Recombination Type	Ideality factor	Description
SRH, band to band (low level injection)	1	Recombination limited by minority carrier.
SRH, band to band (high level injection)	2	Recombination limited by both carrier types.
Auger	2/3	Two majority and one minority carriers required for recombination.
Depletion region (junction)	2	Two carriers limit recombination.

Table-1. ***Relation between recombination process and ideality factor.***

Hence, the ideality factor plays dominance role in remarking the solar cell performance, as it gets affected by the output voltage as well as reverse saturation current though the device. This factor is also beneficial to define the heterojunction in the solar cells. When ideality factor is detected to be greater than 2, then it reveals the presence of shottky diode or heterojunction in solar cell [29].

2.2.2. Effect of temperature

Solar cell is a temperature dependent device, if increase the temperature reduces the band gap of semiconductor. The decrease in the band gap of semiconductor, with increase in temperature, it can be observed as increasing the energy of the electrons in the materials. The impact of temperature on photovoltaic devices or I-V curve, indicated in following **Figure-13**.

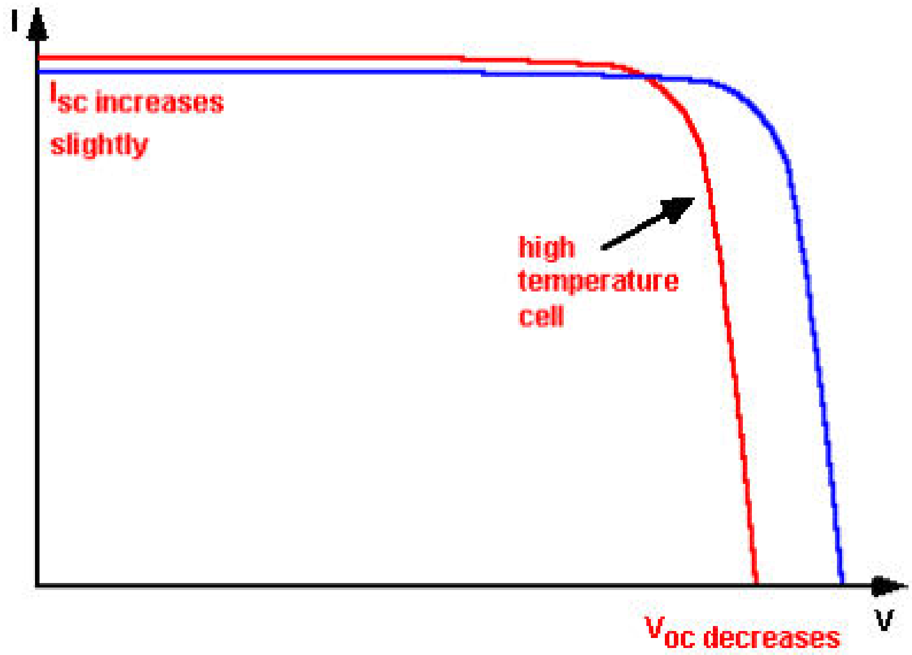

Figure-13. The variation of V_{OC} with temperature (red line).

2.2.3. Effect of light intensity

The solar cell parameters change with changing the light intensity, such as short-circuit current, open-circuit current, fill factor as well as the efficiency and also effect on series and shunt resistance. The intensity of light on solar cell is called the number of suns, i.e., 1 sun corresponds to standard illumination at AM 1.5 or 1 kW/m^2. A photovoltaic module can be designed to operate under low light intensity (0 to 1 sun or 1kW/m^2) conditions is called a flat plate module while the photovoltaic module can be designed by concentrated sunlight (greater than 1 sun i.e., 10 sun illumination or 10 kW/m^2) are called concentrators.

2.3 IPCE Measurement

The IPCE stand for an incident photon to current efficiency and it is also called quantum efficiency. IPCE is used to measure the ratio of photocurrent versus the rate of incident photons for photovoltaic devices and also used to measure the band gap. In the DC IPCE method, at each stage, the wavelength of incoming monochromatic light is altered and the current of the photovoltaic device can be measured as shown in the **Figure-14**. There are two types of IPCE or quantum efficiency i.e., external quantum and internal quantum efficiency. The external quantum efficiency is the number of photo generated electrons per number of incident photons, on the device active area at a given wavelength [30], while internal quantum efficiency is the number of collected carriers per number of all absorbed photons by only the active absorber at a given wavelength [31].

`

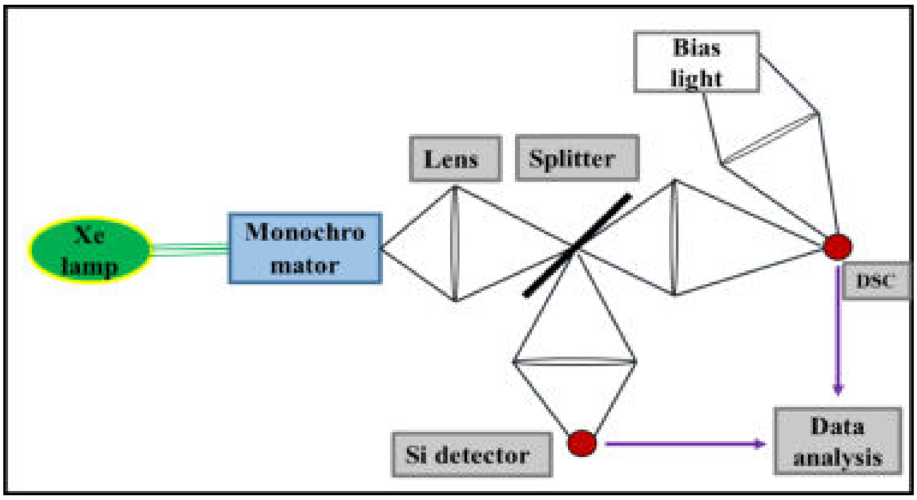

Figure-14. Schematic setup of IPCE technique

The IPCE of the device can be calculated by equation-12,

$$\text{IPCE}=\frac{rate\ of\ number\ of\ collected\ electrons}{rate\ of\ number\ of\ incident\ electrons}$$

$$\text{IPCE} = \frac{Jmeasured/\ [mAcm^{-2}C^{-1}]}{\frac{P_{in}\lambda}{hC/\lambda}.\frac{mWcm^{-2}}{eV}}$$

$$IPCE\ (\lambda) = 1240 \times \frac{J_{sc}}{P_{in}.\lambda}\ \ldots\ldots\ldots\ (12)$$

Where λ is the wavelength of incident monochromatic light (nm), Jsc is the short-circuit photocurrent density (μA/cm^{-2}) and Pin (λ) is the monochromatic light intensity in the unit of (mW/cm $^{-2}$) [32]. Initially, the incoming light intensity calibrated to 1 sun and P_{in} is measured with the help of a conventional Si detector. The primary beam is split into two equal beams, one for the Si detector while the other for the test sample. As well as if the intensity of incoming light is calibrated to 1 sun then we can determine the short circuit current with the help of integrated IPCE (see equation-13) [33].

$$J_{IPCE} = \sum_{near\ UV}^{near\ IR} \mathrm{J_{measured}}\ (\lambda),\ \ = \int_{near\ UV}^{near\ IR} IPCE\ (\lambda).e.{}^{\Phi}in(\lambda)d\lambda\ldots\ldots\ldots(13)$$

Where, ϕ_{in} is the incident photon flux and ‘e’ is the electron elementary charge.

2.4 Electrochemical Impedance Spectroscopy (EIS)

EIS is a non-destructive technique and is used to measure the electrical properties or electrochemical performance of any materials, by using the small amplitude and alternating current. So, this technique is widely used in various fields for the measurement of conductivity such as rechargeable batteries, solar cells, fuel cells, biosensors, coatings, sensors development, etc. In concern with solar cells, this EIS

`

technique is used to study kinetics of interfacial charge transfer process, charge transfer resistance, diffusion length for the charge carriers as well as electronic or ionic process occurring in the solar cells [34]. It is also analysing the corrosion performance of the coated aluminium panel with the use of an electrochemical cell, where alternating current (AC) scanned across a wide range of frequencies to obtain an impedance spectrum of the materials. EIS differs from direct current (DC) techniques; which allows researchers to investigate capacitive, inductive, and diffusion processes in the electrochemical cell or potentiostate. The basic instrumentation set up used in EIS measurement is illustrated in **Figure-15**.

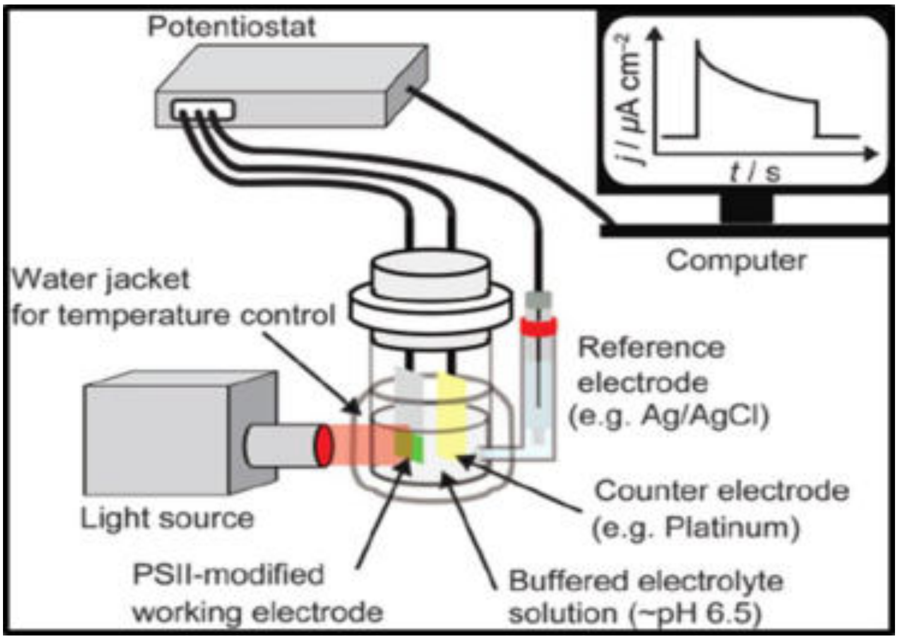

Figure-15. Schematic experimental set up of EIS for PEC measurements reprinted with the permission of reference [35]**.**

Generally, EIS run through the three-electrode system such as working electrode (sample), counter electrode (graphite or platinum) and reference electrode (Saturated calomel electrode or silver/silver chloride). Then these electrodes are attached to the cell and can be filled with an electrolyte solution. The impedance spectra consist the measurement impedance measured as a function of frequency. Low frequency feature is correlated the diffusion of carriers in electrolyte system, intermediate frequency is exemplified the electron transport and back reaction observing at metal oxide/electrolyte interface, and further charge transfer at cathode is associated with high frequency feature. Also, the impedance data represented using Nyquist plot, where Impendence measured as vector. This plot includes the real impedance on X-axis, and imaginary impedance on Y-axis. This can be illustrated by using following **Figure-16** which was investigated by our research group for TiO_2-based DSSCs for

`

studying the interfacial charge transfer behaviour with the variation of dopant [34]. For this investigation, the researchers examined the ohmic resistance and charge transfer resistance.

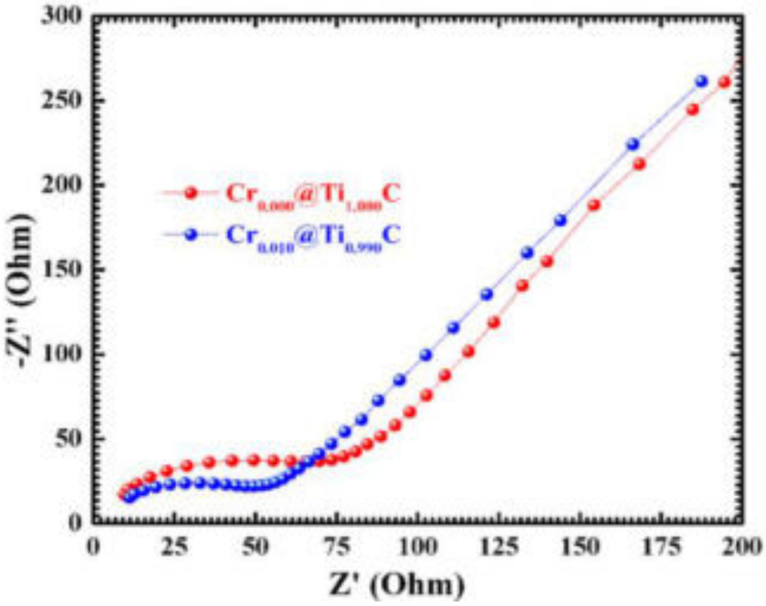

Figure-16. Nyquist plot of the EIS spectra obtained from the representative TiO_2/MWCNTs and Cr0.010@Ti0.990C NCs measured in the frequency range from 0.1 Hz to 1.2 MHz [30].

Impedance can be calculated using following equation-14;

$$Z = \frac{E_t}{I_t} = \frac{E_o \sin(\omega t)}{I_o \sin(\omega t + \varphi)} \text{ ....(14)}$$

Where, Z is impedance, E_t is potential at time, I_t is current at time, E_o is amplitude of the signal, ω is radial frequency and φ is phase shift.

Thereafter, charge transfer resistance at the electrolyte/Pt-FTO interface is typically given for the equilibrium potential. is given by following equation-15;

$$R_{CT} = \frac{RT}{nFi^o} \text{ .... (15)}$$

Where, R_{CT} is charge transfer resistance, R is molar gas constant, T the temperature, n is number of charge carriers, F the Faraday constant, and i^o is the exchange current density of the reaction.

2.5 C-V Measurements (Mott-Schottky Plot)

The technique is used to measure the capacitance as the functions of voltage in order to characterize the conducting behaviour of electrodes through metal-oxide-semiconducting field effect transistor (MOSFET) i.e., Schottky barrier structures. The measurement also delivers the thickness of oxides, oxide charge, and defect

`

present in the materials etc. as well as to the junction of the solar cell in case of reverse bias. The Mott-Schottky (M-S) defines the properties such as flat band potential, doping density, donor/acceptor concentration, type of semiconducting materials, etc., by measuring the capacitance with respect to potential difference between electrode and electrolyte. For this measurement, plot comprises the reciprocal of square of capacitance verses the potential.

This Mott-Schottky (M-S) measurement come to pass with execution of EIS over the range of applied potential. The capacitance of the space-charge layer can be derived from the impedance measurement and its relation with applied potential and flat band potential is given by following equation-16 of M-S analysis,

$$\frac{1}{C_{sc}^2} = \frac{2}{\epsilon\epsilon_0 e N_d}\left(U - U_{FB} - \frac{KT}{e}\right)\ldots\ldots\ldots (16)$$

Where, C_{SC} is capacitance of space-charge layer, ϵ and ϵ_o are dielectric constant and vacuum permittivity, respectively, K is Boltzmann constant, e is the electronic charge, U is applied potential, U_{FB} is flat band potential, N_d is doping density, and T is the temperature. Typical M-S plot is displayed in **Figure-17**.

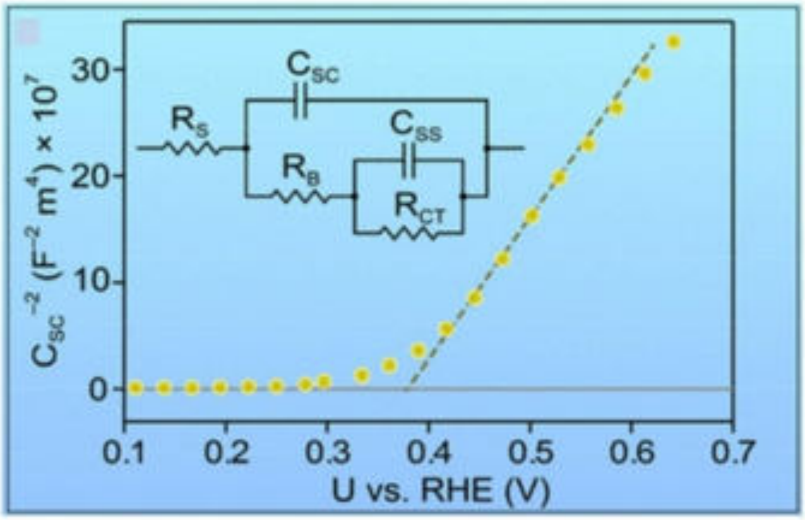

Figure-17. Mott-Schottky plot of reciprocal of square of capacitance with respect to the applied potential. The inset shows the equivalence circuit for the measurement. Where, R_S: series resistance, R_B: bulk semiconductor resistance, R_{CT}: charge-transfer resistance, and C_{SS}: surface-state capacitance [35].

Accordingly, a plot of reciprocal of C_{SC}^2 versus U should disclose U_{FB} as the linearly generalized intercept with the x-axis, while N_d will be proportionate to the inverse of the slope. Since all these parameters playing superseding role to remark the solar cell performance, it is essential to organize these parameters for studying the devices throughout the research investigation for inclusive consequences.

3. CONCLUSIONS

Development of third generation solar cells is one of the vibrant areas of research in energy studies over the employment of first as well as second generation solar cells. Hence, in order to study the said generation of solar cells, present review have been comprised various points. It is conceivable to say that, the emerging hybrid solar devices such as QDSSCs, dyad-sensitized, DSSCs, organic and perovskite solar cells have been focused highly so as overcome the constraints of the existing generation solar cells. Also, in connection to measurement techniques for the performance of solar cells, various strategies such as IV, Impedance, Mott-Schottky analysis, etc. have been emphasized for determination of current efficiency, charge transfer resistance, carrier density, etc. for the synthesized materials.

REFERENCES

1. Gielen, D., Boshell, F., Saygin, D., Bazilian, M. D. (2019) Energy Strategies Review, 24, 38–50.
2. Sharma, D., Mehra, R., Raj, B. (2021) Superlattices Microstructures, 153, 106861.
3. Ahmed, E.M. (2015) Journal of Advanced Research, 6, 105–121.
4. Miller, S. L., Nasby, R. D., Schwank, J. R., Rodgers, M. S., Dressendorfer, P. V. (1990) Applied Physics, 68, 6463–6471.
5. Nayak, P. K., Mahesh, S., Snaith, H. J., Cahen, D. (2019) Nature Reviews Materials, 4, 269-285.
6. Andreani, L. C., Bozzola, A., Kowalczewski, P., Liscidini, M., Redorici, L. (2019) Advance Physics, 4, 1.
7. Płaczek-Popko, E. (2017) Opto-Electronics Reviews, 25, 55–64.
8. Sharmaand, S., Chaujar, R. (2020) Proceding 2nd International Conferance VLSI Device, 18–19.
9. Enayati, M., Gong, Y., Goddard, J. M., Abbaspourrad, A. (2018) FoodChemistry, 266, 508–513.
10. Leeand T.D. (2017) Renewable and Sustainable Energy Reviews, 70, 1286–1297.
11. Kim, B. J., Lee, S., Jung, H. S. (2018) Journal of Material Chemistry A, 6, 12215-12236.
12. Rühle, S. (2016) Solar Energy, 130, 139-147.
13. Eisler, C. N., Abrams, Z. R., Sheldon, M. T., Zhang, X., Atwater, H. A. (2014) Energy & Environmental Science, 7, 3600-3605.
14. Brown A. S., Green, M. A. (2002) Journal of Applied Physics, 92, 1329-1336.
15. Silicon, G. (2009) Optical Photonics News, 20, 18-23.
16. Choudhury, B. D., Lin, C., Soliz-Martinez, J., Huq, H., Uddin, M. J. (2021) Scientific Reports, 11, 1-11.
17. Lietal. M. (2018) Nature Communications, 9, 3-9.
18. Wang, J., Ming, T., Jin, Z., Yan, C. H. (2014) Nature Communications, 5, 1-9.

19. Yan, J. Saunders, B. R. (2014) RSC Advances, 4, 43286-43314.
20. Pawar, P. S., Koyale, P. A., Dhodamani, A. G., Delekar, S. D. In Advances in Metal Oxides and Their Composites for Emerging Applications, edited by Delekar S. D. Elsevier, (2022) pp.263–286.
21. Somasundaranand, P. (2016) International Journal of Photoenergy, 2016, 1-9.
22. Duran, E., Piliougine, M., Galan, J., Andujar, J. M. (2008) Conference Recording: IEEE Photovoltaic Special, 2008.
23. Kishore Kumar, D. (2020) Material Science in Energy Technology, 3, 472-481.
24. Wurfel, U., Cuevas, A., Wurfel, P. (2015) Journal of Photovoltaics, 5, 461-469.
25. Chavali, R. V. K., Wilcox, J. R., Alam, M. A. (2014) Journal of Photovoltaics, 3, 763-771.
26. Saliba, M., Etgar, L. (2020) ACS Energy Letters, 5, 2886-2888.
27. Riquelme, A., Gálvez, F. E., Contreras-Bernal, L., Míguez, H., Anta, J. A. (2020) Journal of Applied Physics, 128, 13.
28. Li, C. (2014) Review of Scientific Instruments, 85, 2.
29. Morifuji, T., Takekuma, Y., Nagata, M. (2019) ACS Omega, 4, 11271-11275.
30. Dhodamani, A. G., Delekar, S. D., More, K. V., Patil, S. M. (2020) Solar Energy, 201, 398-408.
31. Kato, M., Zhang, J. Z., Paul, N., Reisner, E. (2014) Chemical Society Reviews, 43, 6485-6497.
32. Bredar, A. R. C., Chown, A. L., Burton, A. R., Farnum, B. H. (2019) ACS Applied Energy Materials, 3, 66–98.
33. Gelderman, K., Lee, L., Donne, S. W. (2007) Journal of Chemical Education, 48, 685-688.
34. Albery, W. J., Smith, A. L. (1996) Journal of the Chemical Society, Faraday Transactions, 92, 4083-4085.
35. Sivula, K. (2021) Energy Letters, 6, 2549-2551.

`

Aggregation-Induced Emission, Mechanochromism, and Applications of Tetraphenylethene/Triphenylamine-based Molecules

Kishor. S. Jagadhane[a,b], Govind. B. Kolekar[c], Prasad. M. Swami[a], Prashant. V. Anbhule[a,*]

[a]Department of Chemistry, Shivaji University, Kolhapur416004 (MS) India.
[b]School of Nanoscience and Biotechnology, Shivaji University, Kolhapur416004 (MS) India.
[c]Department of Chemistry, Shivaji University, Kolhapur416004 (MS) India.
*Corresponding author: pva_chem@unishivaji.ac.in

ABSTRACT

This Review provides a comprehensive analysis of recent developments in the research of tetraphenylethylene as well as triphenylamine (TPA) luminophores that are active in aggregation-induced emission and mechanochromic luminescence as their applications in a variety of sectors. It begins by going over the wide range of structural motifs that have been specifically useful in sensing. Tetraphenylethene/triphenylamine is used as a mechanoluminescent substance.

KEYWORDS

Tetraphenylethene, Triphenylamine, Aggregation-Induced Emission, Mechanochromic luminescence, aggregation-induced emission luminogens.

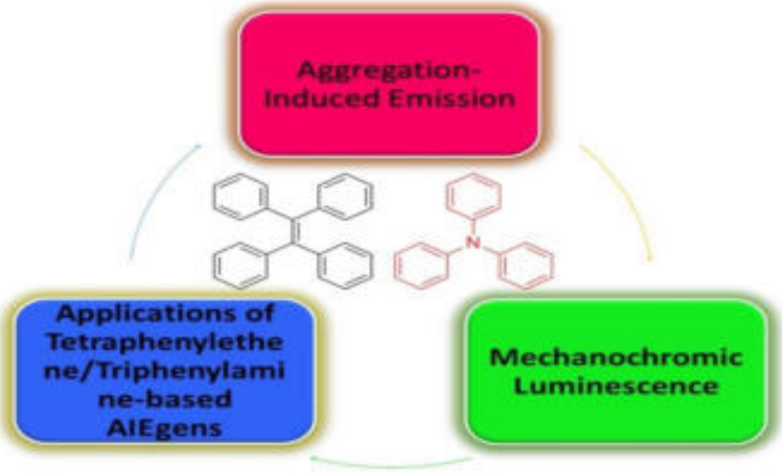

Graphical representation (TOC)

1. INTRODUCTION

In recent years, tetraphenylethylene-based organic compounds have attracted a lot of attention due to their wide range of uses and exceptional selectivity, sensitivity, and outcomes. Aggregation-induced emission photophysical processes frequently include the building block tetraphenylethene/triphenylmethane. Aggregation-induced emission (aggregation-induced emission) compounds exhibit a propeller structural property when exposed to 365 nm UV light. Aggregates and solids should not be stacked [1]. It has long been known that TETRAPHENYLETHENE-derived probes are aggregation-induced emission-active due to tetraphenylethene's hydrophobic properties. Tetraphenylethylene contains an outer ring of revolving aromatic phenyl rings that resemble a propeller. Recent studies have uncovered and demonstrated that the peripheral aromatic rings can freely rotate in diluted solutions [2]. The excited state causes nonradiative disintegration (decay).Tetraphenylethylene derivatives are the most frequently employed chromophore to explain complexation with metal ions because of their "Aggregation-Induced Emission" characteristics. The development of new chemosensors for metal ion detection involves functionalizing tetraphenylethylene-based molecular architecture with pendant coordinating sites for metal ions. Tetraphenylethene's capacity to be detected is determined by its aggregation-induced emission properties, which depend on chromophore receptor sites' interaction with analytes [3].

1.1 Aggregation-induced emission

Aggregation-induced emission, a type of photophysical phenomenon connected to the aggregation of chromophore moiety, was first proposed by B. Z. Tang and his team in 2001 [4]. In an aggregation-induced emission process, the amount of water in the mixture determines how quickly the weak or non-emissive luminogens become emissive as a result of the development of their aggregate. These astonishingly bright luminogens, also known as aggregation-induced emission luminogens have found extensive use as an intriguing material in numerous sectors as shown in **Figure-1**[5-7].

1.1.1 Mechanochromicproperties

In response to mechanical forces like grinding, heating, fuming, and crushing/rubbing, some smart materials, and molecules exhibit a special property known as mechanochromic luminescence (MC). Due to its possible applications in mechanosensory, security documents, and optical storage, the MC luminescence property has attracted considerable interest. When the solid sample was pulverized with a pestle and mortar, the color of tetraphenylethene-based materials changed substantially, as did the emission which is shown in **Figure-2** [1].

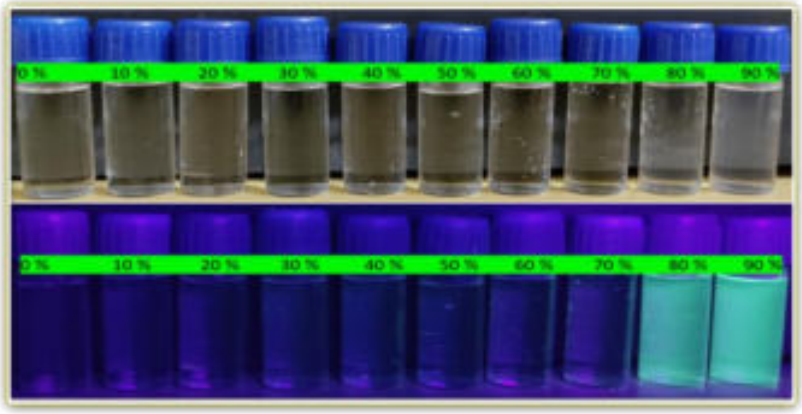

Figure-1. Photographic images of aggregation-induced emission (aggregation-induced emission) in ACN: H_2O mixtures with different water fractions 0 to 90 % - (Top Image) Under ambient light (Daylight) (Bottom Image) Under UV Irradiation (365 nm). ("Photograph courtesy of 'Kishor Jagadhane et al. Copyright ChemistrySelect 2022.").

MC luminogens modify their emission by altering their aggregate shape or molecular structure. Even though the first method is a general technique to control a luminogens emission, only a small number of MC luminogens based on this mechanism have been documented because of the imperfect and irreversible chemical processes in the solid state. Although each system has unique properties, the majority of described luminogens were able to produce MC fluorescence by having their morphology altered by mechanical stimulation. These luminogens can change between crystalline and amorphous states, a stable liquid crystalline phase and a metastable liquid crystalline phase, or between two different crystalline phases depending on the intermolecular interactions that are present before and after the application of mechanical stimuli, such as the -interaction, dipole-dipole interaction, and hydrogen bonding. It has also been discovered that some luminophore-doped polymer composites display the mechanochromism phenomena. Despite the reasonably apparent mechanisms for mechanochromism, few materials exhibiting MC luminescence had been identified before 2008, which was largely due to two factors. First, their syntheses' design strategy is still unclear. Second, the aggregation-caused quenching (ACQ) effect, traps, or flaws in the aggregates cause the emission of several luminogens to be completely or partially quenched upon aggregate formation. As a result, creating MC luminogens becomes a difficult undertaking [8-15].

Mechanochromic materials (also known as piezoceramic) can alter the color of their emission in response to certain external force stimuli, such as pushing, shearing, or grinding. Mechanochromic materials have gained a lot of attention as a type of "smart material" due to their promising uses in optical storage, pressure sensors, rewritable media, and security ink. Due to low-pressure demand and good reversibility, changing the way of molecular packing (aggregation states) or intramolecular conformation to produce mechanochromism is more appealing than solid-state chemical processes for both fundamental research and practical applications. It has been discovered that the phase transition between the crystalline state and the amorphous phase frequently affects mechanochromic performances. The pressured sample's amorphous form makes it impossible to verify the molecular packing modes and configuration, which makes it more challenging to pinpoint the underlying causes of emission shift. The mechanochromic phenomena have thus far been attributed to changes in intramolecular planarity, stacking, H- or J-aggregation, and intermolecular interactions [16-20].

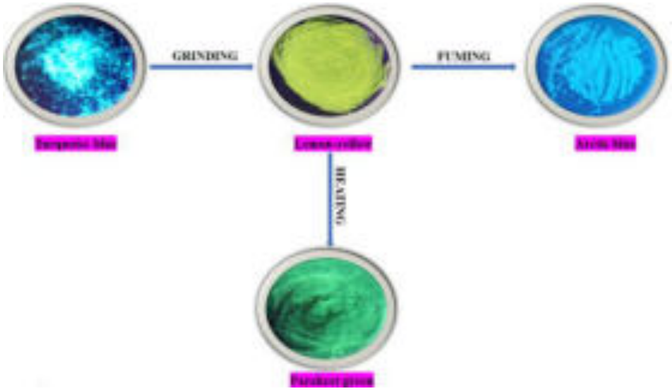

Figure-2. Under UV irradiation (365 nm), photographs of the mechanochromic phenomena of probe 1 exhibit how that color changes after grinding, fuming, and heating. ("Photograph courtesy of 'Kishor Jagadhane et al. Copyright ACS Omega 2022.").

1.1.1.1 Applications

New ideas inspire innovative applications. Wherever the RIR process is present, the aggregation-induced emission effect can theoretically be used to achieve desirable results. The only thing limiting the possibilities is likely our imagination. The aggregation-induced emission effect has been investigated in many laboratories, and much of the work has been focused on its applicability in optoelectronic and sensory systems. Due mostly to the ACQ issue, the device performances of OLEDs based on typical flat luminophores have been subpar. The aggregation-induced emission luminogens are emissive in their aggregate state, making them attractive building blocks for effective OLEDs. This is supported by the fact that an OLED based on silicon exhibits an external quantum yield (ZEL) of up to 8%, which is close to the upper limit for an EL device based on an organic singlet emitter [3,5,6,21]. All the reported and possible applications about the tetraphenylethene are shown in **Figure-**

3and all the reported and possible applications about the triphenylamine are shown in **Figure-4** [22-24].

Figure-3. Graphical Representation of applications of tetraphenylethene-based aggregation-induced emission materials.

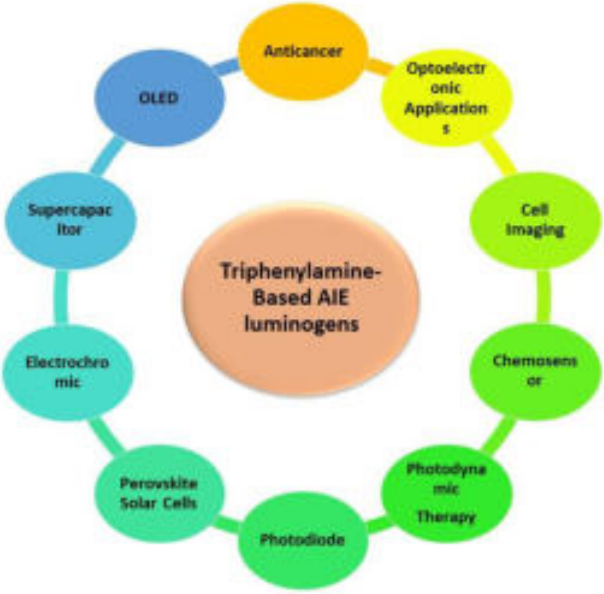

Figure-4. Graphical Representation of applications of triphenylamine-based aggregation-induced emission materials.

2. CONCLUSION

In conclusion, it has been shown that tetraphenylethene and triphenylamine is the best raw material from which to create a variety of useful materials in the future. Because of their particular aggregation-induced emission activity in the solid state, and mechanochromic luminescence behavior upon mechanical force. tetraphenylethene/triphenylamine-based aggregation-induced emission luminogens are simple to create and modify. Although the benefit of aggregation-induced emission in tetraphenylethene derivatives has been used in some applications as described in this Review, we think there are still many other potential applications that have not yet been explored. We also believe that a large community of researchers will continue to build upon the research in this review.

ACKNOWLEDGEMENT

The authors (KSJ and PVA) are thankful to the Department of Chemistry, Shivaji University, Kolhapur, and the School of Nanoscience and Biotechnology, Shivaji University, Kolhapur for providing the all-research facility, and the authors were grateful for the financial support from the Dr. Babasaheb Ambedkar Research and Training Institute (BARTI), Pune. (No. BARTI/Fellowship/BANRF-2018/19-20/3036).

REFERENCES

1. Jagadhane, K., Bhosale, S., Gunjal, D., Nille, O., Kolekar, G., Kolekar, S.,Dongale, T.,Anbhule, P. (2022) ACS Omega, 7, 34888–34900.
2. Xia, M., Li, C., Liu, L., He, Y., Li, Y., Jiang, G.,Wang, J. (2022) Biosensors, 12, 1–11.
3. La, D.D., Bhosale, S.V., Jones, L.A., Bhosale, S.V. (2017)ACS applied materials & interfaces, 10, 12189-12216.
4. Hong, Y., Lam, J. W. Y.,Tang, B. Z. (2011) Chemical Society Reviews, 40, 5361–5388.
5. Mei, J., Leung, N. L. C., Kwok, R. T. K., Lam, J. W. Y.,Tang, B. Z. (2015) Chemical Reviews, 11, 11718–11940.
6. Suman, G.R., Pandey, M., Chakravarthy, A.J. (2021) Materials Chemistry Frontiers, 5, 1541-1584.
7. Deng, L., Wu, W., Guo, H., Zhao, J., Ji, S., Zhang, X., Yuan, X.,Zhang, C. (2011) TheJournal of Organic Chemistry, 76, 9294–9304.
8. Santhiya, K., Sen, S. K., Natarajan, R., Shankar, R.,Murugesapandian, B. (2018) The Journal of Organic Chemistry, 83, 10770–10775.
9. Qi, Q., Zhang, J., Xu, B., Li, B., Zhang, S. X. A.,Tian, W. (2013) The Journal of

Physical Chemistry C, 117, 24997–25003.

10. Hariharan, P. S., Mothi, E. M., Moon, D.,Anthony, S. P. (2016) ACS Applied Materials & Interfaces, 8, 33034–33042.
11. Ito, S., Nagai, S., Ubukata, T., Ueno, T.,Uekusa, H. (2020) Crystal Growth&Design, 20, 4443–4453.
12. Omokawa, R., Kawasaki, R., Sugikawa, K., Nishimura, T.,Nakaya, T. (2021) ACS Applied Polymer Materials, 3, 3708–3713.
13. Huang, B., Gu, X., Feng, Y., Zhang, Y., Jiang, D., Chen, W. C., Dai, G., Ji, Y., Zhao, Q.,Lee, C. S. (2020) Crystal Growth & Design, 20, 2454–2461.
14. Feng, N., Gao, C., Guo, C. Y., Chen, G. (2018) ACS Applied Materials & Interfaces, 10, 5603–5608.
15. Yin, Y., Chen, Z., Fan, C., Liu, G.,Pu, S. (2019) ACS Omega, 4, 14324–14332.
16. Yoon, S. J.,Park, S. (2011) Journal of Materials Chemistry, 21, 8338–8346.
17. Wu, Z., Fang, W., Wu, C., Corrigan, N. A., Zhang, T., Xu, S., Boyer, C. (2022) Chemical Science,13, 11519-11532.
18. Shen, X. Y., Wang, Y. J., Zhao, E., Yuan, W. Z., Liu, Y., Lu, P., Qin, A., Ma, Y., Sun, J. Z.,Tang, B. Z. (2013) The Journal of Physical Chemistry C, 117, 7334–7347.
19. Li, H., Chi, Z., Xu, B., Zhang, X., Li, X., Liu, S., Zhang, Y.,Xu, J. (2011)Journal of Materials Chemistry, 21, 3760–3767.
20. Luo, X., Zhao, W., Shi, J., Li, C., Liu, Z., Bo, Z., Dong, Y. Q.,Tang, B. Z. (2012) The Journal of Physical Chemistry C, 116, 21967–21972.
21. Zhu, C., Kwok, R. T. K., Lam, J. W. Y.,Tang, B. Z. (2018) ACS Applied Bio Materials, 1, 1768–1786.
22. Yen, H. J., Liou, G. S. (2019) Progress in Polymer Science, 89, 250–287.
23. Roquet, S., Cravino, A., Leriche, P., Alévêque, O., Frère, P.,Roncali, J. (2006) Journal of the American Chemical Society, 128, 3459–3466.
24. Duan, J., Pan, H., Wei, C., Xiao, J., Zhai, G.,Su, W. (2017) RSC Advances, 7, 10570–10574.

Greener and Environmentally Benign Methodologies for the Synthesis of Bis(indolyl)methane and Trisindolines

Aboli C. Sapkal[a], Suraj R. Attar[a], Santosh B. Kamble[a,*]
[a]Department of Chemistry, Yashavantrao Chavan Institute of Science, Satara 415 001 (MS) India.
*Corresponding author: santosh.san143@gmail.com

ABSTRACT

According to important position of heterocycles in synthetic organic chemistry world. Bis(indolyl)methane and Trisindolines acquired vital place due to its various important biological activities such as anticancer, antimicrobial, antitubercular, antifungal, anticonvulsant, spermicidal, and antioxidant activities, among others. Therefore, researcher synthesize bis(indolyl)methane and trisindolines by using various methodologies but some methods are required harsh reaction conditions, toxic chemicals therefore researcher go towards green methodologies that minimize use of toxic chemicals, uses green techniques such as ultrasonication, room temperature reaction instead of refluxing etc. So, the main purpose of this review is to provide a comprehensive summary of the various synthetic strategies that follows the green chemistry principles to synthesize Bis(indolyl)methane and Trisindolines.

KEYWORDS

Green Chemistry, Bis(indolyl)methane (BIMs), Trisindolines, Indole, Isatin, heterocycles.

……………………………………………………………………………………

1. INTRODUCTION

Nitrogen containing heterocycles acquire an important position in the pharmaceutical industry. Out of various nitrogen containing heterocycles, indole is a very important biological scaffold. Indole is present in many natural products, including agrochemicals, pharmaceuticals, photochemistry, dyes, and so on [1]. The aromatic bicyclic structure incorporating benzene ring fused with pyrrole ring is known as Indole [2]. Indole contains only one nitrogen atom, which is weakly basic in nature, like pyrrole. Because of its high-energy HOMO, indole is an electron-rich heteroaromatic system [3].

The most famous synthetic method is Fischer indole synthesis, first reported in 1883 [4]. After that lot of methods reported for synthesis of indole such as Nenitzescu synthesis[5], Ullmann reaction[6], Leimgruber-Batcho synthesis, Reissert synthesis[7], Bartoli reaction[8] etc. All of these are interested in the synthesis of indole due to its important role in vital activity in humans and animals, such as the amino acids tryptophan [9], tryptamine, and serotonin, and the mammalian hormone melatonin, responsible for psychiatric health [10].

Among the many advantages of indole are the ability to generate other moieties by combining indole with other organic functionalities such as aldehyde, isatin, and alkyls, among others, to form highly versatile and biologically active scaffolds such as bis(indolyl)methane, tris(indolyl)methane, and trisindolines. Heterocyclic substances are abundantly present in nature and exhibits several biological activities that makes them important part of drug development which are supplements for maintain the healthy life. The majority of the important bis(indolyl)methane is isolated from natural sources in the terrestrial and marine environments. Therefore, they are natural products containing novel structures that show a wide range of significant biological properties. They are also very important according to pharmacy, such as in cancer chemotherapy with bis(3-indolyl)methane [11], where they exhibit antibiotic , antifungal, and antimicrobial activities [12-14].

Trisindolines are obtained by combining two molecules of indole with one molecule of isatin. Isatin is the core structure of various biologically active scaffolds and commercially available medications. Therefore, the combination of isatin and indole produces very potent molecules that are very interesting drugs; one of them is trisindolines. Trisindolines attracted the researcher from its first discovery due to its wide spectrum of pharmaceutical activities, such as anticancer[15], antimicrobial [16], antimycobacterial [17], antifungal, anticonvulsant, a-glucosidase inhibition [18], and spermicidal activities [19].Due to the wide range of biological applications, various synthetic methods for the synthesis of bis(indoyl)methane and trisindolines have been developed, of which only green methodologies are collected in this review. Because green methods reduce the use of toxic chemicals, choosing alternative energy sources to conventional heating such as microwave, sonication, etc., avoids or eliminates the use of solvents and catalysts that protect the environment. All of this is in accordance with Paul Anastas and John Warner's twelve principles of "green chemistry," which were proposed in 1990 and aid in the preservation of the earth's health [20].

As a result, in this review, we collect all such green methodologies from 2003 to 2021, such as ultra-sonication, microwave irradiation, ionic liquids, aqueous medium, grinding, solvents, and catalyst-free synthesis of bis(indole)methane and trisindolines, as follows:

2. DIFFERENT GREEN METHODOLOGIES FOR SYNTHESIS OF BIS (INDOLYL) METHANE AND TRISINDOLINES

Bis(indolyl)methane in which two indole moieties attached to same carbon atom. Indole ring is more reactive at position of 3-carbon atom, therefore here we collected reactions of indole and aldehyde gives 3,3` Bis(Indolyl)methane. In trisindolines reaction between indole and isatin is also takes place at 3-carbon atom of indole ring.

J. S. Yadav et al.[21] demonstrated that ecofriendly process for the synthesis of BIMsby using 1-butyl-3-methylimidazolium tetrafluoroborate ([bmim]BF_4) or 1-butyl-3-methylimidazoliumhexafluorophosphate ([bmim]PF_6) ionic liquids. At room temperature stirring the indole, aldehyde or ketone in ionic liquids [([bmim]BF_4) or ([bmim]PF_6)] for 4-5hrs gives the BIMs in 80-90% yield **(Scheme 1)**. Ionic liquids are environmentally benign reaction media because they having no vapor pressure, increases rate of reaction and selectivity also. Ionic Liquids changes the anion and cation properties. Ionic liquids are alternative reaction media that avoids the use of toxic chemicals, volatile organic solvents which are dangerous to environment. Therefore, ionic liquid follows the green chemistry principle.

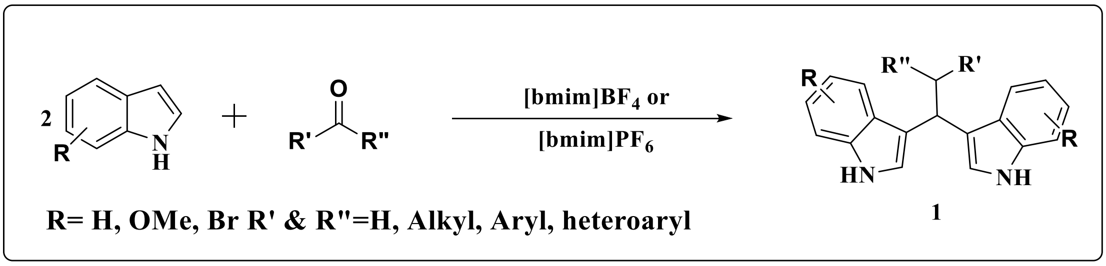

Scheme-1. Synthesis of BIMs in Ionic liquids.

Novel approach discovered by Xiao-Fei Zeng et al. [22] for synthesis of unsymmetrical bis(indolyl)alkanes **(2)** under ultrasonic irradiation. In recent years many organic transformations are catalyzed by ceric ammonium nitrate (CAN) because inexpensive, easily available and soluble in less hazardous organic solvent such as EtOH and MeOH for this reason it can easily participate in oxidation, oxidative addition, nitration, photo-oxidation, deprotection, graft polymerization etc.Reaction of indoles with (1H-indol-3-yl)(phenyl)methanol by using catalyst CAN and 2 ml EtOH was irradiated under ultrasound at r.t. for 2-5 hrs gives desired product with good to excellent yield (70-90%) **(Scheme-2)**.

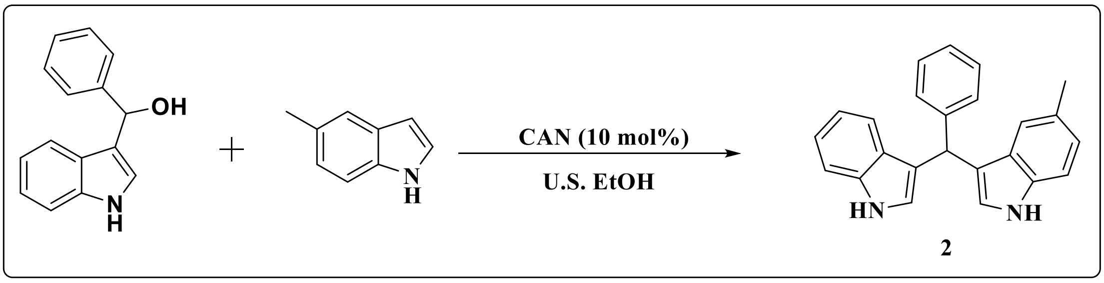

Scheme-2. Synthesis of Unsymmetrical bis(Indolyl)alkanes under U.S.

Parasa Hazarika et al.[23] Develop nonhazardous synthetic methodologies for synthesis of bis- (Indolyl) methane **(3)** and trisindolines **(4)** for that they takealdehyde or ketone (1 mmol) which reacts with indole (2 mmol) and isatin (1 mmol) treated with indole (2 mmol) in presence dodecylsulphonic acid (DSA) in water at room temperature **(Scheme 3 and 4).** Dodecylsulphonic acid acts as a Bronsted acid surfactant; that is, DSA plays a dual role, acting as both a water separator and as Bronsted acid, which catalyses an electrophilic substitution reaction. Dodecylsulphonic acid creates micelles with hydrophobic substances that help dissolve water insoluble reactants, due to which the reaction proceeds and produces the products in good yield. Here develop the economically and environmentally friendly protocol within a short period of time with excellent yield (92% in 30 minute).

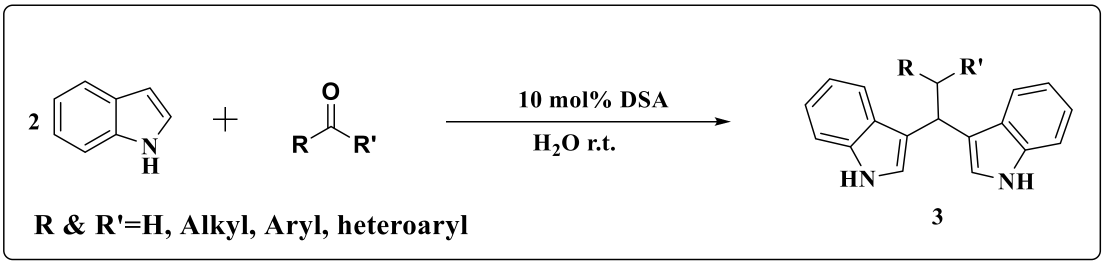

Scheme-3. Synthesis of bis(indolyl)methane in aqueous media.

Scheme-4. Synthesis of Trisindolines in Aqueous media.

Solvent free synthesis is very green protocol demonstrated for synthesis of bis-indolylmethanes(5) and3,3’-indolyloxindole(6) derivatives by HeshmatollahAlinezhad et al. [24] by using cellulosic sulphuric acid (CSA).CSA is a solid acid catalyst which is easy to handle, non-explosive and eco-friendly. After the reaction, the catalyst can be easily recovered by simple filtering and reused in subsequent reactions with a slight decrease in yield.Mixture of indole, aldehyde or ketone with CSA (5mol%) was ground at room temperature for 15min gives BIMs in 73-90% yield **(Scheme-5)**. Then mixture of indole, isatin with CSA (5mol%) was ground at room temperature for 15min gives 3,3’-indolyloxindole in good yield (85%) **(Scheme-6)**.

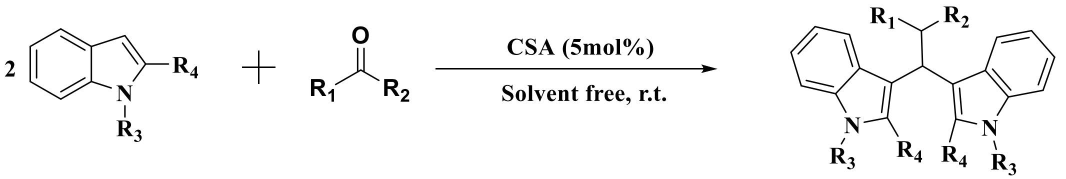

R_1=R_2= H, Alkyl, Aryl and R_3=R_4= H, CH_3

5

Scheme-5. Solvent free synthesis of BIMs by using CSA.

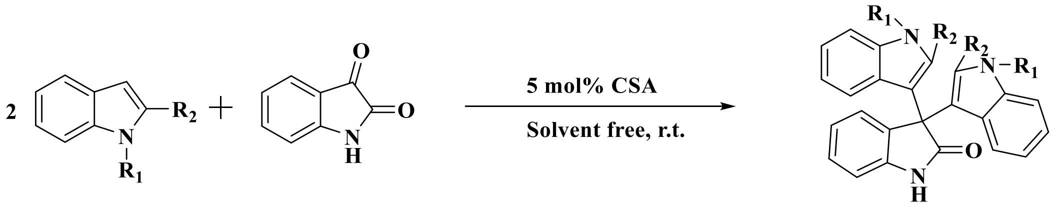

R_1=R_2= H, CH_3

6

Scheme-6. Solvent free synthesis of 3,3'-indolyloxindole by using CSA.

Alum ($KAl(SO_4)_2$-$12H_2O$) catalyzed synthesis of bis(Indolyl) methane(7) under ultrasound irradiation without solvent developed by Swapnil S Sonar et al. [25] in which indole (5mmol) and aldehyde or ketone derivatives (2.5mmol) with 10 mol% Alum powder was irradiated under ultrasonication at ambient temperature for spectacular time (5-30 minute) gives Bis(Indolyl)methane (**Scheme-7**) with good yield (92%). Ultrasound and solvent free reaction save the energy, time, produce high yield, avoid use of toxic solvents and protect the environment.

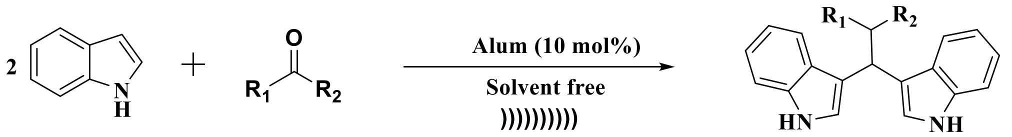

7

R_1 & R_2= H, Aryl, Heteroaryl, Cyclohexyl

Scheme-7. Ultrasound assisted, solvent free Synthesis of Bis(indolyl)methane.

Developed simple green methodology with excellent yield by Ratnadeep S. Joshi et al. [26] under Ultrasound irradiation. They mention 1-Hexenesulphonic acid sodium salt used as catalyst for organic transformation first time which is easy to handle that makes the reaction pathway very smooth and simple. A mixture of 1H-indole (1 mmol), aldehyde (2 mmol) and 1-hexenesulphonic acid sodium salt (10 mol%) was dissolved in minimum quantity of water with constant stirring then reaction mixture was irradiated under ultrasonic irradiation at ambient temperature for appropriate time (45minute) which gives the derivatives of bis(indol-3-yl)methanes (8) with 92% yield **(Scheme-8).**

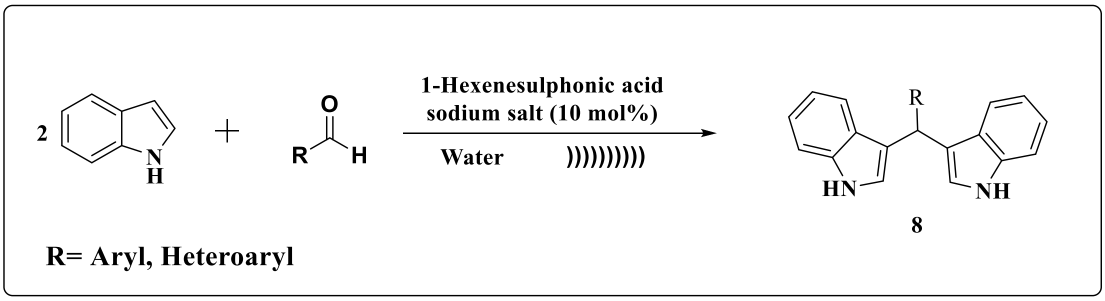

R= Aryl, Heteroaryl

Scheme-8. In aqueous media Synthesis of bis(indol-3-yl) methane's under ultrasound waves.

Ji-Tai Li et al. [27] synthesize bis(indolyl)methanes(9) under ultrasound irradiation in aqueous media for that they use ABS (Dodecylbenzenesulfonic acid) as a catalyst which play dual role it acts as acid catalyst and also emulsifier in reaction due to which use of water as a reaction medium is possible.They take indole or N-methylindole(2mmol), aromatic aldehyde (1 mmol), ABS (0.05 mmol), in 5ml water then reaction mixture was irradiated under ultrasonication(U.S.) at temperature 23-25^{o}C for appropriate time (10min) gives the good to excellent yield (85-98%) **(Scheme-9)**. It is green synthesis of bis(indolyl)methanes by the use of ultrasonication which is clean, energy convenient, required less time, then next is aqueous medium which is cheap, abundantly available and last one is catalyst ABS which is less hazardous to environment and economically favorable.

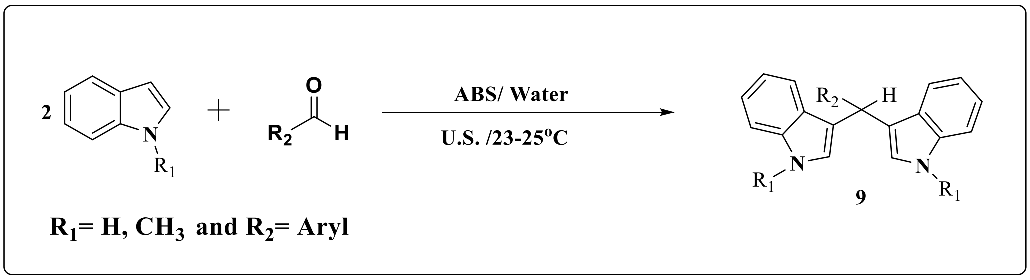

R_1= H, CH_3 and R_2= Aryl

Scheme 9. Ultrasonic assisted Synthesis of bis(indolyl)methane.

Karimi, Narges et al. [28] synthesized Oxindoles(10) Derivatives by using Brønsted Acidic Ionic Liquid [$(CH_2)_4SO_3HMIM$][HSO_4] in aqueous that is on water.This ionic liquid also catalyzes esterification reaction, acetalization of carbonyl compounds and prins reaction.Reaction is carried out by indole, isatin and 12 mol% ionic liquid[$(CH_2)_4SO_3HMIM$][HSO_4] in 5ml water was stirred at room temperature for 35-70min thatafforded oxindole in good yield (85-92%) **(Scheme-10)**.

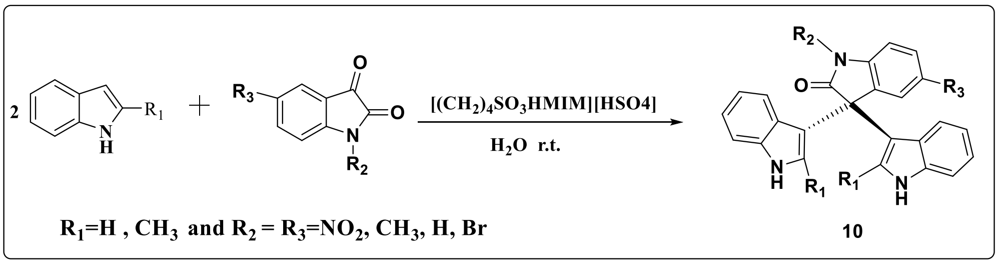

Scheme-10. Synthesis of Oxindoles catalyzed by ionic liquid.

Aqueous hydrotropic medium is a very attractive green solvent, which increases solubility of sparingly soluble organic reactants. Hydrotropes reduce the surface tension of water, which is a greener reaction medium. Hydrotrope is simple to make in a laboratory, lowering the final cost and making it less hazardous and easier to handle. Kamble et al. [29] developed the greener medium for the synthesis of bis(indolyl)methane (11) that avoids the use of organic solvent.Mixture of Indole and aldehyde in 50% Aq. Sodium paratoulene sulphonate (NaPTS) was stirred at room temperature for 20minute gave the bis(indolyl)methane in 91% yield **(Scheme-11)**.

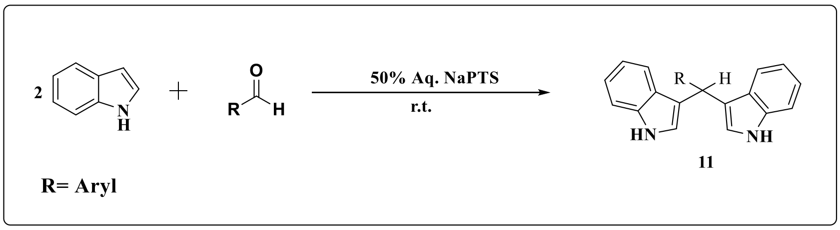

Scheme-11. Synthesis of Bis(indolyl)methane in aqueous hydrotropic medium.

YaghoubSarrafi et al. [30] prepared derivatives of 3,3-di(indolyl)oxindoles **(12)** in 88-95% yield within 30 minutes employing 0.3 g Amberlyst-15 catalysed reaction of indole (1mmol) and isatin (0.5 mmol) in aqueous medium at 70°C **(Scheme-12)**. Amberlyst-15 is highly effective that can increase reactivity and selectivity of several organic synthesisIt is a green protocol because first, Amberlyst 15 is a heterogeneous catalyst that is recovered after completion of the reaction and reused, and second, the solvent system is water, which is easily available andenvironmentally friendly because it reduces the use of toxic chemicals, which reduces the cost of final synthesis. These are some notable features of given protocol.

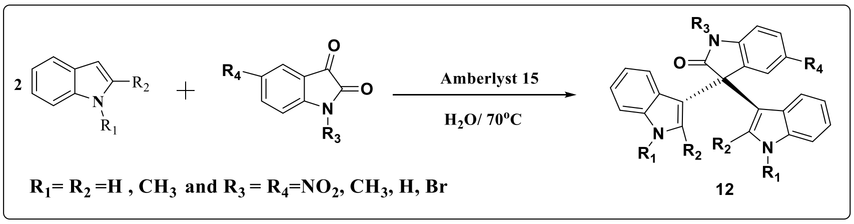

Scheme 12. Synthesis of 3,3-di(indolyl)oxindoles by using Amberlyst 15 in Aqueous media.

Organic synthesis in aqueous medium is one of the important green prospective due to aqueous medium having lots of advantageous such as nonhazardous to human and also to the environment, its availability. sulfonic acid-functionalized mesoporous silica Nanoparticles (SAMSNs) are heterogenous acid catalyst easy to separate, non-corrosive, environmentally and economically compatible.Therefore Ebrahim Mehrasbiet al. [31] prepare 3,3di(indolyl)oxindoles (13) by using sulfonic acid-functionalized mesoporous silicaNanoparticles (SAMSNs) in aqueous media. Indole (2mmol), isatin (2mmol) and SAMSNs (0.06gm) taken in 3ml water was stirred at 60^{o}C for 10 minute at high temperature they found 98% yield **(Scheme-13)** and room temperature required more time and yield is also less (88%).

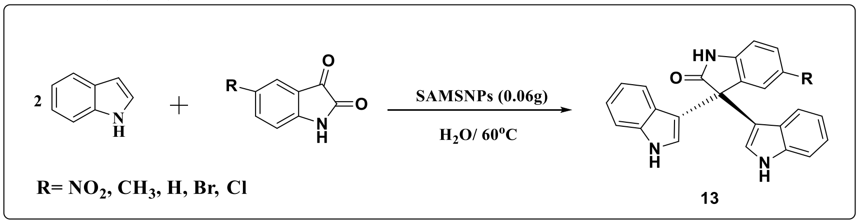

Scheme-13. Synthesis of 3,3-di(indolyl)oxindoles catalyzed by SAMSNs.

An efficient ultrasound-promoted synthesis of bis(indole) (14) derivatives was disclosed by Somayeh Rahimi et al. [32] using 12-tungstophosphoric acid ($H_3PW_{12}O_{40}$). 12-tungstophosphoric acid ($H_3PW_{12}O_{40}$) is a heteropolyacids (HPAs) and highly stable catalyst.Reaction between indole and 2-(pyridylmethylene) malononitriles or 3-(pyridyl) acrylates using 12-tungstophosphoric acid (3 mol%) in water was refluxed at 90^{o}C under silent and ultrasound irradiation gave the bis(indole) in 94-93% within time of 11hrs for salient and 15min. for sonication **(Scheme-14).**

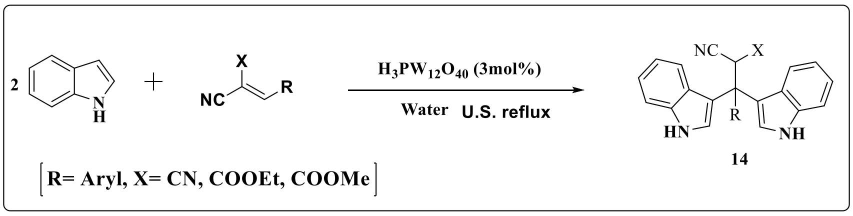

Scheme-14. Synthesis of bis(indole) derivatives in the presence of $H_3PW_{12}O_{40}$.

Deep eutectic solvents are good alternatives to regularly used organic solvent because they are environmentally friendlier, nonflammability, having low melting points and cheaper. Deep eutectic solvent has analogous physicochemical properties to ionic liquids.So NEDA SEYEDI et al. [33] utilized $ZnCl_2$/Urea as a Deep Eutectic Solvent (DES) under ultrasonication for the preparation of Bis(indolyl)methane (15). Reaction between carbonyl compound (1mmol), indole (2mmol), DES (1eq) was irradiated under ultrasonication at $60^{o}C$ for 10-25 min. which given the Bis(indolyl)methane with 80-92% yield **(Scheme-15)**.

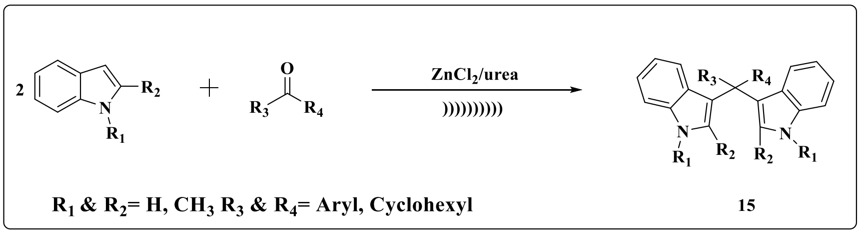

Scheme-15. Synthesis of Bis(indolyl)methanes in DES.

Mohammad Ali Amrollahi et al. [34] again used $H_3PW_{12}O_{40}$ in aqueous media for the synthesis of Bis(indolyl)methane under ultrasound irradiation**.**12-tungstophosphoric acid ($H_3PW_{12}O_{40}$) acts like heteropolyacids (HPAs) that catalyzed several organic reaction in aqueous medium such as Diels–Alder reactions, oxidative dehydrogenation of alcohols and amines, preparation of dihydropyrimidinones, preparation of oximes.Here they perform reaction between aldehyde (0.5mmol), indole (1mmol) and active methylene compound (0.5mmol) and catalyst $H_3PW_{12}O_{40}$ (3.4 mol%) in 8ml water which was irradiated under ultrasonicated at $90^{o}C$ for 10-15min. gave the Bis(indolyl)methane (16) in 80-95% yield **(Scheme-16)**. In this methodology aqueous media and ultrasonication both are green protocols that save the energy, economy and also environment.

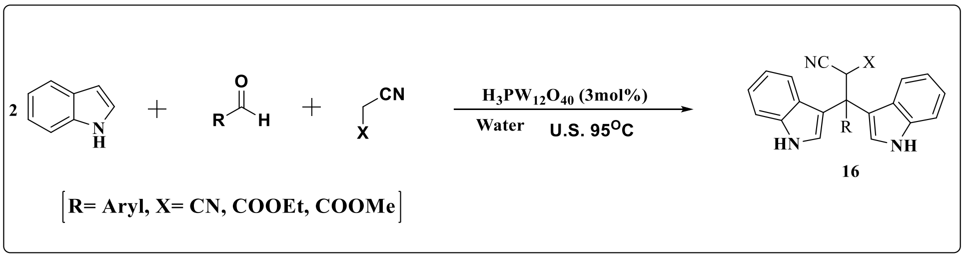

Scheme-16. $H_3PW_{12}O_{40}$ Catalyzed Synthesis of Bis(indolyl)methane in aqueous media.

Expanded Perlite-PPA (EP-PPA), as a novel, green and efficient heterogeneous catalyst developed by Marzieh Esmaielpour et al. [35] for the green synthesis of derivatives of bis(Indolyl)methane (17) in aqueous media.Expanded Perlite-Polyphosphoric acid (EP-PPA) is a protic acidic heterogenous catalyst. The catalytic activity of expanded perlite-PPA is effective up to six cycles.Mixture of indole (2 mmol), Benzaldehyde (1 mmol) and EP-PPA (0.04 g) in H_2O (3 mL) was stirred at 60°C for 10min gave the desired product in 98% yield **(Scheme-17)**. EP-PPA is an inexpensive and efficient catalyst for the electrophilic substitution reactions.

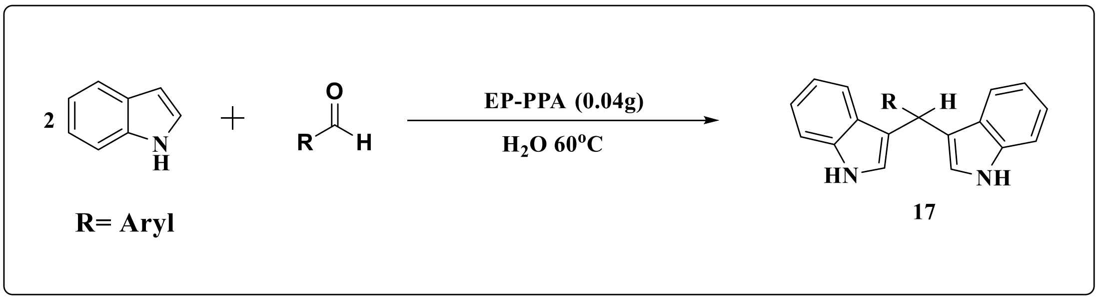

Scheme-17. Synthesis of Bis(indolyl)methane in presence of EP-PPA.

Catalyst free synthesis is one of the vital green perspectives which follow the green chemistry principle such as avoids the use of toxic and harmful chemicals. Under this circumstances Ge Gao et al.[36] demonstrated that in aqueous Ethyl Lactate (EL), catalyst free synthesis of Bis(Indolyl)Methane (18) and 3,3-Bis(Indolyl)oxindoles (19). Under ultrasound irradiation indole reacting with aldehyde or isatin in EL: H_2O (3:2) that obtained the product with good to excellent yield (85-95%) at room temperature **(Scheme 18 and 19)**.

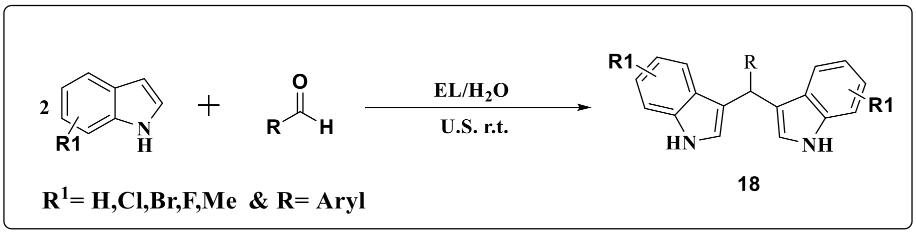

Scheme-18. Catalyst free synthesis of bis(indolyl)methane.

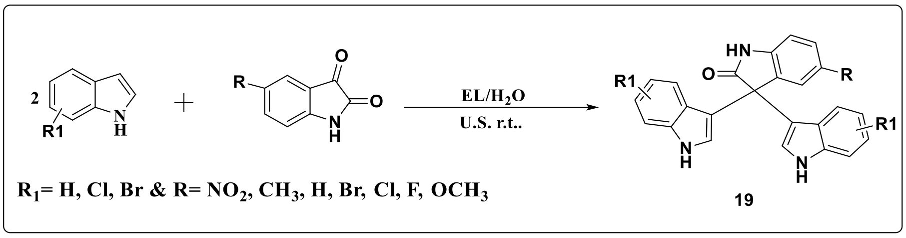

Scheme-19. Catalyst free synthesis of 3,3-bis(indolyl)oxindoles.

Nikofar et al. [37] prepare the Symmetrical and Unsymmetrical Di(indolyl)indoline-2-ones (20) by two methods such as solvent free stirring and grinding by using HNO$_3$@nano SiO$_2$ as catalyst. They compare the results obtained from these two methods; both methods give 80–90% yield, but the difference is the time required to complete the reaction; grinding requires less time (2–5 minutes) and stirring requires more time (20–40 minutes).That is catalyst not only increases yield but also reduces time. Nanoparticle catalyses the reaction in very less amount that reduces waste generation after completion of reaction. Symmetrical and Unsymmetrical trisindolines were prepared by reacting isatin (1 mmol) and two same or different indoles (2 mmol) without solvent only in presence of catalyst HNO$_3$@nano SiO$_2$ **(Scheme-20).**

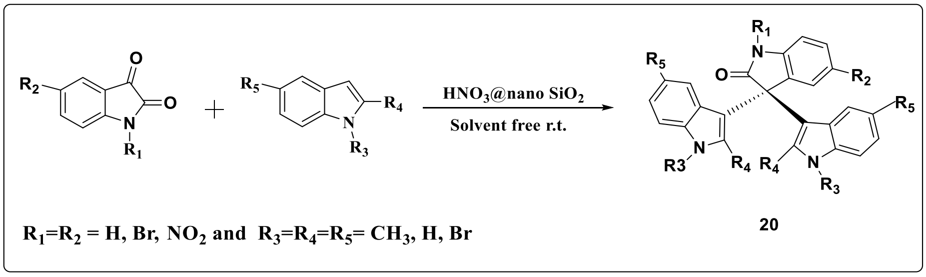

Scheme-20. Solvent free synthesis of Symmetrical and Unsymmetrical Di(indolyl)indoline-2-ones.

A green protocol for catalyst free synthesis of BIMs(21) was disclose by Yi-Shu Zhao et al. [38]. Reacting 2-methylindole and aryl aldehydes in EtOH-H$_2$O (1:1) under blue LEDs for 4hrs produces series of BIMs with good yields (90-98%) **(Scheme-21)** has been accomplished. Reactions assisted under visible light in the absence of a catalyst can fully fulfill the requirements of a mild reaction pathway and ecological friendliness; as per the author, implementation of visible light is the best strategy for the synthesis of BIMs.

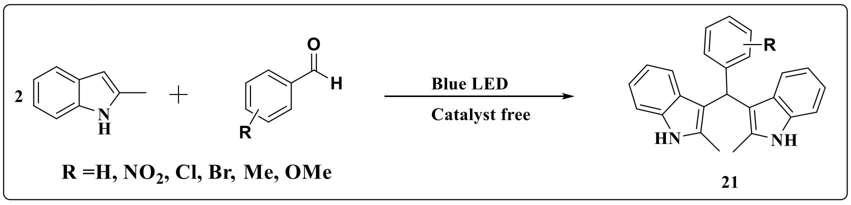

Scheme-21. Catalyst free Synthesis of bis(indolyl)methane under Blue LED.

According to Green Chemistry principles thiamine hydrochloride showed high atom economy and a small E-factor for the reaction. Therefore SivagamiMathavan et al. [39] utilizes environmentally and economically friendly, recyclable aminocatalyst thiamine hydrochloride for synthesis of bis(indolyl)methane (22) and tris(indolyl)methane (23). Indole reacted with aldehyde in presence of catalyst thiamine hydrochloride (1 mol%) at room temperature for 1-3hrs gave bis(indolyl)methane in 80-92% yields **(Scheme-22).** tris(indolyl)methane prepared by reaction between indole, isatin and thiamine hydrochloride (1 mol%) at room temperature within 1-3 hrs with 80-90% yield **(Scheme-23).** Thiamine hydrochloride (vitamin-B$_1$) (VB$_1$) is a non-toxic, biodegradable, easily available, inexpensive and environmentally benign catalyst.

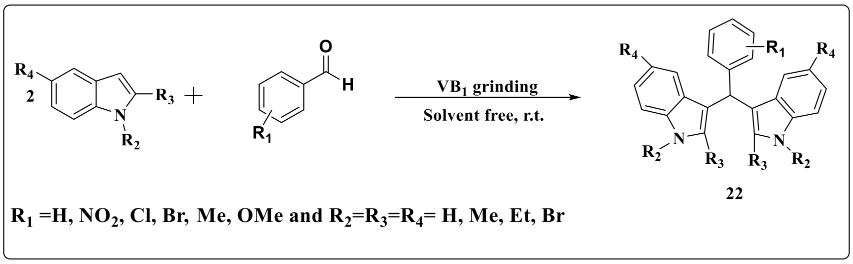

Scheme-22. Thiamine hydrochloride catalyzed solvent free synthesis of bis(indolyl)methane.

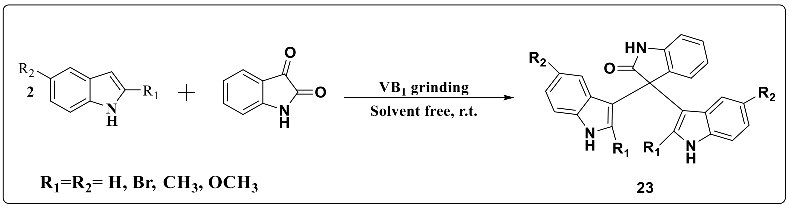

Scheme-23. Thiamine hydrochloride catalyzed solvent free synthesis of tris(indolyl)methane.

One more green protocol such as solvent and catalyst free synthesis of BIMs under visible light reported by Baliram S. Hote et al. [40]. Without any solvent and catalyst indole and aldehyde reacted with each other under visible light irradiation produces BIMs (24) in 25-40min. with 80-90% yield **(Scheme 24)**. Photochemical reactions are a well-known example of green methodology because they decrease or eliminate the generation of hazardous waste. According to them, these photochemical reactions are significantly advantageous because they take place by absorption of a photon, which does not generate any residue. As a result, overall reactions performed under light irradiation are very mild and environmentally friendly.

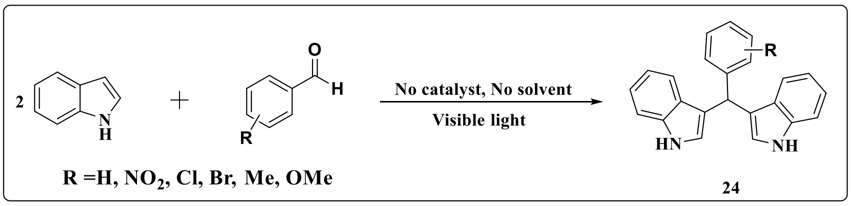

Scheme-24. Synthesis of bis(indolyl)methane under visible light.

Harish K. Indurthi et al. [41] reported microwave (MW) assisted synthesis of Bis(Indolyl)methane (25) without use of solvent. Reaction is catalyzed by Seralite SRC-120 which is commercially available, cheap and strongly acidic cation exchange resin that shows the good reactivity under microwave heating. The catalyst seralite SRC-120 support the reactants under microwave irradiation. Microwave reduces the reaction time with good yield. In reaction vial, indoles (1.0 mmol), aldehydes/ketones (0. 5 mmol), and seralite SRC-120 were mixed well. The sealed reaction vial was irradiated under microwave at 450W within 5-10minute gave the BIMS with good yield (80%) **(Scheme-25)**.

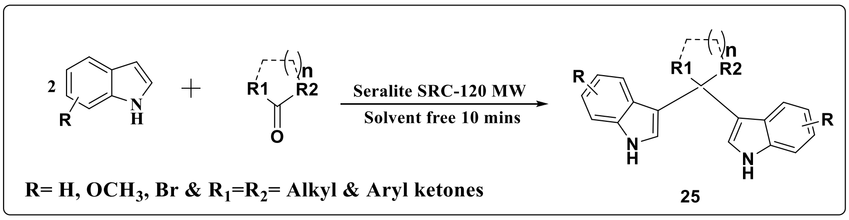

Scheme 25. Microwave assisted synthesis of bis(indolyl)methane.

Xiaohan Yuan et al. [42] was reported first HFIP-promoted catalyst-free synthesis of 3,3-di (indolyl)indolin-2-ones (26). Hexafluoro-2-propanol (HFIP) is used green solvent in organic transformations due to its strong H-bond donating (HBD) properties. HEIP gives nucleophilic substitution reactions, heteroarylation due to which it easily promotes the synthesis of 3,3-di (indolyl)indolin-2-ones. Here model reaction obtained at various temperature and study shows that as temperature increases yield increases and reaction time decreases. Then at 75°C indole and isatin in HFIP (2 ml) gives 94% of 3,3-di (indolyl) indolin-2-ones within 1hr **(Scheme-26)**.

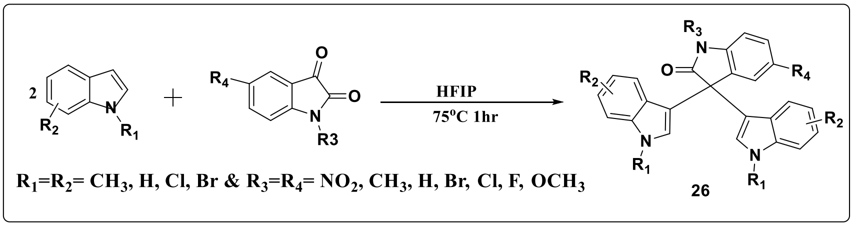

Scheme-26. HFIP-promoted catalyst-free synthesis of 3,3-di (indolyl)indolin-2-ones.

Synthesis of bis(indolyl)methanes (27) under solvent drop-grinding (SDG) method was coined by Kiyoshi Tanemura et al.[43] By using small amounts of organic solvents or ionic liquids. In this protocol they use different solvents and observe the effect of solvents out of which few are organic solvents eg. MeCN or THF and remaining are ionic liquids such as 1-butyl-3-methylimidazolium tetrafluoroborate ([bmim]BF_4), 1-ethyl-3-methylimidazolium trifluoromethanesulfonate ([emim]OTf), 1-butyl-3-methylimidazolium bis(trifluoromethylsulfonyl) imide ([bmim]NTf_2), 1-ethyl-3-ethylimidazolium bis(trifluoromethylsulfonyl)imide ([emim]NTf_2), and [bmim]PF_6. Among them, THF, [emim]NTf_2, and [bmim]PF_6 was effective for the synthesis of bis(indolyl)methane. Solvent drop-grinding (SDG) requires very little solvent and is extremely valuable for expensive ionic liquids. The reaction between indole, isatin and in presence of catalyst $Sc(OTf)_3$ gives BIMs within 10-20 min in 90-92% yield **(Scheme-27)**.

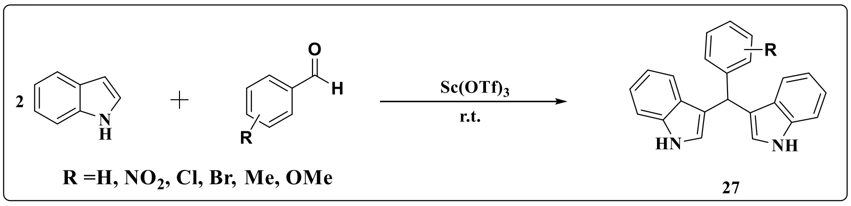

Scheme-27. Synthesis of BIMs by Solvent Drop-Grinding method.

Zhiqiang Wuet al.[44] was developed ball milling solvent free synthesis of unsymmetrical bis(indolyl)alkanes (28) using Lewis acid-surfactant-SiO_2 composite nanocatalyst (LASSC) ($AlCl_3.6H_2O$+SDS+SiO_2).It is a Friedel-Crafts alkylation without solvent under ball milling produces bis(indolyl)alkanes at room temperature is newly developed strategies. LASSC catalysts are easy to prepare, less toxic, readily recovered and recycled several times. Sample tube containing aromatic aldehyde (0.5 mmol), different substituents indoles (0.5 mmol) and nanocatalyst (0.5 mmol) was placed in ball mill at 60Hz gives 93% yield within 8mins **(Scheme-28)**. This protocol is operationally simple and required mild reaction conditions.

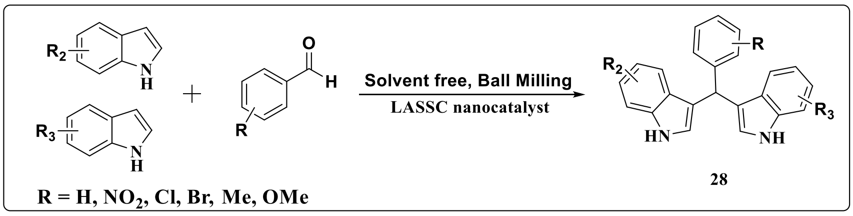

Scheme-28. Solvent-free synthesis of unsymmetrical bis(indolyl)alkanes.

Table-1. Comparative study of Synthesis Bis(indole)methane and Trisindolines.

Sr. No	Reagent	Condition	Time	Yield (%)	References
1	[([bmim]BF_4) or ([bmim]PF_6)]	R.T.	4-5 hrs	80-90	[17]
2	ceric ammonium nitrate (CAN)	EtOH/US/RT	2-3 hrs	70-90	[18]
3	Dodecylsulphonic acid (DSA)	H_2O/ RT	30 min	90	[19]
4	Cellulosic sulphuric acid (CSA)	RT	15 min	90	[20]
5	Alum ($KAl(SO_4)_2$-I2H_2O)	RT/US	5-30 min	92	[21]
6	1-Hexenesulphonic acid sodium salt	H2O/US	45 min	92	[22]
7	Dodecylbenzenesulfonic acid	23-25°C	10 min	85-98	[23]
8	Ionic Liquid $[(CH_2)_4SO_3HMIM][HSO_4]$	H_2O/ RT	35-70 min	85-92	[24]
9	Sodium paratoulene sulphonate (NaPTS)	H_2O/ RT	20 min	91	[25]
10	Amberlyst 15	H_2O/ 72°C	30 min	88-95	[26]
11	sulfonic acid-functionalized mesoporous silica Nanoparticles (SAMSNs)	H_2O/ 60°C	10 min	98	[27]
12	12-tungstophosphoric acid ($H_3PW_{12}O_{40}$)	H_2O/ 90°C/US	15 min	94-93	[28]
13	Deep Eutectic Solvent (DES) - $ZnCl_2$/Urea	60°C/US	10-25 min	80-92	[29]

14	$H_3PW_{12}O_{40}$	H_2O/ 90°C/US	10-15 min	80-95	[30]
15	Expanded Perlite-PPA (EP-PPA)	H_2O/ 60°C	10 min	98	[31]
16	HNO_3@nano SiO_2	RT	20-40 minutes	80-90	[32]
17	Blue LEDs	EtOH-H_2O (1:1)	4 hrs	90-98	[33]
18	Thiamine hydrochloride (vitamin-B_1) (VB_1)	RT	1-3 hrs	80-92	[34]
19	Visible light		25-40 min	80-90	[35]
20	Seralite SRC-120	microwave at 450W	5-10 min	80	[36]
21	Hexafluoro-2-propanol (HFIP)	75°C	1 hrs	94	[37]
22	$Sc(OTf)_3$	RT	10-20 min	90-92	[38]
23	($AlCl_3.6H_2O$+SDS+SiO_2)		8 min	93	[39]

3. CONCLUSION

Bis(indolyl)methane and Trisindolines are very important biological scaffolds due to this more than century researcher works on synthesis and proceed towards to developing more greener methodologies that minimizes environmental pollution, reduce use of toxic chemicals, less energy consumption techniques. Therefore, in this review we collect all such green methodologies and gives idea to developed more greener and sustainable techniques in upcoming years.

ACKNOWLEDGEMENTS

We sincerely thank the Rayat Institute of Research and Development (RIRD) and Y.C.I.S. Satara (Autonomous) for financial support and also for providing necessary facilities. One of the authors A.S. thanks to Government of Maharashtra for awarding Sarthi Research Fellowship.

CONFLICT OF INTEREST

The authors declare no conflict of interest.

REFERENCES

1. Shiri, M., Zolfigol, M. A., Kruger, H. G., Tanbakouchian, Z. (2010) Chemical Reviews, 110, 2250-2293.
2. Wati, F. A., Santoso, M., Moussa, Z., Fatmawati, S., Fadlan, A., Judeh, Z. M. (2021) RSC Advances, 11, 25381-25421.
3. Sundberg, R. J. In Indoles, edited by Sundberg, R. J. Elsevier (1996) pp.1-5.
4. Roussel, P. A. (1953) Journal of Chemical Education, 30, 122.
5. Nenitzescu, C. D. (1929) Romanian Chemical Engineering Society Bulletin, 11, 37-43.
6. Melkonyan, F. S., Karchava, A. V., Yurovskaya, M. A. (2008) The Journal of Organic Chemistry, 73, 4275-4278.
7. Noland, W. E., Baude, F. J. (1973) Organic Synthesis, 5, 567-571.
8. Bartoli, G., Leardini, R., Medici, A., Rosini, G. (1978) Perkin Transactions, 1, 692-696.
9. Corey, E. J., Czakó, B., Kürti, L. In Molecules and medicine, edited by Corey, E. J., Czakó, B. and Kürti, L. John Wiley & Sons (2007) pp.2-32.
10. Wu, Y. J. In Heterocyclic Scaffolds II: Reactions and Applications of Indole, edited by Gribble, G. W. Springer Berlin, Heidelberg (2010) pp.1-29.
11. Safe, S., Papineni, S., Chintharlapalli, S. (2008) Cancer Letters, 269, 326-338.
12. Kobayashi, M., Aoki, S., Gato, K., Matsunami, K., Kurosu, M., Kitagawa, I. (1994) Chemical and Pharmaceutical Bulletin, 42, 2449-245l.
13. Sivaprasad, G., Perumal, P. T., Prabavathy, V. R., Mathivanan, N. (2006) Bioorganic & Medicinal Chemistry Letters, 16, 6302-6305.
14. Kamal, A., Khan, M. N. A., Srinivasa Reddy, K., Srikanth, Y. V. V., Kaleem Ahmed, S., Pranay Kumar, K., Murthy, U. S. N. (2009) Journal of Enzyme Inhibition and Medicinal Chemistry, 24, 559-565.
15. Reddy, B. S., Rajeswari, N., Sarangapani, M., Prashanthi, Y., Ganji, R. J., Addlagatta, A. (2012) Bioorganic & Medicinal Chemistry Letters, 22, 2460-2463.
16. Praveen, C., Ayyanar, A., Perumal, P. T. (2011) Bioorganic & Medicinal Chemistry Letters, 21, 4072-4077.
17. Annuur, R. M., Titisari, D. A., Dinarlita, R. R., Fadlan, A., Ersam, T., Nuryastuti, T., Santoso, M. (2018) In AIP Conference Proceedings, 2049, 020088.
18. Wang, G., Wang, J., Xie, Z., Chen, M., Li, L., Peng, Y., Deng, B. (2017) Bioorganic Chemistry, 72, 228-233.

19. Paira, P., Hazra, A., Kumar, S., Paira, R., Sahu, K. B., Naskar, S., Mondal, N. B. (2009) Bioorganic & Medicinal Chemistry Letters, 19, 4786-4789.
20. Polshettiwar, V., Varma, R. S. (2008) Accounts of Chemical Research, 41, 629-639.
21. Yadav, J. S., Reddy, B. V. S., Sunitha, S. (2003) Advanced Synthesis & Catalysis, 345, 349-352.
22. Zeng, X. F., Ji, S. J., Wang, S. Y. (2005) Tetrahedron, 61, 10235-10241.
23. Hazarika, P., Sharma, S. D., Konwar, D. (2008) Synthetic Communications, 38, 2870-2880.
24. Alinezhad, H., Haghighi, A. H., Salehian, F. (2010) Chinese Chemical Letters, 21, 183-186.
25. Sonar, S. S., Sadaphal, S. A., Kategaonkar, A. H., Pokalwar, R. U., Shingate, B. B., Shingare, M. S. (2009) Bulletin of the Korean Chemical Society, 30, 825-828.
26. Joshi, R. S., Mandhane, P. G., Diwakar, S. D., Gill, C. H. (2010) Ultrasonics Sonochemistry, 17, 298-300.
27. Li, J. T., Sun, M. X., He, G. Y., Xu, X. Y. (2011) Ultrasonics sonochemistry, 18, 412-414.
28. Karimi, N., Oskooi, H., Heravi, M., Saeedi, M., Zakeri, M., Tavakoli, N. (2011) Chinese Journal of Chemistry, 29, 321-323.
29. Kamble, S., Rashinkar, G., Kumbhar, A., Salunkhe, R. (2012) Synthetic Communications, 42, 756-766.
30. Sarrafi, Y., Alimohammadi, K., Sadatshahabi, M., Norozipoor, N. (2012) Monatshefte für Chemie-Chemical Monthly, 143, 1519-1522.
31. Mehrasbi, E., Sarrafi, Y., Tajbakhsh, M. (2015) Research on Chemical Intermediates, 41, 6777-6787.
32. Rahimi, S., Amrollahi, M. A., Kheilkordi, Z. (2015) Comptes Rendus Chimie, 18, 558-563.
33. Seyedi, N., Khabazzadeh, H., Saeednia, S. (2015) Synthesis and Reactivity in Inorganic, Metal-Organic, and Nano-Metal Chemistry, 45, 1501-1505.
34. Amrollahi, M. A., Kheilkordi, Z. (2016) Journal of the Iranian Chemical Society, 13, 925-929.
35. Esmaielpour, M., Akhlaghinia, B., Jahanshahi, R. (2017) Journal of Chemical Sciences, 129, 313-328.
36. Gao, G., Han, Y., Zhang, Z. H. (2017) ChemistrySelect, 2, 11561-11564.
37. Nikoofar, K., Khalili, Z. (2018) National Academy Science Letters, 41, 361-364.

38. Zhao, Y. S., Ruan, H. L., Wang, X. Y., Chen, C., Song, P. F., Lü, C. W., Zou, L. W. (2019) RSC advances, 9, 40168-40175.
39. Mathavan, S., Kannan, K., Yamajala, R. B. (2019) Organic & Biomolecular Chemistry, 17, 9620-9626.
40. Hote, B. S., Siddiqui, T. A., Pisal, P. M., Mandawad, G. G. (2022) Polycyclic Aromatic Compounds, 42, 1761-1769.
41. Indurthi, H. K., Virdi, R., Koli, P., Nageswara Rao, D., Sharma, D. K. (2021) Synthetic Communications, 51, 139-150.
42. Yuan, X., Wang, S., Cheng, J., Yu, B., Liu, H. M. (2020) Chinese Chemical Letters, 31, 2465-2468.
43. Tanemura, K. (2021) Tetrahedron Letters, 82, 153391.
44. Wu, Z., Wang, G., Li, Z., Feng, E., Liang, Y., Zhan, H., Liu, W. (2021) Synthetic Communications, 51, 1206-1217.

GUIDELINES FOR CONTRIBUTORS

1] **Journal of Shivaji University : Science & Technology** is the publication of Shivaji University, Kolhapur (Maharashtra, India), being published twice a year. It is an academic peer reviewed ISSN approved Journal.

2] The Journal welcomes research articles based on original research, review papers, research communication/notes by the faculty and research scholars working in various fields of Science and Technology. Articles/Papers can be submitted in English language only.

3] The length of manuscripts should not exceed 6000 words for review article, 5000 words for research article, 2000 words for research communication and 1000 words for research note.

4] The article/paper must accompany an **abstract not exceeding 200 words.**

5] During writing and submission of a manuscript, please follow the author guidelines arakble on the home page of Journal of Shivaji University: Science and Technology.

6] All the sources of literature referred to while writing the article/paper must be properly cited in the text. The serial numbers of End Notes, if any, must also be indicated within text at appropriate places.

7] The listing of references must follow the standard format.

8] Tables, charts, maps, figures etc. should be placed at appropriate places in the text of the article/paper and must be numbered serially with suitable headings. The tables should be referred to by their numbers within the text. Art-work for maps, figures and charts should be provided separately, if necessary.

9] Only articles evaluated and approved by the subject Experts/Referees/Departmental editorial board are considered for their publication in the Journal. The referees evaluate Article/ Paper drafts in term of structure and organization of paper/argument, originality of the research, appropriateness of abstract and introduction, literature review, methodology and data sources, data/evidence and conclusions, and quality of language.

10] The name of the author/co-author of the article being submitted should mentioned on the first page of the article/paper below title of that article. An asterisks (*) is used for defining corresponding author/s of a manuscript.

11] For any other information and for inquiries regarding submitted articles/papers preferably use e-mail communications. **(E-mail : editor.jscitech@unishivaji.ac.in)**

12] Manuscript should be sent to email of the Editor (**editor.jscitech@unishivaji.ac.in**) {or associate editor of the concerned subject}, Journal of Shivaji University: Science and Technology, Kolhapur with e-copy only (single M.S. word as well as PDF file).

Only research articles/review papers/research communication/notes prepared strictly in accordance with the above guidelines will be sent to referees for their evaluation and opinion about their acceptability or otherwise. We do not send back rejected articles.


शिवाजी विद्यापीठ कोल्हापूर
ज्ञानमेवामृतम्